ABSTRACT

Title of Dissertation:	ENABLING RAPID PHENOTYPIC DETECTION OF CEPHALOSPORIN RESISTANCE BEYOND THE CENTRAL LABORATORY
	Hieu Thuong Nguyen Doctor of Philosophy 2019
Dissertation directed by:	Associate Professor Ian White Fischell Department of Bioengineering

The so-called bacterial "superbugs" are largely resistant to some of the most commonly prescribed antibiotics, including a drug class known as *cephalosporins* used to treat many hospital and community-acquired infections. This major public health threat has been acknowledged for decades by the Centers for Disease Control (CDC) as a major concern; yet, the detection of superbugs has not been made routine since standard testing practices have been limited to specialized "central" laboratories with sophisticated yet bulky and expensive equipment and highly trained personnel. As a result, the lack of simpler testing methods that can be used in everyday clinics and doctor's offices can be viewed as a source of error contributing to incorrect antibiotic treatment and poorer patient outcomes, factors that drive even more advanced resistance, depleting our drugs or last resort.

In this dissertation, we explore new strategies for simplified methods to test for cephalosporin resistance in order to give higher accessibility in the timely detection of superbugs to support the improvement of patient care. To do this, we take an organic chemistry and biochemical approach to develop new detection molecules that report resistance activity in bacteria expressing extended-spectrum β-lactamase (ESBL) enzymes, one of the most prolific resistance strategies used by superbugs. Next, we describe methods of integrating these detection molecules into practical testing methods, and detail the engineering of simpler assays that allow for rapid readout of ESBL phenotypes using commonplace laboratory plate readers, portable Raman devices, and even handheld personal glucose meters (used for diabetes monitoring) purchased from the drugstore.

ENABLING RAPID PHENOTYPIC DETECTION OF CEPHALOSPORIN RESISTANCE BEYOND THE CENTRAL LABORATORY

by

Hieu Thuong Nguyen

Dissertation submitted to the Faculty of the Graduate School of the
University of Maryland, College Park, in partial fulfillment
of the requirements for the degree of
Doctor of Philosophy
2019

Advisory Committee:
Associate Professor Ian White, Chair
Professor Philip DeShong
Professor Peter Kofinas
Professor Daniel Stein
Professor William Bentley

Dedication

To all those who have ever suffered or lost at the hands of incurable disease.

Acknowledgements

To my advisors, Professors Ian White and Philip DeShong for their mentorship, wisdom, and encouraging visions that provide light to my callow eyes;

To Dr. Imaly Nanayakkara, for her continued support, companionship, and MATLAB wizardry to produce a few beautiful figures and schematics (Figs. 3.13, 5.6, 5.7); And the rest of the White Noise for their unbridled willingness to help;

To undergraduate student Connor Hall, for his helpful assistance in performing SERS experiments and analyses (Figs. 5.8, 5.9);

To Dr. David Watts, for his insightful analyses of MS data and chemical substrate characterization (Fig. 3.8, Appendices 2 and 3);

To Dr. Shweta Ganapati, for her contributions to chemical characterization (Appendix 1);

To my dear Friends with jobs who occasionally sponsor my leisure out of pity but are always fierce in their belief in my potential;

To my siblings, for their empathy; To my mother, for listening;

I give my deepest gratitude.

Table of Contents

List of Tables

List of Figures

List of Abbreviations

AMR: antimicrobial resistant
AST: antibiotic susceptibility testing
CDC: Centers for Disease Control and Prevention
Cep-glucose: cephalosporin detection substrate releasing glucose signaling molecule
Cep-diNTP: cephalosporin detection substrate releasing diNTP reporter molecule
Cep-pNTP: cephalosporin detection substrate releasing pNTP reporter molecule
CFU: colony forming unit
CLSI: Clinical Laboratory Standards Institute
CV: cyclic voltammetry or cyclic voltammagram
DDST: disk diffusion susceptibility test
diNTP: 2,4-dinitrothiophenol
DNA: deoxyribonucleic acid
DTNB: Ellman's reagent (5,5'-dithio-bis-[2-nitrobenzoic acid])
EDTA: Ethylenediaminetetraacetic acid
ESBL: extended-spectrum beta-lactamase
ESI-MS: electrospray ionization-mass spectrometry
GOx: glucose oxidase
HGT: horizontal gene transfer
HIV: human immunodeficiency virus
HPLC: high performance liquid chromatography
HRP: horseradish peroxidase
IR: infrared (spectroscopy)
IVD: *in vitro* diagnostic
LCR: ligase chain reaction
LC-MS: liquid chromatography-mass spectrometry
MBL: metallo-beta-lactamase
MIC: minimum inhibitory concentration
MS: mass spectrometry
NAG: *N*-acetylglucosamine
NAM: *N*-acetylmuramic acid
NMR: nuclear magnetic resonance
PBP: penicillin binding protein
PCR: polymerase chain reaction
PCR-RFLP: polymerase chain reaction restriction fragment length polymorphism
PCR-SSCP: polymerase chain reaction single-strand conformation polymorphism
PGM: personal glucose meter
POC: point-of-care
pNTP: *para*-nitrothiophenol
RT: real-time
RXN: reaction (chemical)
SNP: single nucleotide polymorphism
SERS: surface-enhanced Raman spectroscopy
UV-vis: ultraviolet visible (spectrophotometry)

Chapter 1: Introduction

1.1 Overview

Antimicrobial resistance (AMR) to *β*-lactam compounds poses a critical and mounting challenge in the treatment of community and hospital acquired infections. The Centers for Disease Control and Prevention (CDC) listed extended-spectrum *β*-lactamase (ESBL) producing *Enterobacteriaceae* as one of the biggest threats in its 2013 Antimicrobial Resistance Threats Report.[1,2] Though enumerated under "serious threats," ESBL pathogens are a direct evolutionary forerunner of carbapenem-resistant *Enterobacteriaceae*, declared as an "urgent threat" to public health. The etiology of resistant cases lies largely in Gram negative *Enterobacteriaceae* which produce and disseminate plasmid-encoded enzymes capable of hydrolyzing *β*-lactam antibiotics which range from older (*-cillins*) to more advanced (*cephalosporins, carbapenems*). Incorrect antibiotic treatment not only leads to poor patient outcomes, but also places selective pressure on the pathogen, driving AMR advancement. Therefore, timely and accurate testing is crucial for good patient outcomes and for safeguarding public health.

As recommended by the Clinical and Laboratory Standards Institute (CLSI), the current standard in antimicrobial susceptibility testing (AST) relies on bacterial culture (disk diffusion susceptibility test, Etest, broth dilution).[3] Results require days-long turnaround; in cases of sepsis, this timeline can prove to be too long, giving the clinician no choice but to administer advanced *β*-lactams of last resort despite

antibiotic stewardship recommended guidelines.[4] The need for faster reporting has led to the adoption of four US FDA-approved automated systems that can produce susceptibility results in the range of 3.5 hours to overnight: MicroScan WalkAway (Siemens Healthcare Diagnostics), BD Phoenix Automated Microbiology System (BD Diagnostics), Vitek 2 System (bioMérieux), and Sensititre ARIS 2X (Trek Diagnostic Systems).[5] These high-throughput systems measure minimum inhibitory concentration (MIC) either by colorimetric, turbidimetric, or fluorometric means, with a variable time-to-result for each readout method depending on the pathogen. In the case of the MicroScan WalkAway, fluorogenic substrates are used to test Gram negative susceptibility, and have a generally faster turnaround time (3.5-7 hours) than turbidimetric end-point measurement for general AMR pathogens (4.5-18 hours). Genotypic tests (ESBL Array, Check-Points) may also provide resistance confirmation, but require more involved sample preparation than simple broth inoculation, and are typically reserved for cases with discrepant phenotypic test results. Furthermore, as genotypic methods are designed to detect single nucleotide polymorphisms (SNPs), the established testing repertoire has been limited to the TEM and SHV families of ESBLs, and only include a small handful of CTX-M variants.[6] Though TEM and SHV evolutionary expansion via SNPs represents a large portion of enzyme mutations that are conducive to resistance,[7] sequencing efforts are far from fully encompassing the widening scope of this rapidly evolving gene.

Rapid phenotypic tests including acidimetric and iodometric methods exist as convenient, quick indicators of β-lactamase presence by way of color-change

readouts. The acidimetric test relies on the generation of a carboxylic acid from the hydrolyzed *β*-lactam, which acidifies unbuffered systems, and methodologies to measure the resultant pH change have been reported in the literature using aqueous phenol red in a tube format or bromocresol purple in the form of strips.[8] The iodometric test is limited to the detection of penicillinase activity, as it relies on the production of penicilloic acid to reduce iodine which changes color when in complex with starch.[9] Though rapid, there exists a critical tradeoff: these tests are susceptible to producing false positives as reduction of iodine and solution acidification are highly subject to variabilities in sample and environment, often causing them to occur nonspecifically;[10] furthermore, the *β*-lactamase enzymes detected by these methods do not encompass the broad- or extended-spectrum genetic permutations whose ascertainment is currently of crucial clinical and public health consequence.[10]

As more refined specificity is required to categorically identify a pathogen as ESBL-positive and differentiate from penicillinase-only producers, several *β*-lactam derived chromogenic compounds (Nitrocefin, pyridine-2-azo-*p*-dimethylaniline cephalosporin (PADAC), CENTA) have previously been described as "reporters" or "sensors" of the resistance phenotype, to better serve as effective detection substrates in the study of ESBL activity.[11,12] Nitrocefin has been established as a clinical laboratory test, and is rapidly hydrolyzed by a range of *β*-lactamases upon incubation with bacterial isolates from overnight culture. Single colonies are placed in a tube containing a buffered solution of Nitrocefin, or dropped onto paper disks impregnated with the compound in a commercial product marketed under the name Nitrocef Disks (Hardy

Diagnostics). Uncleaved Nitrocefin is visually observable as a yellow color and has an optical absorbance peak at 390 nm, a spectral property that would preliminarily indicate a β-lactamase-negative sample due to the apparent lack of enzymatic activity. In the presence of β-lactamase capable of cleaving early-generation cephalosporins, the amide bond of the β-lactam ring in Nitrocefin is hydrolyzed, producing an observable red color change and optical absorbance peak shift to 486 nm from 389 nm at neutral pH, which can be measured spectrophotometrically using a sufficiently sensitive absorbance reader to quantify a given β-lactamase-positive sample. Since single colonies positive for β-lactamase would generally produce copious amounts of the enzyme, especially if grown in selective media containing inducing factors, the absorbance shift can be expected to be visually observable without instrumentation as a yellow to red color change within 5 minutes. In recommended protocols, access of the detection substrate to β-lactamase is further enhanced by CFU concentration via centrifugation, and by cell wall disruption via sonication.[13] However, Nitrocefin and CENTA are generally cleavable by most β-lactamases, and therefore do not distinguish a given isolate explicitly as an ESBL producer.

Commercially available resistance testing agar plates containing multiple chromogenic substrates (chromID ESBL, CHROMagar ESBL, bioMérieux; Brilliance ESBL, Oxoid) can provide a convenient format for culling more specific resistance information.[14] Single colonies from a pre-cultured sample are streaked onto the plates and incubated overnight; specific color change in each colony occurs depending on the combination of different chromogens liberated in the process of

bacterial growth and metabolism. This can provide identifying information by narrowing down to groups of putative bacterial species based on the enzyme producer profile (e.g., earlier generation β-lactamases producers, gluconuridase producers, galactosidase producers). More specific ESBL determination can be performed in plates additionally supplemented with specific cephalosporin antibiotics (e.g., cefpodoxime, cefepime) in addition to Nitrocefin. Though these methods can determine specific resistance information, each with their own set of advantages, they all require extended culture times.

As fluorescence measurement is generally accepted to have higher sensitivities than chromogens, which rely on absorbance spectrophotometry, the development of fluorogenic ESBL substrates has expanded the phenotypic detection repertoire with the promise of lower limits of detection.[15–20] They include substrates that have been designed to release well-characterized coumarins upon specific cleavage by advanced ESBLs including metallo-β-lactamases (MBLs), an improvement on substrates unable to distinguish β-lactamases with extended-spectrum profiles from narrow-spectrum.[21]

Yet, as previously described methodologies require the specialization of a central microbiology lab facility, resistance testing away from equipped central labs, such as in disadvantaged regions, remains an underserved goal. Electrochemical readouts of a redox-active reporter have the potential to meet this paradigm, as demonstrated by the handheld personal glucose meter (PGM). Recently the PGM has been re-envisioned and implemented as a handheld reader for general *in vitro* diagnostics (IVD) beyond

blood glucose biomarkers.[22,23] Biomedical research groups have engineered schemes incorporating a variety of materials into pathways to ultimately produce glucose for endpoint quantitation; this has been described for DNA aptamer-based HIV diagnostics as well as detection of contaminants such as melamine in milk.[24,25] Amperometric measurements of hydrolyzed Nitrocefin have also been reported in the literature, with the aim toward rapid detection of ESBL activity using disposable screen-printed sensors with small sample volumes to enable robust, field-portable instrumentation.[26]

1.2 Public health implications

Numerous public health organizations such as the Centers for Disease Control and Prevention (CDC), World Health Organization (WHO), Infectious Diseases Society of America (IDSA) have declared the rapid emergence of resistant bacteria to be a major "crisis", describing the situation in such dire terms as a "nightmare scenario" that has potentially "catastrophic consequences". As we are now in a "post-antibiotic era" as declared by the CDC in 2013, several other agencies including the Institute of Medicine and federal Interagency Task Force on Antimicrobial Resistance have evaluated that multidrug resistance is an impending threat to both public health and national security for the United States. The antibiotic pipeline has in essence "dried up" since the 1980s, starving the medical field of new resources to continually battle the rising threat of multidrug resistance. Having decreased steadily over last 3 decades, with 30 new antibiotics developed between the years of 1980-1989 dropping to a mere seven new drugs between 2000-2009, this divestment is hugely attributed to

the low economic appeal that fails to yield worthwhile returns for many large companies in the pharmaceutical industry. Other discouraging factors include the larger challenges posed by the smaller market of Gram negative pathogens, as they more rapidly acquire resistance phenotypes and are therefore more unpredictable (in contrast with more widespread and slowly evolving Gram positive methicillin-resistant Staphylococcus aureus). These considerations paired with regulatory approval barriers prove to be a major disincentivizing obstacle to even more optimistic companies.

Maintenance of proper antimicrobial stewardship through judicious use of our remaining antibiotics serves as one of the most implementable strategies available. Overuse or inappropriate prescribing of antibiotics is currently the main driver in the evolution of resistance: incorrect treatment occurs in 30-50% of cases (either by choice of agent or duration of therapy),[4] and up to 60% of antibiotics prescribed in intensive care units have been determined to be unnecessary, inappropriate, or suboptimal.[5] Subtherapeutic or subinhibitory administration promotes evolution of resistance genes by way of mutagenesis, horizontal gene transfer (HGT), or altered gene expression, leading to bacterial strain diversification.

1.3 Management efforts and stewardship

Currently, management strategies for the ongoing antibiotic resistance crisis have been generally two-fold: revitalization of antimicrobial drug discovery programs by the pharmaceuticals industry, and implementation of public initiatives through support by the European Commission[27] (ND4BB, or "New Drugs for Bad Bugs") and

Infectious Diseases Society of America[28] (10x'20 Initiative). Though new drugs have reached advanced stages in the development pipeline, general consensus maintains emphasis on antibiotic stewardship programs that mandate behavioral practices for control and reduction of resistant pathogens: surveillance, infection control, and selection of optimal therapeutic combinations and dosing regimens. The rapid detection of ESBL at the point-of-care can strengthen antimicrobial stewardship not only by aiding in treatment measures in the case of susceptible pathogen detection, but also contribute surveillance data for Antibiogram-assisted resistance incidence tracking and monitoring.[29] The CDC has published guidelines to be taken every time antibiotics are prescribed:[30]

1) Order recommended cultures before antibiotics are given and start drugs promptly.
2) Make sure indication, dose, and expected duration are specified in the patient record.
3) Reassess within 48 hours and adjust Rx if necessary or stop Rx if indicated.

Results from culture-based follow-up testing can later confirm initial rapid-test readouts, as well as determine MIC; however, there are yet two considerations: standard clinical practices typically recommend administering the highest effective dose that is still physiologically safe for the patient, rendering MIC determinations under this dose generally irrelevant; and culture based in vivo testing is not always

able to predict resistance/ susceptibility patterns in the patient, posing an added challenge.[31]

Ultimate goals of this work. The assay methodologies described in the current work can be conceived as future *ex vivo* clinical tests as they aims to directly interrogate bacteria within patient samples. Further, in addition to directly impacting patient health outcomes and contributing to public health assessment in positive ways, the present work aims to bring rapid antibiotic resistance testing out of highly specialized central laboratories and into standard laboratories found in hospitals, clinics, and doctor's offices. Ultimately, the work aims to bring rapid resistance testing to any low-resource setting such as underserved communities or even geographically isolated regions without complete access to healthcare facilities, through compatibility engineering of our assays for the implementation of portable equipment such as store-bought personal blood glucose monitors or portable SERS devices.

Chapter 2: Background

2.1 Beta-lactam antibiotics

2.1.1 Brief history of Cephalosporins

Once considered a medical blessing, the first β-lactam antibiotics eventually fell to newly emerging strains of resistance-harboring bacteria. Newer generation β-lactams known as cephalosporins were developed to have broad-spectrum bactericidal properties while also having lower toxicity and allergenicity. However, the conundrum to their popularity also lay in their broad targeting scope: these antibiotics had differential efficacies against bacteria, exerting evolutionary pressure that selected for resistant organisms and drove their overgrowth and diversification. Among common pathogens that have been selected, some constitutively possess a lower degree of resistance to cephalosporins, but may develop into more broadly resistant mutants that are capable of secondary transfer into other species. One such example is *Pseudomonas aeruginosa*, whose enhanced resistance commonly arises from treatment with oral cephalosporins (namely ceftriaxone or ceftazidime) prescribed for urinary tract infection, and can transfer plasmid-encoded ESBL capacity into Enterobacteriaceae.[32]

Overgrowth, or increased population densities of potentially pathogenic bacteria, occurring in multiply resistant strains can be especially troublesome in the hospital environment.[31] The majority of patients and healthy individuals given cephalosporins develop enterococcal overgrowth in the gastrointestinal tract due to the drug's disproportionate microbicidal effect on other bacterial species. This disruption of the

microbiome—caused more often by cephalosporins than other antibiotic types—can result in associated diarrhea and colitis, clinical diseases often attributed to *Clostridium difficile* overgrowth. Though treatment options include vancomycin, metronidazole, or a combination of both, a high frequency of treatment failures has been documented.[31] As a result, *C. difficile* has gained widespread notoriety due to costly and debilitating hospital outbreaks, with incidences on the rise in the UK over the last decade. As the association of cephalosporins and *C. difficile* has been well established, treatment restrictions put in place in clinical practice have already reduced the incidence of *C. difficile* cases among the elderly.[33,34] This modified practice strategy has proven successful in reducing deleterious repercussions of cephalosporin use, epitomizing improved clinical stewardship. We therefore posit that a more informed practice enabled by a timely resistance test can further improve the resolution of treatment on a case-by-case basis, zeroing in on instances that necessitate last resort administration.

2.1.2 Mode of action

The β-lactam class of antibiotics exert their antibacterial effects through the inhibition of bacterial cell wall synthesis.[35] They interrupt the transpeptidation process that links individual peptidoglycan components of the cell wall together. The bacterial cell wall is a highly complex, rigid structure whose main building block is peptidoglycan, a molecule composed of sugars and amino acids. Chains of peptidoglycan are cross-linked to form tight, mesh-like networks outside the plasma membrane and serve to maintain cell shape by counterbalancing the high internal osmotic pressure. The rigid

sugar-based glycan component consists of chains of alternating *N*-acetylmuramic acid (NAM), to which a short, three- to five- amino acid chain is attached, and *N*-acetylglucosamine (NAG).[36] Crosslinking occurs between these short peptides in adjacent glycan chains to yield the structural lattice that forms the cell wall. Specialized bacterial enzymes known as penicillin binding proteins (PBPs) are essential transpeptidases that catalyze the crosslinking reaction by recognizing the D-Ala-D-Ala motif of the short peptides attached to NAM. As β-lactams have high steric similarity to the D-Ala-D-Ala motif, they can act as a substrate due to their resultant high affinity to PBPs.[37] Upon binding to PBPs, β-lactams exert their antibiotic action acylating the PBPs to form an irreversible covalent bond, thereby inactivating their cross-linking ability and arresting cell wall synthesis. Meanwhile, autolytic restructuring enzymes present in bacteria continue to degrade the cell wall, causing membrane permeability and a consequent shift in osmotic pressure that

results in cell lysis.[38,39]

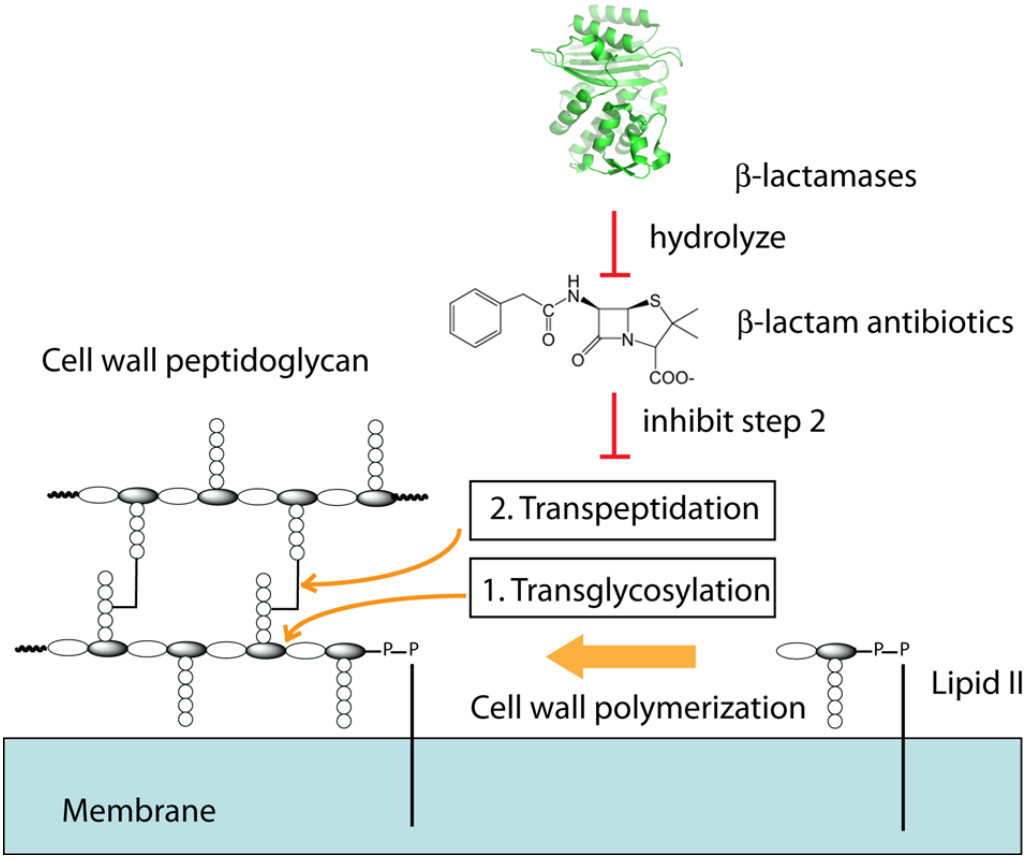

Figure 2.1. Schematic of beta-lactamase activity against beta-lactam antibiotics that inhibit Gram negative bacterial cell wall synthesis. *Image from The Chen Lab © 2019, Univ. of South Florida. Used with permission.*

2.1.3 Classes of β-lactams

Penicillins. In the penicillins (Fig. 2.2), the β-lactam ring is fused to a five-membered thiazolidine ring. Newer penicillins have been formulated through modifications of the acyl side chain attached to the C_6 carbon (R^1). Most examples of this give rise to ampicillin derivatives such as carbenicillin (carboxy group in place of amino group), ticarcillin (substitution of phenyl group for thiophene in addition to carboxy group in place of amino group), and other iterations of acyl side chain modification (ureido groups) that yield azlocillin, mezlocillin, and piperacillin.[40] These acidic side chain

substitutions in carbenicillin and ticarcillin decrease binding to PBPs of *S. faecalis*, and therefore are less effective against the pathogen; however antibiotics of the latter modifications have greater binding affinities to PBPs as well as increased penetration into the cell walls of Gram negative rods including *Pseudomonas aeruginosa* thereby giving them greater effectiveness overall.

Cephalosporins. Cephalosporins (Fig. 2.2) have a β-lactam ring fused to a six-membered dihydrothiazine ring. The cephalosporin nucleus is inherently more resistant to β-lactamase hydrolysis than that of penicillins, making it the next iteration in the advancement of the β-lactam antibiotics after the spread of penicillin resistance, especially among *Staphylococcus aureus* and *E. coli*. There is also greater drug development potential in the cephalosporins because of a greater number of therapeutically important modification sites: the 1-position sulfur, 7-position carbon directly or via its acyl group, and the 3-position carbon.[41–45]

Carbapenems. This class of β-lactam antibiotics is marked by its resistance to hydrolytic inactivation by β-lactamases, and maintain their inhibitory mode of action by reacting with the active-site serine residue to form a long-lived acyl-enzyme intermediate.[46,47] The structure of carbapenems (Fig. 2.2) consists of a β-lactam ring fused to a penicillin-like five-membered ring that has a carbon replacing the sulfur at C-1, and also possesses a double bond between C-2 and C-3. Their small size allows greater penetrability through Gram negative bacterial cell walls. A hydroxyethyl side chain in *trans* configuration—in contrast to the acylamino moiety in penicillins and

cephalosporins—has given the carbapenems marked resistance to β-lactamase hydrolysis, as in the case of imipenem. Yet, recent evolution of β-lactamase-mediated resistance driven in the past 1-2 decades by poor antibiotic stewardship has resulted in the rise of class A carbapenemases and class B metallo-β-lactamases.[46,47] (This will be detailed in the next section under "metallo-β-lactamases".)

Monobactams. These are a group of novel compounds related to the β-lactams that only have a single ring structure as opposed to the bicyclic structure characteristic of the other β-lactams (Fig 2.2). As with the previous β-lactams, the monobactams can be similarly modified to diversify the therapeutic portfolio. The 1-sulfonic acid facilitates binding interactions with PBPs by lowering the activation energy, as in aztreonam.[48]

Inhibitors. β-lactamase inhibitors come in two types: clavulanic acid and sulbactam. These compounds structurally resemble the penicillins (Fig. 2.2) and while not effective by themselves as an antibiotic, when administered in combination formulations, help to enhance *in vitro* activity for diagnostic purposes as they exert protective effects over certain β-lactam antibiotics. Their inhibitory activity is sometimes described as "suicide-like" as they are designed to preferentially bind to β-lactamases but in doing so are destroyed.[49–54]

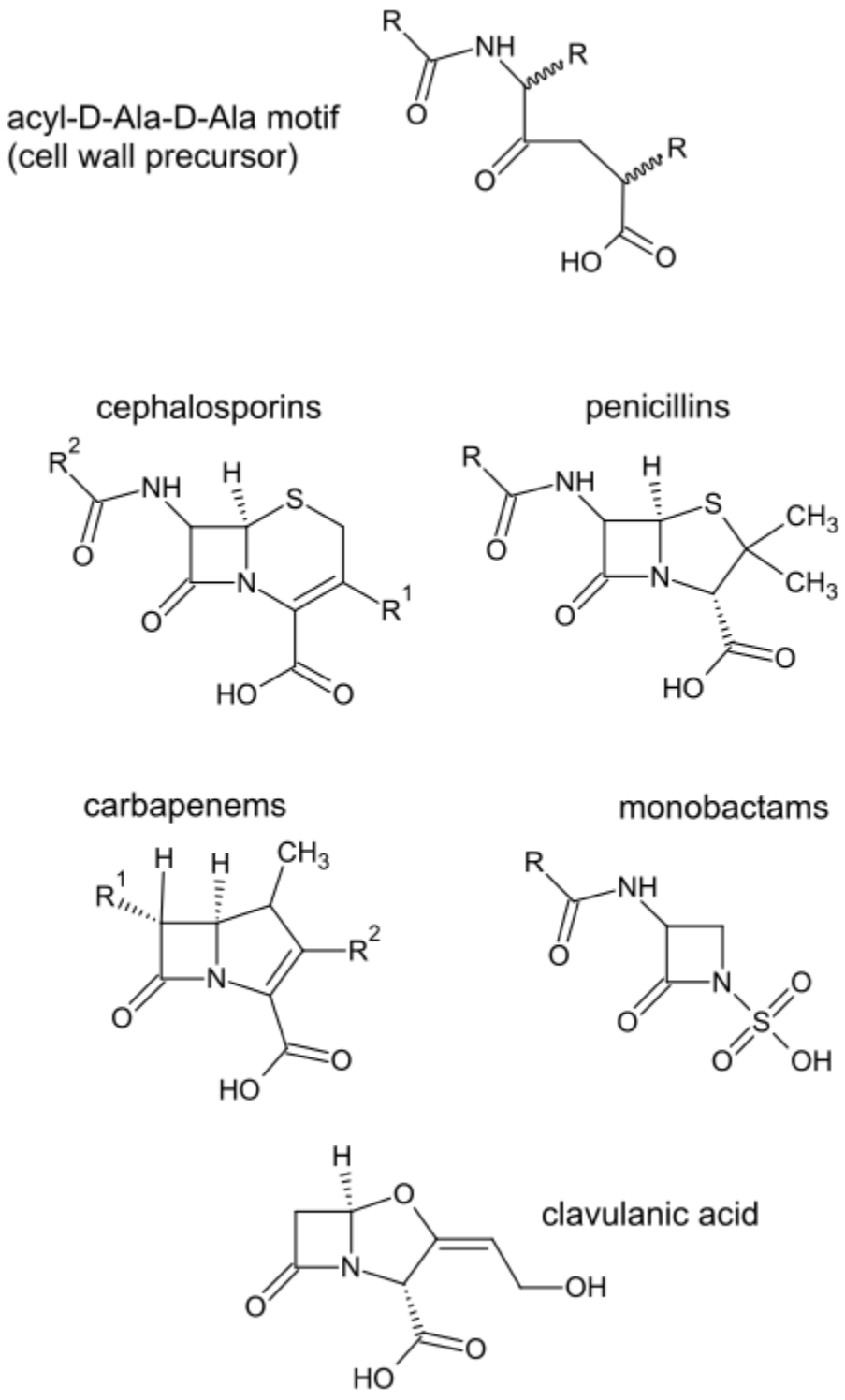

Figure 2.2. Chemical structures of β-lactams and related compounds

2.1.4 Clinical use

Clinical uses - penicillins. Extended-spectrum penicillins are used for *P. aeruginosa* and other aerobic Gram negative rods and anaerobes, with high response rates (60-80%) in bacteremias, intraabdominal infections, female genitourinary tract infections, bone and soft tissue infections, and pneumonias.[55–71] Notably, no differences in efficacy are observed in comparative trials with extended-spectrum penicillins. However, monotherapeutic treatment has been associated with colonization by resistant organisms in 6 to 39 percent of cases;[66,67] superinfection in 7-12 percent of cases; failures to eliminate organisms despite patient clinical improvement in 25-50 percent of cases.[63,70–72] Therefore, as single-agent treatment yields poor response in compromised hosts, they have been recommended for use in combination with aminoglycosides especially for serious infections. Combination therapy has marked improvements in patient response rates, improving efficacy in a variety of clinical situations: 56-97 percent response rates in compromised hosts (e.g., patients with neutropenia), 30-60 percent of hosts harboring *P. aeruginosa* (e.g., bacteremia, endocarditis, osteomyelitis, malignant otitis externa, keratitis, central nervous system infection), 20-50 percent of hosts harboring *Enterobacteriaceae* infection.[71] For anaerobe colonization of intraabdominal or pelvic spaces, or mixed aerobic-anaerobic infections of the lung, extended-spectrum penicillins have produced response rates of 70-90 percent.[73–75] Monotherapy is associated with recurrence in up to 20% of patients; combination therapy is therefore recommended for its high efficacy. Though the ureido penicillins are also effective prophylactic agents for treatment of pelvic,

inflammatory, and biliary surgery, first-generation cephalosporins are equally effective and less expensive.[72–78]

Clavulanic acid with ticarcillin (Timentin, 3 g ticarcillin and 100 mg clavulanic acid, intravenous administration) improves ticarcillin's efficacy against ticarcillin-resistant strains of *Enterobacteriaceae, H. influenzae, S. aureus,* and *bacteroides* by 60-80 percent; however, no increased activity is reported in *P. aeruginosa*. Clavulanic acid and amoxicillin (Augmentin, 250-500 mg amoxicillin and 125 mg clavulanic acid, oral preparation) provides enhanced activity against β-lactamase producers of *Staphylococcus, Branhamella catarrhalis, H. influenzae, Neisseria gonorrhoeae,* and *bacteroides.*[40]

Clinical uses – cephalosporins & carbapenems: Treatment and outcome of infection by ESBL producers. The efficacy of penicillins and its related compounds flounders in the face of β-lactamase enzymes with mutuations rendering them capable of inactivating these older-generation antibiotics.[79–82] Therefore, the range of therapeutic options is reduced when facing infections by ESBL-producing organisms able to hydrolyze many β-lactam antibiotics. Plasmids that these organisms harbor often carry genes that also encode for resistance to aminoglycosides and other antimicrobial agents such as trimethioprim and sulfamethoxazole; plasmid-encoded resistance to cephalosporins is also associated with susceptibility decrease to quinolones including ciprofloxacin.[83–86] Interestingly, in *Klebsiella pneumoniae* clinical isolates, porin loss was only observed in those strains that produce ESBL,[87] with a significant number

expressing active quinolone efflux activity. B-lactam/ β-lactamase inhibitor combinations are generally effective against organisms possessing a single ESBL; however, it has become the case that many organisms now produce multiple ESBLs,[87–90] thereby reducing the effectiveness of such combinations. A 1994-1998 study involving isolates from 35 intensive care units in Europe showed a rise from 31 percent to 63 percent resistance to piperacillin-tazobactam β-lactam/ inhibitor combination over the span of that four year period.[91] Evidenced *in vitro*, the carbapenems (imipenem, meropenem, ertapenem) have the most reliable activity against ESBL-producers as they are stable to hydrolytic activity by these enzymes. Cephamycins (alpha-methoxy cephalosporins modified at the 7-position carbon) have also shown stability toward the ESBLs; however, ESBL-producers tend to lose outer membrane proteins that lead to an ESBL-unrelated form of resistance to these antibiotics.

Serious infections that include the presence of ESBL-producers should not be treated using third-generation cephalosporins: elevated cephalosporin MICs (4-8 μg/ mL) that still lie within the susceptible range can result in high failure rates.[92–94] Though stochastic modeling studies of cefepime (a fourth-generation cephalosporin) have suggested high probability of successful pharmacokinetic/ pharmacodynamics target achievement,[95] empirical data gained from clinical studies has been limited.[94,96] However, a randomized trial of cefepime versus imipenem for hospital-acquired pneumonia showed perfect clinical response (100 percent, 10 of 10 patients) to the carbapenem versus only 69 percent response (9 of 13 patients) to cefepime for a

cohort of patients infected by ESBL-producers.[97] As a rule of principle common among many extended-spectrum cephalosporins, MICs for the antibiotic rise in tandem with the inoculum of the infecting organism.[98–100] CTX-M-type ESBL producers tend to more frequently exhibit resistance activity toward cefepime,[101] as a result, cefepime should not be used as first-line therapy against ESBL-producers. The recommended treatment for cefepime for organisms showing any *in vitro* MIC activities below a certain threshold (<2 μg/mL) is either high dosage (≥2g twice a day) or in combination with amikacin.[102,103]

Cephamycins are also not recommended as a first-line therapeutic in ESBL-producing infections. Despite having reportedly good *in vitro* activity in the treatment of ESBL producers,[104–106] use of cephamycins (including cefoxitin) have resulted in treatment failure and relapse of infection due to selection of porin resistant mutants during therapy. Furthermore, treatment of *Klebsiella pneumoniae* infection outbreak using combined cephamycin and carbapenem has been faced with resistant organisms.[105]

Even in combination with β-lactamase inhibitors, β-lactam MICs rise in tandem with rising inoculum.[100] Since ESBL-producers also often still harbor the parent enzymes (e.g., TEM-1, SHV-1), hyperproduction of these classical β-lactamases together with porin loss can result in decreased efficacy of β-lactamase inhibitors. Carbapenems have been shown to be more effective than β-lactam/ β-lactamase inhibitor combinations in some animal studies in the treatment of ESBL-producing infections.[107] Stochastic pharmacokinetic/ pharmacodynamics modeling has shown

lowered probabilities of reaching targets correlated with success; clinical experience with the drug-inhibitor combinations is limited. Therefore, drug-inhibitor combinations are also not recommended as the first line of treatment for serious infections with ESBL-producing organisms.[95]

Other clinically relevant antibiotics. Quinolones have previously been shown to be a treatment of choice for complicated urinary tract infections with ESBL-producers when there is no detectable *in vitro* resistance. However, *in vitro* resistance is on the rise, and the development of newer quinolones are of marginal benefit. Carbapenems have been found to be equivalent or of greater effectiveness when compared to quinolones.[103,108–111]

2.2 Beta-lactamase enzymes

2.2.1 Molecular mechanism

This dissertation will focus on the most prominent and therefore most important mode of β-lactam resistance, namely, the production of β-lactamases. These enzymes are able to hydrolyze the β-lactam ring through a similar acylation mechanism to render the antibiotic inactive toward PBP targets. However, unlike PBPs, the structure of β-lactamases enables them to coordinate a water molecule in the hydrolysis of the acylated substrate from their active site, thereby allowing them to turn over more β-lactam substrates without themselves becoming inactivated.[112]

ESBLs, most of which are derived from classical TEM and SHV lineages of β-lactamase, are of increasing concern.[113] A few key features that distinguish ESBLs from typical β-lactamases is that ESBLs possess a number of mutations allowing them to hydrolyze expanded-spectrum β-lactam antibiotics. This functional expansion of hydrolytic ability is accompanied by a physical expansion of the active site that allows for the steric accommodation of extended-spectrum β-lactams having bulkier side chains; however this physical expansion may also result in increased susceptibility of the ESBL active site to binding by β-lactamase inhibitors.[114] ESBLs do not exhibit activity against the cephamycins (alpha-methoxy cephalosporins). Interestingly, though most ESBL-expressing strains are thusly susceptible to cephamycins, the loss of an outer membrane porin protein may thereby confer compensatory resistance to cephamycins such as cefoxitin and cefotetan.[104,115,116]

It is also important to note two other common modes of β-lactam resistance:
Altered PBPs exhibiting lower affinity for β-lactam antibiotics. Mutations in the PBPs of certain species such as Streptococcus pneumonia and Staphylococcus aureus have exhibited some resistance to inactivation by penicillins, and their continued function may compensate for inactivated PBPs[117].
Diminished or eliminated expression of outer membrane proteins (OMPs). Gram negative bacteria have been found to lower or eliminate the expression of OMPS in order to restrict the entry of certain β-lactams into the periplasm where PBPs are located[118].

2.2.2 ESBL producers

The greatest threats among microorganisms are Gram negative producers of ESBL and include include A*cinetobacter baumannii, Pseudomonas aeruginosa*, vancomycin-resistant *Enterococcus faecium*, methicillin-*resistant Staphylococcus aureus* (MRSA), and *Aspergillus spp*.[119] Gram positive bacteria, especially *Staphylococcus aureus* and *Enterococcus spp*. pose major threats to antibiotic treatments, though this affront is relatively still under control as the majority of resistance is via horizontally acquired *mec* genes that encode modified PBPs (PBP2A in the case of MRSA) that have low affinity to "conventional" β-lactams (penicillin-like antibiotics).[117] Though widespread in its dissemination, MRSA can still be combatted by a variety of drugs including the glycopeptides and later-generation β-lactams (cephalosporins).[33]

Conversely, Gram negative bacteria are yet particularly worrisome, presenting a more serious challenge in facing the antibiotic crisis. They are especially prevalent in hospital and community settings, with *Pseudomonas aeruginosa, Acinetobacter spp*., and *Enterobacteriaceae* (*Klebsiella pneumoniae*) representative of nosocomial infections. In the community, *Escherichia coli* is the main producer of extended-spectrum ESBLs, and *Neisseria gonorrhea* has developed chromosomally-encoded resistance to expanded-spectrum cephalosporins, including ceftriaxone.[81]

The prevalence of β-lactamases have been fueled by the plasmid capture of normally chromosomal genes from *Enterobacter cloacae, Citrobacter freundii*, or *P. aeruginosa*, which have been able to confer multiple resistance types to genetically

labile *Klebsiella pneumoniae* or *Escherichia coli* against both earlier (alpha-methoxy-β-lactams cefoxitin, cefotetan) and later generation cephalosporins (oxyimino-β-lactams cefotaxime, ceftriaxone, and ceftazidime).[120] ESBL-producing bacteria that express resistance (or reduced susceptibility) phenotypes to the oxyimino-cephalosporins (e.g., cefotaxime, ceftriaxone, ceftazidime) are most largely represented by *Enterobacteriaceae*, namely *Eschericia coli* and *Klebsiella pneumonia*e. These two bacterial species are the main sources of community- and hospital-acquired infections.[121] Carbapenem resistant *Enterobacteriaceae* (CRE) are one of the latest challenges facing human health. Some carbapenemase-producing strains have become resistant to most or all available antibiotics, causing infections extremely difficult to treat, and in some cases can contribute to death in up to 50% of infected patients.[47,122] ESBL-producing (non-carbapenemase) *Enterobacteriaceae* are already responsible for 26,000 hospital-acquired infections, resulting in 1,700 deaths per year.[123]

Here we focus on Gram negative pathogenic bacteria whose main resistance strategy is the production of extended-spectrum β-lactamase (ESBL). As some physicians recognize cephalosporins' role in ESBL selection, so have they begun reverting to older antibiotic combinations for community-acquired pneumonias or surgical prophylaxis.[72–74,77] Hospitals exhibit a greater concentration of resistant coliforms that can disseminate throughout the community environment.[90,108] Therefore, in addition to eliminating cephalosporins as the prophylaxis of choice, further reduction of suboptimal or incorrect treatment is also necessary to preserve the cephalosporin

arsenal. Though ESBL producers can be inhibited by such remaining newer cephalsporins as cefepime, it must be ensured as the best choice before treatment.[35]

2.2.3 Classification

Functional and molecular grouping. Most ESBLs are considered as Ambler's molecular class A,[124] a key feature of which is possession of an active site serine residue, preferential hydrolysis of penicillins, and a molecular weight of approximately 29 kDa.[125] Ambler classification differentiates ESBLs by amino acid sequence similarity, and class A includes families such as TEM-1, SHV-1, and *S. aureus* penicillinase, yet it does not sufficiently differentiate many types of class A enzymes. More recently, a classification scheme devised by Bush, Jacoby, and Medeiros uses the biochemical properties of the enzyme (i.e., substrate/ inhibitor profile) in addition to molecular structure and nucleotide gene sequence (for sufficient characterization of ESBLs by lineage origin) to classify ESBLs into distinct functional groups.[126] Following this scheme, ESBLs are defined under functional group 2be as β-lactamase enzymes capable of hydrolyzing oxyimino-cephalosporins and are inhibited by clavulanic acid.

Classification	Description
Ambler Class A/ Bush Group 2	Penicillinases susceptible to β-lactamase inhibitors. Ex: *S. aureus* PC1 (Group 2a); *E. coli, K. pneumonia* TEM-1, SHV-1 (Group 2b)
Ambler Class B/ Bush Group 3	Carbapenemases, metallo-β-lactamases (MBLs), require Zn^{2+} atoms, resistant to clavulanic acid, sulfones. Ex: *P. aeruginosa* IMP-type, VIM-type, SPM, NDM
Ambler Class C/ Bush Group 1	Cephalosporinases. Resistance to penicillins, β-lactamase inhibitors, cefoxitin, cefotetan, ceftazidime, ceftriaxone, cefotaxime. Ex: Chromosomally encoded AmpC (*C. freundii, E. aerogenes, E. cloacae, M. morganii, P. aeruginosa, S. Marescens*)

Table 2.1. An abridged table comparison of Amber and Bush classifications of ESBL.

2.2.4 Classical origins of ESBL

TEM β-lactamase family. TEM-1, the classical parent version of this β-lactamase family, is the most commonly encountered β-lactamase in Gram negative bacteria, accounting for up to 90% of ampicillin resistance in *E. coli*.[113] It also accounts for increasing incidences of ampicillin and penicillin resistance in *H. influenzae* and *N. gonorrhoeae*. In addition to penicillins, TEM-1 is active against first-generation cephalosporins such as cephalothin and cephaloridine. TEM-3, first reported in 1989, is the first TEM-type to display the ESBL phenotype;[127] since this first report over 90 additional TEM derivatives have been described, the majority of which are ESBLs, some of which are inhibitor-resistant enzymes.

SHV β-lactamase family. *K. pneumoniae* are the main genetic reservoirs of the SHV-1 β-lactamase which accounts for up to 20% of the plasmid-mediated ampicillin

resistance in the species,[128] with many strains integrating the *bla*$_{SHV-1}$ gene into their chromosome.[113] Unlike TEM-types, there exist relatively fewer derivatives of SHV-type β-lactamases, and the changes that do give rise to derivatives occur in fewer positions within the structural gene.

CTX-M β-lactamase family. This plasmid-encoded family of ESBL is characterized by their ability to preferentially hydrolyze cefotaxime, and have been identified in *Salmonella enterica* (Typhimurium) and *E. coli* among other *Enterbacteriaceae*. Prominent members of this enzyme family include CTX-M-1, CTX-M-2, CTX-M-10, and Toho enzymes 1 and 2.[129,130] The CTX-M-type family is more genealogically distinct from TEM- or SHV-types, only showing approximately 40% homology.[131] Interestingly, studies comparing the genetics between CTX-M-type ESBL and AmpC of *Kluyvera ascorbata* have provided evidence that there is a high degree of homology between the CTX-M-type plasmids and chromosomally encoded AmpC enzymes, suggesting the chromosomal origination of the former from the latter.[132] Kinetic studies show CTX-M-type ESBLs hydrolyze cephalothin or cephaloridine (first-generation cephalosporins) more efficiently than benzylpenicillin, in addition to preferentially hydrolyzing cefotaxime over ceftazidime. Importantly, though they exhibit low-level activity against cefotaxime, this is not sufficient to display a survival resistance phenotype. The Ser-237 residue present in all CTX-M enzymes plays an important role in their extended-spectrum activity.[133] The nonessential Arg-276 residue, which is equivalent to the Arg-244 residue in TEM- and SHV-type ESBLs, may play a role in expanding the activity spectrum of CTX-M-types into the

oxyimino-cephalosporins.[134] Toho-1 crystallographic studies (CTX-M family) have suggested increased flexibility of the CTX-M-type (thanks to marked differences in the β-3 strand and omega loop compared to other class A β-lactamases), and attributed the extended-spectrum phenotype to the lack of hydrogen bonding near the omega loop.[135] Notably, CTX-M-types are better inhibited by tazobactam than other β-lactamase inhibitors sulbactam and clavulanate.[129,131,136,137]

OXA β-lactamase family. Here we will briefly mention this genetically unrelated (with respect to TEM-, SHV-, and CTX-M-types) but growing family of ESBLs. These ESBLs belong to the molecular class D (Ambler) and functional group 2d (Bush-Jacoby-Madeiros). They have high hydrolytic activity against oxacillin and cloxacillin, from whence they derive their name, and also confer resistance to ampicillin and cephalothin (first-generation cephalosporin); they are additionally poorly inhibited by clavulanic acid. OXA-type ESBLs are mainly found in *P. aeruginosa* but also in many *Enterobacteriaceae*. Interestingly, OXA-type ESBLs provide only weak resistance activity against the oxyimino-cephalosporins when cloned into *E. coli* but fairly high-level resistance in *P. aeruginosa*.[138] In a similar story to the previously mentioned ESBLs, whereas most OXA-types exhibit activity against ceftazidime, OXA-17 in particular appears to have traded off its ceftazidime activity to take on cefotaxime and ceftriaxone resistance.[139]

*AmpC β-lactamases***.** AmpC β-lactamases are capable of hydrolyzing the alpha-methoxy-β-lactams (cefotetan, cefoxitin) and are not inhibited by clavulanate or

sulbactam. AmpC expression is governed by chromosomal determinants and overproduction of AmpC is known to produce braod-sectrum resistance to both cephamycins and oxyimino-β-lactams.

Class B metallo-β-lactamases (MBLs). To address the growing concern of carbapenem resistance, we must discuss their culprits, the highly transmissible plasmid-mediated metallo-β-lactamases capable of inactivating this entire class of antibiotics. MBLs boast great breadth in their substrate activity spectrum and can catalyze the hydrolysis of virtually all β-lactam antibiotics with the exception of monobactams.[140] Unlike the class A serine β-lactamases, MBLs are not inhibited by clavulanate, sulbactam, or tazobactam.[141,142] Interestingly, they are additionally not effectively inhibited by NXL-104, an inhibitor of class A and C enzymes currently in clinical trials.[143] However, as they rely on metal ions for their activity, MBLs are accordingly inhibited by metal chelators such as EDTA.[141]

Genetics. Initially discovered nearly half a century ago, and found to be chromosomally encoded in non-pathogenic organisms,[144,145] MBLs have in recent decades become a critical threat to human health with the advent and spread of IMP- and VIM-types in Gram negative pathogenic *Enterobacteriaceae*, *P. aeruginosa*, and *A. baumanii*.[146,147] Additionally, the genetic promiscuity and transmissibility of IMP- and VIM-type enzymes is due to their encoding as gene cassettes residing within the integron structures of other resistance genes, and are associated with transposons that can insert in either the bacterial chromosome or plasmids.[147,148] Integrons are

essentially genetic stockpiles in bacteria that can undergo site-specific promoter recombination to allow expression of new genes. The activation and movement of resistance genes within plasmids is facilitated by integrons; once on plasmids, the transfer of resistance genes between different bacteria is achieved with much greater ease compared to genes that are chromosomally encoded.[149] That this identifiable phenomenon plays a critical role in the emergence of so-called multidrug resistant "superbugs" in the wake of carbapenem treatment failure thus becomes obvious and undeniable.

The more recent NDM-1 MBL first discovered in 2008 in *Klebsiella pneumonia* and *E. coli* demonstrates the dissemination potential of MBLs. Found on several plasmid types, bla_{NDM-1} can be transferred among Gram negatives by conjugation. Though not associated with integron structures, NDM-1 nonetheless has rapidly spread worldwide,[122,150] perhaps facilitated by its association with transfer-promoting insertion element ISAba125.

2.3 Genetic detection of ESBL

2.3.1 Genetics and evolution of ESBL

As an overview, we will begin with some important behavioral features of ESBL genes that impact its genetic detection:

- The β-lactamase gene (*bla*) can be encoded chromosomally, on plasmids, or on transposons. Their expression behavior (constitutive or inducible) depends on the genetic environment in which they are situated.
- Extended-spectrum β-lactamases give rise to resistance against oxyimino-cephalosporins (e.g., cefotaxime, ceftazidime, ceftriaxone, and aztreonam, an oxyimino-monobactam, etc.).
- Plasmid-mediated enzymes confer resistance to alpha-methoxy-cephalosporins, such as cephoxitin and cefotetan, as well as the oxyimino-β-lactams. These are the class C β-lactamases which are normally chromosomally encoded in Gram negatives.
- Class B metallo-β-lactamases confer resistance to the carbapenems such as imipenem and meropenem, and include the oxyimino- and alpha-methoxy-cephalosporins.
- Chromosomally encoded class A extended-spectrum enzymes are found in *Klebsiella oxytoca* and other nosocomial pathogens, though these are outside the relevant scope of this review and will not be discussed here.

TEM-1 is the most common plasmid mediated β-lactamase in enteric organisms except in *Klebsiella pneumoniae* (SHV-1 dominates). Single amino acid substitutions may yield identical enzymatic properties, but in some cases may result in low-level enhancement of activity toward a few oxyimino-cephalosporins, as in the case of TEM-7 or TEM-12 which differ by Ser substitution at position 164, or TEM-11 which has a His substitution at the same position, and exhibit modest enhancement

toward cefotaxime, ceftazidime, and aztreonam.[151] Notably, marked relative increases in activity toward ceftazidime and aztreonam occur when the 164-positional substitutions are accompanied by one of the following: Lys-104, Lys-240 or Thr-237, and Lys-240 appearing in the arising ESBLs TEMs -5, -6, -9, -10, -16, -24, or -26. Interestingly, these subsitutions are always associated with greater ceftazidime activity over cefotaxime.[152] In contrast, TEMs -3, -4, and -8, which possess a Ser-238 residue change, exhibit higher activity against cefotaxime over other oxyimino-β-lactams. Enzyme-substrate activity trends of striking similarity also appear within the SHV family with Ser-238 association with higher cefotaxime hydrolysis over ceftazidime, and Lys-240 (SHV-4, SHV-5) correlating to a concomitant increase in ceftazidime activity.

It is of high importance to note that mutations yielding an advantageous increase in relative activity is in fact a double-edged sword: the broader substrate specificity afforded by substitutional changes from the classical enzymes, extended-spectrum β-lactamases suffer from lowered catalytic efficiency. TEM-1 is a wonderfully efficient enzyme[153]; kinetic studies of extended-spectrum TEMs -3, -5, -9, and -10 reveal they only exhibit 0.4 to 2.2% of the specific activity of the classical TEM-1 enzyme.[154] In nature, bacteria compensate for this grave loss in catalytic efficiency by pushing the metabolic production of these broader β-lactamases into overdrive. To do this, more efficient promoter-possessing genes such as TEM-2 are 4 to 30 times more efficient than TEM-1, making it the likely progenitor of the later ESBL evolutions.[154,155] Hybrid promoters produced from the portions upstream of the TEM-6 gene related to

insertion sequence IS1 can also increase expression efficiency. Enzyme hyperproduction by way of new combinations of promoter elements can play a fundamental role in increasing resistance; hyperproduction of SHV-1 enhances resistance to ceftazidime and aztreonam.[156]

The genes for TEM- and SHV-type ESBLs are typically encoded by large, multiresistant plasmids thought to carry associated virulence factors that can aid bacterial colonization and dissemination.[157] Interestingly, and perhaps as a result, strains producing ESBL often also produce TEM-1,[158] potentially to compensate for the loss in activity concomitant with substrate spectrum expansion. Yet this often reduces the effectiveness of β-lactam-inhibitor combination treatments, as in the example of *E. coli* expressing TEM-3, TEM-7, and SHV-4, but also TEM-1 thus reducing or completely nullifying synergistic effects of ceftazidime with added inhibitor sulbactam. The majority of SHV-type derivatives exhibit the ESBL phenotype, and one variant, SHV-10, which possesses a glycine 130 to serine substitution, is reported to be inhibitor-resistant.[159] Importantly for purposes of enzyme-substrate behavior prediction, the Ser140Gly mutation appears to override the strong ESBL phenotype seen in SHV-type enzymes with the Gly238Ser and Glu240Lys mutations. SHV-type ESBLs though mainly seen in *K. pneumoniae* have also been observed in *Citrobacter diversus, E. coli*, and *P. aeruginosa*.[160–163]

It is believed that fluctuating selective pressure from multiple β-lactam agents within an institutional setting are responsible for ESBL incidence rather than selection by a single agent.[151] Though *E. coli* and *K. pneumoniae* are largely the genetic reservoirs

for TEM-type ESBLs, their spread to other Gram negatives is occurring with increasing frequency with reports in *Enterobacteriaceae* such as *Enterobacter aerogenes*, *Morganella morganii*, *Proteus mirabilis*, *Proteus rettgeri*, and *Salmonella* spp., as well as non-*Enterobacteriaceae* Gram negatives (e.g., TEM-42 in *P. aeruginosa*; TEM-17 in *Capnocytophaga ochracea*).[101,164–168]

2.3.2 Genetic methods of antibiotic resistance detection

Since its inception in 1985, polymerase chain reaction (PCR) has proven to be a powerful technology for the precise detection of specific gene sequences. This tool can be used for the identification of pathogens and characterization of resistance and virulence factors, shedding light on not just etiology but also phylogeny for classification purposes. As such, the detection of the presence of resistance genes can provide crucial evidentiary support for antimicrobial therapies in the clinic, and many techniques exist for this purpose. However, there exists a strong *caveat emptor* of admonition: the confirmed presence of a resistance gene within a clinical sample does not necessarily portend treatment failure.[169] Additionally, there are many challenges in the genetic detection of resistance determinants, including: false-positive results due to silent gene or pseudogene amplification; low sensitivity on mixed flora samples due to PCR inhibition; susceptibility to contamination with extraneous or residual nucleic acids; generation of false-negatives due to primer binding site mutations; unwieldiness in screening for new resistance mechanisms in general (especially ones due to highly varied point mutations).[170–172]

Here we will briefly mention a few developed methods providing greatest utility for the genetic detection of antibiotic resistance.

PCR (polymerase chain reaction). This very common standard methodology can be applied to colony hybridization for the detection of OXA-type ESBL. DNA from positive isolates is extracted, PCR amplified using OXA-specific primers, and digested using restriction endonucleases; restriction fragment sizes are compared to distinguish groups of OXA-related genes. Though this technique does not directly identify specific OXA genes present, it can distinguish between ESBL and non-ESBL OXA-type genes.

PCR-Restriction Fragment Length Polymorphism (PCR-RFLP). This is one of the simplest methods most commonly used to detect SHV derivatives by identifying the specific mutation at peptide position 238.[173] The extracted DNA is first amplified by PCR, then digested with restriction enzyme *Nhe*I to detect the G to A nucleotide change that gives rise to the G238S amino acid substitution. This substitution is common in many early variants of the SHV-type ESBLs.

PCR-Single-Strand Conformational Polymorphism (PCR-SSCP). Able to detect single base mutations within the bla_{SHV} gene[174,175], this test first generates a 475-bp amplimer using oligonucleotide primers internal to the coding sequence of the bla_{SHV} gene, then is digested with restriction enzyme *Pst*I. Fragments are run on a 20% denaturing polyacrylamide gel, and the electrophoretic pattern of the digested

amplimer fragments can be used to identify SHVs -1 through -5, and SHV-7. Combining PCR-SSCP and PCR-RFLP can allow for the identification of a total of 17 SHV genes.[176]

Ligase Chain Reaction(LCR). LCR can be used to identify DNA sequences by a single base pair difference. This method uses a thermostable ligase and four oligonucleotide primers complementary to the target sequence that hybridize adjacent to each other. Subsequent amplification will only occur if there is no base mismatch, which allows the ligase to act to produce an amplifiable sequence. LCR is performed by first denaturing the target DNA containing the bla_{SHV} gene, then allowing biotinylated primers to bind, detecting mutations at four positions. An enzymatic reaction with NADPH-alkaline phosphatase allows for detection readout. Because this detection methodology identifies single base pair differences, new oligonucleotides must be designed for every suspected single nucleotide polymorphism (SNP), posing a great feasibility challenge for practical implementation of LCR into clinical workflows.

Sequencing. Nucleotide sequencing is the fall-back standard method to determine presence of a specific β-lactamase gene. Many methods exist for this purpose, but high skill is required for processing and reading of sequencing autoradiographs.[177] Next-Generation Sequencing (NGS) holds great promise in providing resistance gene detection in a timely manner[178], though it is outside the scope of this dissertation.

2.3.3 Considerations in the genetic detection of ESBL in Gram negatives

The proliferation of new subtypes within each ESBL family giving rise to an ever-increasing number of variants poses a gargantuan challenge to genetic methods of ESBL mediated resistance detection as these methods face inherent limitation in their ability to encompass the full range of ESBL morphs. As such, the identification and monitoring of ESBL by genetic methods should be reserved for reference laboratories receiving difficult-to-type strains often exhibiting complex resistance. For molecular epidemiological purposes, PCR-RFLP is viewed as one of the most appropriate techniques for the most common ESBL types,[179] as type-specific PCRs combined with PCR-RFLP can cover a number of TEM, SHV, and CTX-M subtypes.[176,180–182] Importantly, as phenotypic methods face difficulties from variable levels of resistance expression, genotypic methods carried out in reference laboratories should accompany phenotypic assessment, especially to discern any discrepancies which may arise between the two.[183] Still, direct sequencing remains the gold standard for identifying any unknown amplification products of a given reaction. As the automation of running and analysis of sequence gels advances, this provides an expansive method for determining any resistance gene or mutation.[184]

2.4 Phenotypic detection of ESBL

2.4.1 Clinical & Laboratory Standards Institute (CLSI) Laboratory Guidelines.

Documents provided by CLSI have for many years provided laboratories with comprehensive, up-to-date standards for antimicrobial susceptibility testing. Items

covered by the guidelines include most relevant drugs to test, report updates on specific organisms, quality control measures for assurance in accuracy and reproducibility of results, MIC breakpoints and interpretive criteria for disk diffusion zone measurements.[185],[186] The M2 document provides performance criteria for disk diffusion tests and the M7 document details performance criteria for MIC testing. These two documents address testing of common, rapid-growing aerobic bacteria (e.g., staphylococci, enterococci, Enterbacteriaceae, and specific species of Pseudomonas, Acinetobacter, *Burkholderia cepacian, Stenotrophomonas maltophilia, Vibrio cholerae, Haemophilus influenzae, Neisseria gonorrhoeae, Streptococcus,* and *Neisseria meningitidis*). The M100 is a supporting document containing supplemental tables with recommended drugs for testing and reporting, interpretive breakpoints, and quality control ranges.[186] The M11 document details culturing and testing methodologies for anaerobic bacteria, such as agar and broth microdilution for MIC determination.[187]

CLSI Breakpoint Methodology. Breakpoint determination or MIC interpretive criteria for new antimicrobials, organisms yet to be characterized, or modifications to previous criteria are established as outlined by the CLSI publication (document M23-A2) based on four types of required data: (1) establishment of the new antimicrobial agent's MIC performance in wild-type isolates that lack known resistance mechanisms, and comparisons with MIC performance in strains of isolates that have known resistance mechanisms affecting the antimicrobial agent's drug class; (2) examination of pharmacokinetics of the drug in body fluids and tissues of healthy

patients, and comparisons with the examination of pharmacokinetics of the drug in body fluids and tissues of in patients with infections of various types; (3) pharmacokinetic studies (empirical evidence with the option of mathematical modeling) to enable the observation of peak serum level of the drug and its potential maintenance at levels above proposed MIC breakpoints (especially useful for β-lactams and glycopeptides); (4) exhaustive review of clinical and bacteriological response data collected over large clinical trials performed regarding a new antimicrobial agent to substantiate potential U.S. Food and Drug Administration (FDA) approval.

2.4.2 Gold standard techniques for ESBL determination

To address this need, the standards for testing established since the early days of resistance incidence rely on several methods which will be described in this section.

Double-disk synergy test (DDST). The inception of this test began in epidemiological studies on the spread of ESBL-producing Enterobacteriaceae in French hospitals in efforts to distinguish observed cefotaxime resistance as due to ESBL production or cephalosporinase overproduction.[188] This test is based on the synergy between a third-generation cephalosporin and clavulanate. The two are placed at a certain distance from each other on a lawn of petri dish cultured from isolated single colonies derived from clinical samples and are examined after an overnight period.

Hyperproduction of cephalosporinase can confound results attempting to pinpoint ESBL presence; the use of a fourth-generation cephalosporin (cefepime) that is less easily inactivated by cephalosporinase than ESBL can therefore improve the detection of synergetic effects with clavulanate. Similarly, specific detection of ESBL over β-lactamase classes capable of hydrolyzing both third-generation cephalosporins and carbapenems (metallo-β-lactamases) can be performed by the inclusion of EDTA to chelate essential metal ions in the synergetic test alongside clavulanate[189].

ESBL Etest. These tests are designed to quantify the synergy between extended-spectrum cephalosporins and clavulanate. They contain gradients of cephalosporin either alone on one end of the strip or in combination with clavulanate on the other end. Positive results are determined by a MIC ratio of 8 or more (three or more two-fold dilution steps) with clavulanate, the appearance of a rounded "phantom" zone below the lowest antibiotic concentration, or a deformation of the inhibition ellipse. The latter two indicate the likely presence of ESBL production. ESBL detection in the presence of metallo-β-lactamases can be determined using Etests containing EDTA and comparing the inhibition zones corresponding to similar MIC dilution zones as the typical Etest. Interpretation of these results can be variable and requires training for higher accuracy, and suffers from a 30% failure rate.[190]

Combination Disk Method. This method involves measurement of the inhibition zones around a cephalosporin disk compared to the same disk containing clavulanate. A zone expansion of 50% or a difference of 5 mm or greater between the two

diameters are considered positive for ESBL production. The presence of clavulanate may result in an enlarged inhibition zone (5 mm or more) for ESBL-producing organisms in comparison to a smaller inhibition zone (1 mm or less) in AmpC overproducers.

Distinguising from cephalosporinase overproduction (AmpC). The standard DDST cannot provide distinguishing information between cephalosporinase overproducers and ESBL producers. As a result, in ESBL producers, a modified Etest performed on cloxacillin-containing agar will show positive results (MIC ratios 8 or greater) for an Etest strip containing the cefepime-clavulanate combination. In contrast, ESBL non-producers will show non-interpretable results for Etest strips comtaining cefepime-clavulanate or cefotaxime-clavulanate without the presence of cloxacillin in the media.

Automated methods. Two prominent automated MIC determination systems are the VITEK 2 ESBL test (bioMérieux, Marcy l'Etoile, France) and Phoenix ESBL test (Becton Dickinson, Sparks, MD, USA). These systems both rely on the bacterial growth response to a panel of expanded-spectrum cephalosporins (cefepime, cefotaxime, ceftazidime) with or without clavulanate. Turbidimetric measurements are made at regular intervals following inoculation, and a computerized system compares the proportional reduction of cell growth between wells containing the cephalosporin alone or with clavulanate to determine ESBL status. Broth microdilution testing may determine MICs of cephalosporins for producers and often

correspond to inhibition zones from disc diffusion test methods within the range of resistance producers (0.5-2 mg/L), yet may still result in clinical failures; thus, reliable detection still remains of high importance.[191,192]

Though the standard methodologies outlined above do provide high reliability in susceptibility testing, MIC determination, and often also bacterial species identification, they suffer from the requirement of culturing, and can only be carried out in specialized, central laboratory spaces with highly trained personnel to operate sophisticated equipment, and have expertise in interpretive determination which is not always apparent (as in the case of inhibitory zones using DDST). Rather than solely relying on turbidimetric measurement, rapid determination can be aided by the use of chromogenic substrates that quickly produce measurable and sometimes visual readout in a more convenient format. In the next section we will detail the chromogenic substrates that have been developed as part of a toolkit for newer methods of phenotypic AMR detection.

2.4.3 Newer methods in phenotypic detection

Chromogenic cephalosporins. While the rate of hydrolysis of β-lactam compounds can be monitored by measuring the loss of absorbance at 235-260 nm (indicative of lactam bond cleavage), this method suffers from poor analytical sensitivity due to a few main factors: a) small molar extinction coefficients of the substrate (< 1000 M^{-1} cm^{-1}), b) short optical path lengths in microtiter assay plates (< 1 cm), and c) other components that share the same absorbance range (e.g., proteins).[193] Chromogenic

substrates provide much higher extinction coefficients in comparison, often enhancing sensitivity one to two orders of magnitude. Further, chromogenic substrates are by definition within the visible range, making easy visual assessment a feature for higher concentration samples.

Chromogenic substrates are designed by taking advantage of the cephem core's β-lactam ring opening mechanism as a trigger: intramolecular bond rearrangement will release "reporters" (chromogens or small molecules capable of downstream reaction) if the 3-position of the cephem ring is a methyl halide. CENTA (3-(4-nitro-3-carboxyl-phenylthiol)-methyl-(6R,7R)-7-(2-thienyl-acetamido)-ceph-3-em-4-carboxylate) is one such substrate (**1** in Fig. 2.3). Upon hydrolysis, this substrate releases 2-nitro-5-sulfanylbenzoic acid, which has an absorbance peak at 405 nm. PADAC (**2** in Fig. 2.3) is a similar substrate that releases N,N-dimethyl-4-[(Z)-pyridin-2-yldiazenyl]aniline which has a maximum asorbance peak at 550 nm.[193–195] An interesting synthetic compound (**3** in Fig. 2.3) releases ethanioic S-acid when hydrolyzed, resulting in a thiolate that can reduce tetrazolium salt in solution to form an insoluble colored precipitate as a cleavage activity readout.[196,197]

Release of leaving groups on the 3-methyl of the cephem ring does not necessarily occur in a concerted fashion with regard to β-lactam ring opening.[198,199]
In the case that the 3-methyl within the cephem ring is designed as a continued alkene, without a halide but rather a carbon, designed chromogenicity may still occur due to a bathochromic shift in maximal absorbance also spectrophotometrically

measurable. (**4**-**9** in Fig. 2.3) shows styryl groups at the 3-methyl position functionalized with various chromophores. One of the best-known of this type is Nitrocefin (**4** in Fig. 2.3) which displays a striking visual color change from an initial maximal absorbance at 386 nm that shifts to 482 nm upon hydrolysis. As Nitrocefin is cleavable by classical β-lactamases such as TEM-1, toward an attempt to make a diagnostic substrate that can differentiate ESBL, compound (**9** in Fig. 2.3) has been designed to possesses an oxyimino modification similarly to third-generation cephalosporins. Nitrocefin (**4** in Fig. 2.3) and Chromacef (**8** in Fig. 2.3) have been used in screening studies of metallo-β-lactamase inhibitors, highlighting the usefulness of these chromogenic reporter substrates in drug discovery.[200–204]

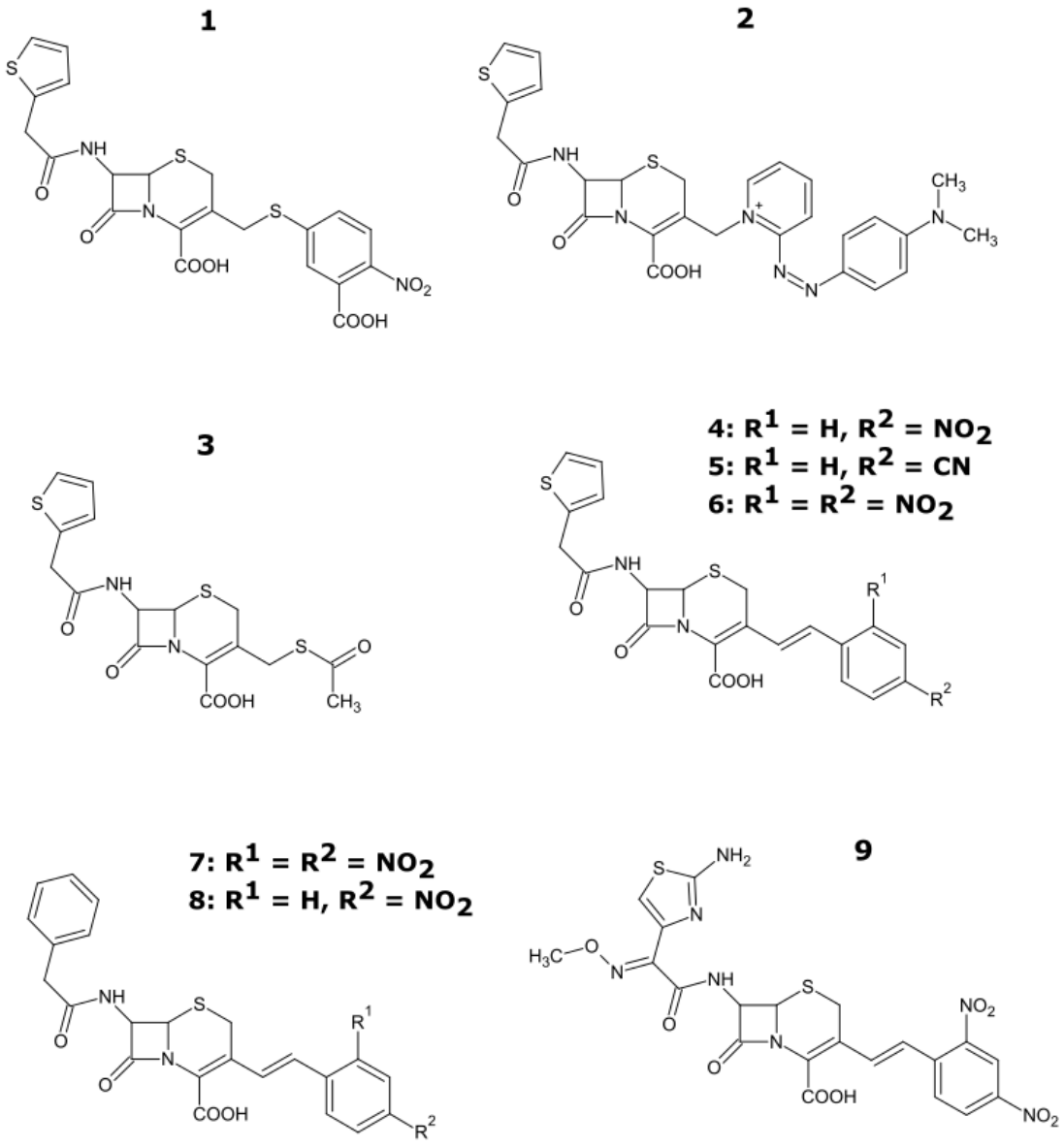

Figure 2.3. Chromogenic cephalosporin substrates for phenotypic detection.

Chromogenic substrate containing media. These are considered the latest generation in the "rapid" culture-based detection as they are designed to combine ESBL detection with organism identification. Engineered chromogenic substrates build up as colored dyes in bacterial colonies expressing the target hydrolytic enzyme of

interest, allowing easy visual differentiation of (potential) pathogens from non-expressers within a culture plate.[205] However, chromID ESBL displays low specificities (11-44%) due to interference from the growth of AmpC-overproducers,[205–208] and Brilliance ESBL suffers from similar complications. The incorporation of cloxacillin in EbSA demonstrated significant suppression of AmpC producers and higher specificities over chromID ESBL (78% versus 44%).[206] Growth of non-ESBL K1-OXY penicillinase overproducing *K. oxytoca* and some OXA-30 penicillinase-producing *E. coli* also compromises the specificities of chromID ESBL and Brilliance ESBL. CHROMagar CTX which specifically targets CTX-M-type ESBLs showed 100% sensitivity; however, this was reduced to 64% when non-CTX-M-type ESBLs were recovered. Notably, only 14% of AmpC producers grew on CHOMagar CTX versus 76% on chromID ESBL, indicating suppression of AmpC producers in the former media.[209]

Currently commercially available chromogenic media include chromID ESBL (bioMérieux), Brilliance ESBL (Oxoid Ltc., Basingstoke, UK), and CHROMagar ESBL (CHROMagar, Paris, France). These are offered as either ready-to-use media, or a proprietary selective mix that is added to a commercial product such as CHROMagar Orientation agar base. CHROMagar also provides a product for detection of CTX-M producers, the CHROMagar CTX supplement that is added to the CHROMagar ECC base. These media have been shown to have almost uniformly high sensitivities (>95%).[14,206–209]

Antibiotics as selective agents. Media selectivity can be tuned using antibiotic combinations at certain concentrations to suppress the growth of Gram positive organisms and yeasts in order to select for ESBL producing Gram negatives. Though full combinations are not entirely disclosed by the company, cefpodoxime (4 μg/ mL) is the cephalosporin of choice to select for ESBL producers and is incorporated into the chromID ESBL and Brilliance ESBL products. The reason for this choice is because cefpodoxime is known as a reliably selective substrate for most TEM- and SHV-derived ESBLs, and is preferred for its effectiveness in being a single selective substrate; this is in constrast with ceftazidime which must be combined with cefotaxime for the reliable selection of CTX-M producers and ceftazidime-hydrolyzing TEM-type variants. The superior performance of these commercial chromogenic media containing cefpodoxime has been demonstrated over MacConkey agar supplemented with ceftazidime (2 μg/ mL).[208,208] However, the growth of cephalosporinase overproducers (AmpC and K1) has presented much challenge in the use of cefpodoxime disks, and as a result cefpodoxime concentration must be carefully chosen as MICs in the indeterminate ("ambiguous window") range of 2-4 μg/ mL for *E. coli* cannot rule our resistance mechanisms arising from changes in porin or AmpC overexpression states.[210] The chromID ESBL product also incorporates additional antibiotics to allow better inhibition of adjunct flora.[14]

Efficacy of chromogen combinations to differentiate genera/ species. ChromID and Brilliance ESBL contain chromogens that can differentiate *E. coli* from a grouping of similar bacteria known as KESC (*Klebsiella, Enterobacter, Serratia, Citrobacter*).

One of the chromogens in chromoID ESBL is a substrate for β-glucuronidase that is highly specific to *E. coli* (indicated by development of colonies that are pink to burgundy in color); Brilliance ESBL agar contains chromogens that can also detect β-galactosidase/ β-glucuronidase co-producers (indicated by the development of blue colonies, pink colonies if β-glucuronidase-only producer). Presence of KESC colonies are indicated by a green/ green-blue (due to β-galactosidase expression) or brown-green (due to β-glucosidase expression) on Brilliance and chromID ESBL. Additional supplementation with tryptophan can enable the detection of *Proteus, Morganella, and Providencia* (PMP grouping) that appear tan with a brown halo due to tryptophan deaminase production.

2.5 Enzymology

2.5.1 Motivation

Enzymes from the different Ambler classes of β-lactamases hydrolyze β-lactam antimicrobial agents at different rates. Because β-lactamases can be encoded chromosomally, on plasmids, or encountered alongside a variety of resistance mechanisms that may be co-expressed, resistance determination via phenotypic measurement may give rise to a range of MIC values due to this continuum of antimicrobial activities. In this dissertation, resistance determination is evaluated through the characterization of readout modalities (e.g., colorimetric or fluorescence signal accumulation, enzyme-coupled redox activity for amperometric measurement, photon counts quantified by spectroscopic methods) in their responses to β-lactamase enzymatic activity. Because the majority of studies herein presented involve either

direct or indirect biochemical observation, enzyme activity will be expressed using the international convention in terms of unit activity (international unit, abbreviated as IU or just U), which is defined as the amount of enzyme that catalyzes the hydrolysis of one micromole of substrate (the β-lactam benzylpenicillin, also known as Penicillin G) per minute under standard conditions (aqueous buffer of neutral pH 7.0 at 25 °C).

2.5.2 Rationale

In light of bringing our biochemical studies toward clinical relevance as established by gold standard methodologies, we must attempt to translate enzyme unit activity into terms approximating MIC. To do this, we will take into account substrate conversion rates described by enzymatic unit activity, and consider MIC as the primary determining factor of substrate transport equilibrium at the bacterial outer membrane-external media interface.

Minimum inhibitory concentration (MIC) is defined as the lowest concentration of an antimicrobial agent (i.e., the β-lactam antibiotic in question) that will inhibit the visible growth of a microorganism after overnight incubation. Given this definition, it can be logically deduced that the microorganism in question would achieve growth at an antimicrobial concentration just below the MIC threshold. Therefore, we may conceive of this threshold as representing the cumulative whole of the microorganism's resistance activities that enable its replicative survival. Though this is not the case in actuality (as natural pathogens are known to harbor multiple

resistance mechanisms), for demonstrative purposes we may model an initial translation of our *in vitro* biochemical analysis to clinical MIC under the assumption that 100% of the resistance activity present in a given test sample is due to β-lactamase mediated inactivation of β-lactam antibiotics present in the test media (e.g., the cleavage of β-lactam derivative by ESBL). This implies that in order to survive, the theoretical bacterial strain (acquiring 100% of its resistance through ESBL production) must inactivate the antibiotic at the same rate at which it diffuses into the periplasm (site where the PBP targets reside), which is proportional to the extracellular concentration given by MIC, as described by Fick's law of diffusion.

2.5.3 Modeling

Mathematical characterization of antibiotic penetration into the bacterial periplasmic space where they encounter ESBL can be related in terms of rates of drug diffusion across the outer membrane.[211,212] These uptake rates are described as a permeability coefficient (P in nm s^{-1}) according to Fick's law of diffusion:

$$V = P \; x \; A(S_o - S_i)$$

where V is the rate of diffusion (nmol mg $cells^{-1}$ s^{-1}), A is the area of the cell surface per unit weight (nm^{-2} mg $cells^{-1}$) through which antibiotic diffusion (flux) occurs, and S_o and S_i are the substrate concentrations (nmol mL^{-1}) outside and inside the bacterial outer membrane, respectively, with their difference representing the concentration gradient.

We can think of the flux based on concentration gradient (determined by MIC) to be less than or equal to the rate of enzymatic product turnover as both processes would

be at equilibrium for the bacterial cell to maintain cell wall synthesis and survival. Therefore, assuming overall MIC (bulk media) remains constant, the flux over time would equal product generated over the same period of time. Product generation can therefore be considered in terms of IU, which would depend on the enzyme's expression level to provide enough inactivation activity to match or overtake the antibiotic MIC.

Chapter 3: Design and synthesis of ESBL detection substrates

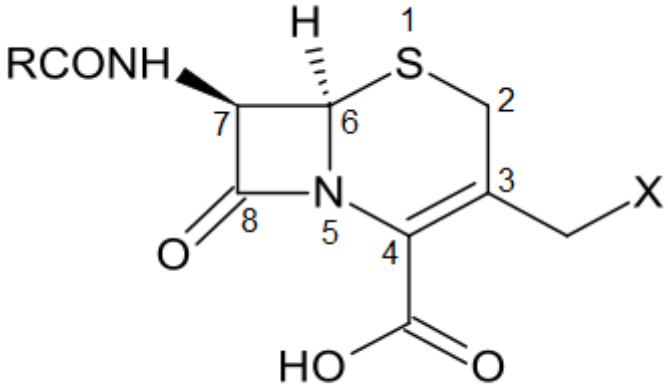

Figure 3.1. Cephem ring, structure, and positional numbering.

Cephalosporins are a class of β-lactam antibiotics related to penicillins that also share the same four-membered β-lactam ring. Whereas penicillins possess a five-membered thiazolidine ring, the classical cephalosporins possess a six-membered dihydrothiazine (cephem) ring fused to the β-lactam. The cephem ring also possesses a double bond between the 3- and 4- position carbons, and a 4-position carboxylic acid (which becomes a carboxylate at physiological pH, aiding with solubility in aqueous environments).

3.1. Rational design of detection substrates

Basis. Our design of synthetic detection substrates is based on one well-known critical feature of the cephalosporin stereochemistry: the opening of the β-lactam ring in cephalosporins is associated with release of a suitable leaving group on the side chain at the C-3 position (Figs 3.1, 3.2).[198] Attack on the β-lactam ring by a

nucleophile can occur as a base-catalyzed hydrolysis event (as seen *in vitro*), or as an acylation of the carboxypeptidase/ transpeptidase enzymes responsible for peptidoglycan synthesis *in vivo* (thus constituting the primary mode of action of β-lactam antibiotics). Example leaving groups liberated in the breaking of the β-lactam ring are acetate, pyridine, and azide groups corresponding to antibiotics cephalothin, cephaloridine, and any 3-(azidomethyl)cephalosporin.[37,213,214] An important property of the cephem structure that enables leaving group liberation is the functional group substitution at the 3-position which allows stabilization of a negative charge upon β-lactam ring opening, an event occurring from breaking of the 1-8 amide bond. This negative charge stabilization aids an increase in the overall reactivity of the β-lactam ring, a property that can enhance interactivity of the cephalosporin with bacterial transpeptidase enzyme targets.[106] Thus, previous substrates designed to assay the activity of β-lactamase have been based on the detection of leaving groups as the decomposition product. In this work we describe the employment of glucose and SERS-active benzylic molecules as leaving groups enabling ESBL reporting.

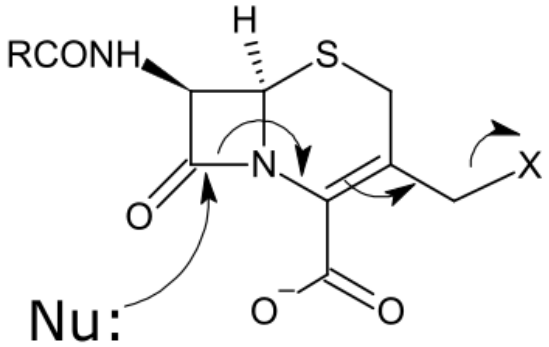

Figure 3.2. Electronic rearrangement within the cephem core structure following ring opening via nucleophilic attack, resulting in the expulsion of leaving group X.

Leaving groups. Upon opening of the β-lactam ring, it is known that the departure of the leaving group is spontaneous.[198] The electronic details describing the exact nature behind this spontaneous departure was initially thought to be reliant on a concerted mechanism based on quantum mechanical studies.[215] However, leaving group elimination as a concerted event has since been countered by subsequent studies suggesting this is not a necessary case.[199] By spectrophotometrically following PADAC (pyridine-2-azo-4'-(*N',N'*-dimethylaniline) cephalosporin), an intermediate wherein the leaving group is still attached at the C-3 position post-ring opening has been observed. Though this implies PADAC's leaving group is a poor one, further evidence suggests the departure of known good leaving groups such as acetoxy or pyridinium may be concerted in the presence of certain enzymes.[199]

Side chains. (Here we will refer to the side chains at the C-7 position as "amide" and the ones at the C-3 position as "leaving group".)

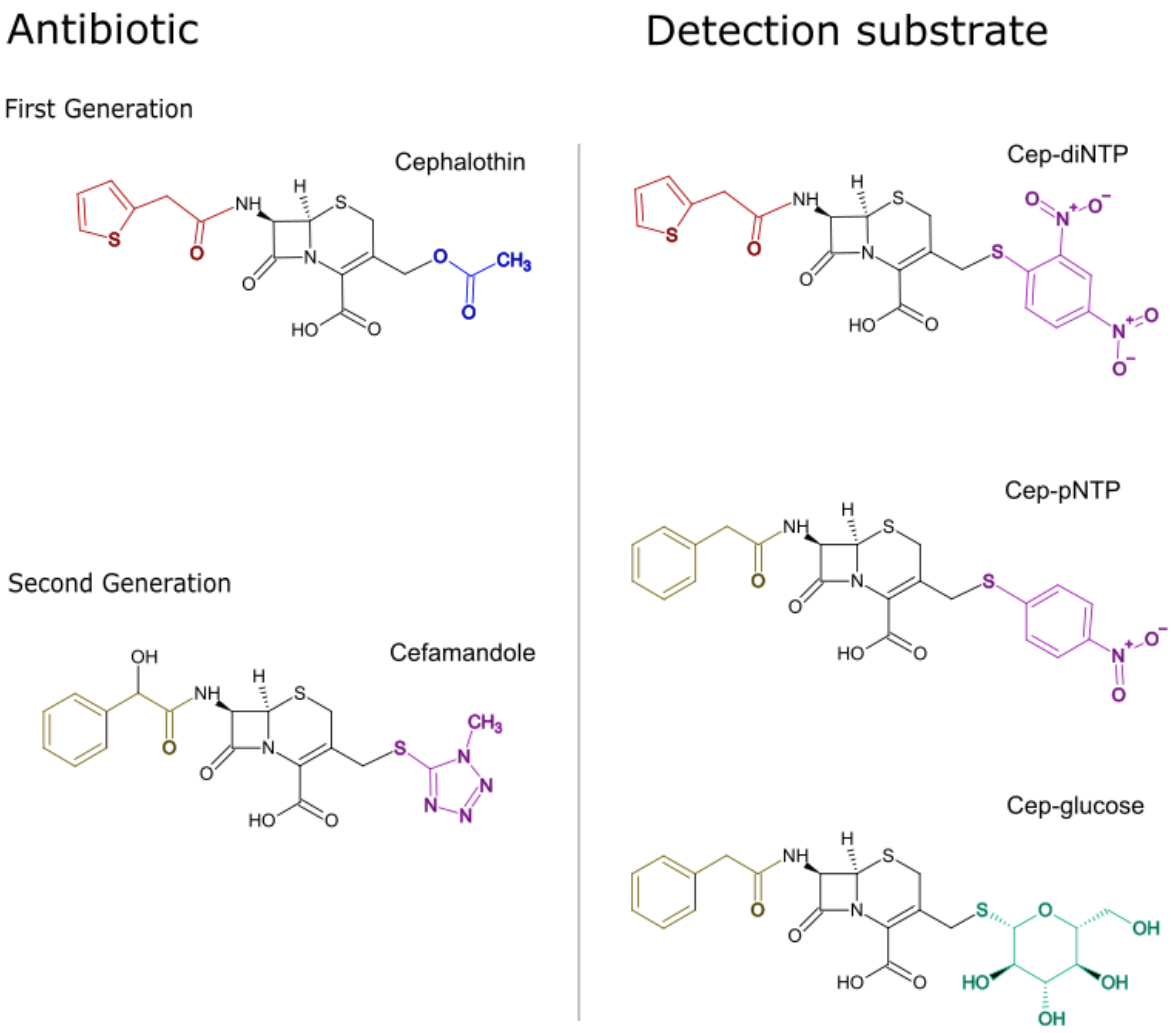

Figure 3.3 Antibiotics of different generations and their side chains corresponding to synthesized detection substrates. (Magenta colored groups indicate SERS-active or potentially SERS-active moieties).

Our design of detection substrates was done with the intention that each would roughly correspond to a certain cephalosporin generation, and thus display specificity for narrow- versus extended-spectrum β-lactamases. As we can see in Fig. 3.3, the first-generation antibiotic cephalothin has a (2-thienylacetyl)nitrilo moiety (red) as

the amide side chain and an acetoxymethyl moiety (blue) as the leaving group. We correspondingly designed our Cep-diNTP SERS-active reporter substrate to have the same amide side chain as the first-generation cephalothin. Second-generation cefamandole has a (R)-mandelamido amide side chain and a N-methylthiotetrazole leaving group side chain; we began with a starting material (Fig. 3.5, 4-Methoxybenzyl-3-chloromethyl-7-(2-phenylacetamido)-3-cephem-4-carboxylate, or "PMB-Cep-Cl") with a similar (benzylacetyl)nitrile side chain which is not exactly the same as the first-generation cephalosporin but would perhaps experimentally show similar enzyme specificities (this has been confirmed in the following studies). Important to note is that the leaving groups also play an important role in the enzyme reactivity and thus also antimicrobial effects of cephalosporin antibiotics.[216] Thus, it is necessary to acknowledge that changing the amide side chain in design approach for engineering enzyme specificity is inherently incomplete. Though Cep-pNTP and Cep-glucose share the same amide side chains, the differing leaving groups may also play a critical role in specificity in enzyme active site binding. Further, as thio-glucose constitutes a poor leaving group whereas pNTP constitutes a good leaving group, the observable kinetics of spontaneous leaving group expulsion will be discussed in a later section (see: 3.4.2 and 5.3).

3.2 Reaction mechanisms

3.2.1 Nucleophilic substitution (S_N2 reaction)

One step in the organic synthesis of our ESBL detection substrates relies on nucleophilic substitution of an alkyl halide at the 3-position of the cephem ring. Functionalization of the 3-carbon substituent with small molecules capable of ESBL reporting as the leaving groups occurs in an S_N2-concerted displacement in which a potent nucleophile displaces the halide (Scheme 3.2.1). The nucleophile we employ for this scheme is the thiolate anion produced from 1-thio-β-D-glucose upon deprotonation with diisopropylethylamine (DIEA), a hindered base. The displacement of chloride results in 3-position carbon substituent functionalization of the cephalosporin core structure with thio-glucose as the R2 variable group. In terms of solvent choice, to enhance the reactivity of the nucleophile, an aprotic solvent is employed. Though solvent polarity is not as critical to S_N2 reactions, the use of acetone allows facile solvation of the PMB-Cep-Cl starting material.

3.2.2. Finkelstein exchange.

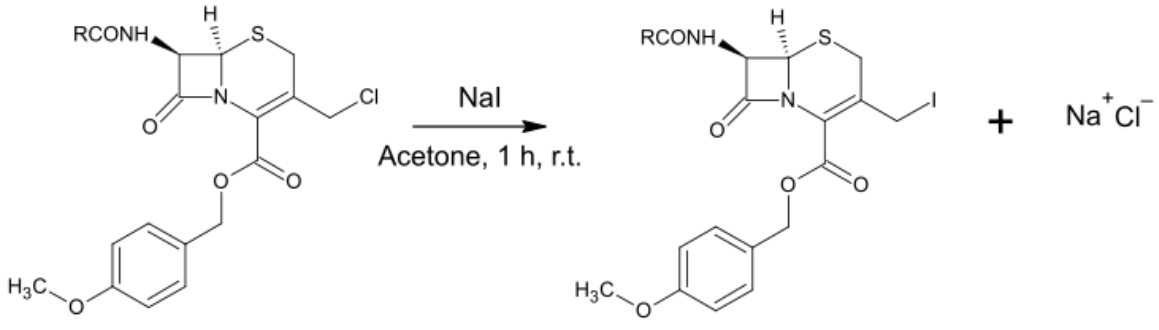

Figure 3.4. Finkelstein exchange for lower-temperature alternative synthesis

Nucleophilic substitution can be carried out by alkoxides as well as thiolate-bearing ones. However, as alkoxides are less nucleophilic than thiolates, the S_N2 reaction can be enhanced by the inclusion of a Finkelstein exchange step in which the chloride leaving group is replaced by iodide. In our synthesis scheme, reaction of the PMB-Cep-Cl starting material with sodium iodide (NaI) for approximately one hour in acetone at room temperature is sufficient for completion of the Finkelstein exchange; displaced chloride anions form an ionic salt with the sodium cations and precipitate out of solution as NaCl is insoluble in acetone, thereby excluding chloride from participating in any potential secondary reactions. However, alternative to inclusion of the Finkelstein exchange step, an increase in temperature from RT to reflux conditions is sufficient for halide displacement and alkylation by thiolate to occur.

3.3 Synthesis of Cep-glucose: Reaction schemes and spectral verification

3.3.1 Cep-glucose synthesis scheme

All solvents were purchased from Fisher Scientific, 4-methoxybenzyl-3-chloromethyl-7-(2-phenylacetamido)-3-cephem-4-carboxylate was purchased from TCI, and 1-thio-β-D-glucose was purchased from Cayman Chemical Company.

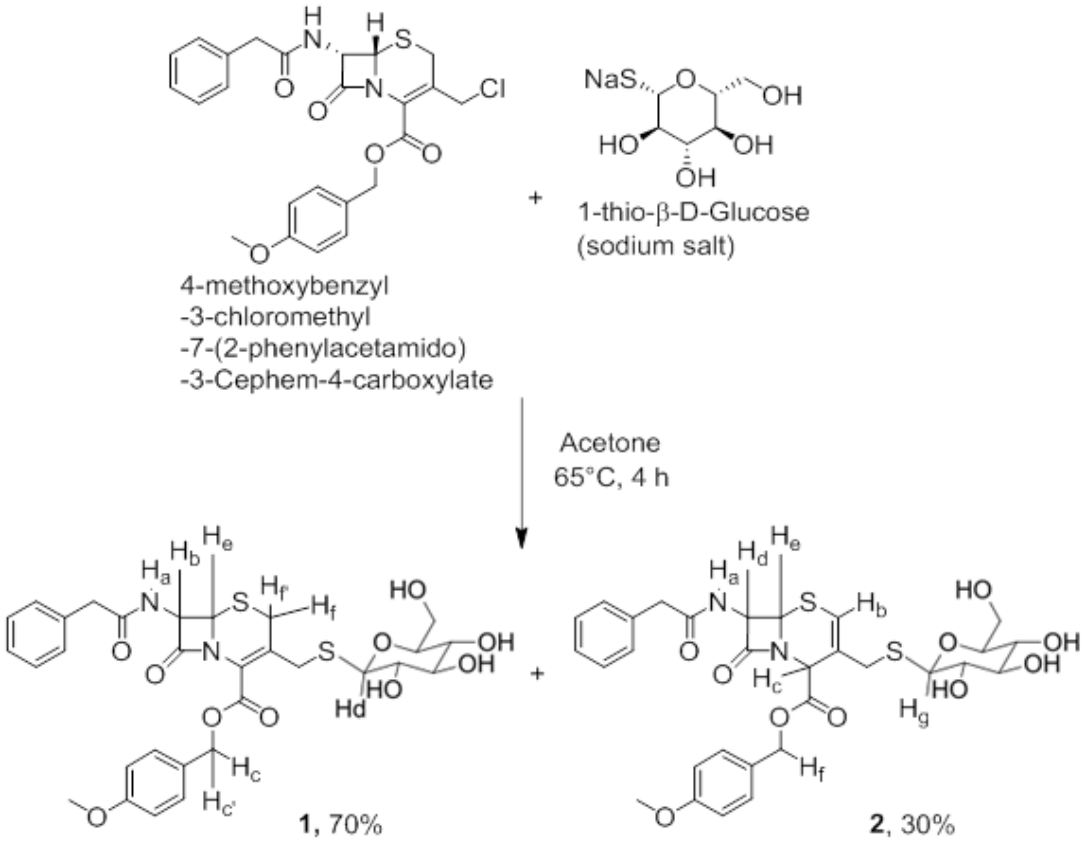

Figure 3.5. Synthesis scheme and product ratios of the PMB-protected Cep-glucose substrate (PMB-Cep-glucose).

4-Methoxybenzyl-3-chloromethyl-7-(2-phenylacetamido)-3-cephem-4-carboxylate (400 mg, 0.200 mmol, 1 eq) was dissolved in 15 mL of acetone and 1-thio-β-D-glucose (sodium salt, 132 mg, 0.6 mmol, 3 eq) was added to the reaction flask and the resulting suspension stirred at reflux for 4 h. The reaction mixture was cooled to room temperature and the solvent removed *in vacuo* to yield an orange oil. The crude mixture was dissolved in dichloromethane (10 mL) and washed with water (10 mL). The aqueous layer was extracted twice with dichloromethane (15 mL) and the combined organic extracts were dried over $MgSO_4$. The solvent was evaporated *in vacuo* to yield a dark, sticky brown-orange oil. Compounds **1** (Rf = 0.32) and **2** (Rf =

0.29) (Fig 3.5) were purified on a silica column with dichlormethane-methanol (94:6) to yield 89 mg (0.14 mmol, 70%) and 38 mg (0.06 mmol, 30%) of products **1** and **2** respectively and a total product yield of 24%. Noting this relatively low yield, inclusion of the Finkelstein step (Fig 3.4) in an alternate lower-temperature synthesis can improve the yield.

*For spectral verification data of Compounds **1** and **2**, please see Appendix I (^{1}H NMR, ^{13}C NMR, COSY, IR, MS).*

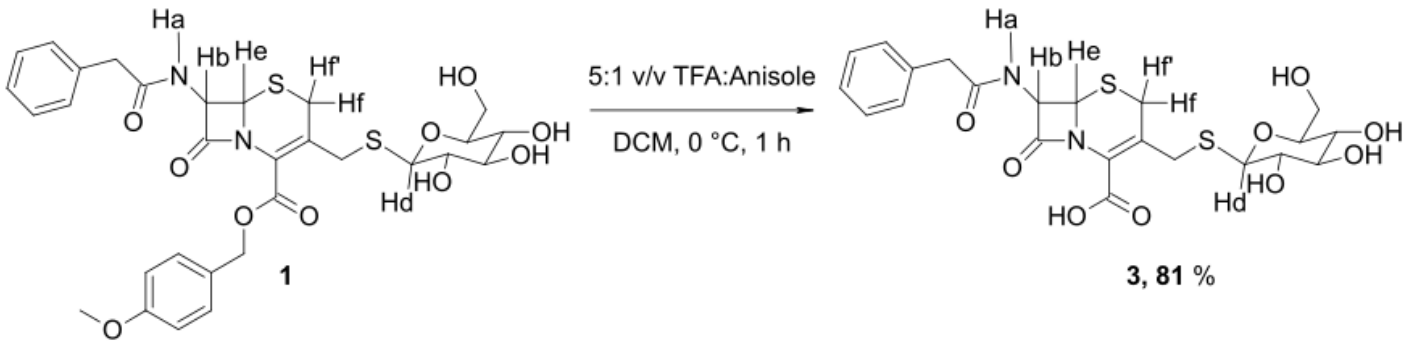

Figure 3.6. Synthesis of Cep-glucose (Compound **3**) from PMB-Cep-glucose (Compound **1**).

In a 1-dram vial, dried **1** (35 mg, 0.052 mmol) was dissolved in 1 mL of DCM and a Teflon coated stir bar was added. The solution was cooled to 0 °C in an ice bath before adding 2 mL of a 5:1 v/v TFA:anisole solution. After stirring for 1 h at 0 °C, the vial was taken from the ice bath and the solvent removed *in vacuo*. To remove anisole as well as deprotection byproducts, the residue was dispersed in 3.5 mL cold Et_2O and then centrifuged at approximately 6000 rpm in a benchtop IEC clinical centrifuge for 10 min. The supernatant was decanted and the solid residue then resuspended in another 3.5 mL of cold Et_2O and the centrifugation-decantation

process repeated an additional three times. Residual Et_2O was removed from the resulting white solid *in vacuo* to yield cep-glucose, **3**, (22 mg, 0.042 mmol, 81%) as an off-white powder (Figure 3.6). The ^{1}H-NMR shows and HPLC-MS support > 90 % product purity, however some NMR invisible trifluoroacetate impurities are present as evidenced by trifluoroacetate complexed ions observed by mass spectrometry. Samples of **3** were stored in a -20 °C freezer until needed.

*For spectral verification data of Compound **3**, please see Appendix II (^{1}H NMR, ^{13}C NMR, COSY, IR, MS).*

3.4 Cep-glucose substrate-enzyme kinetic studies with ESBL

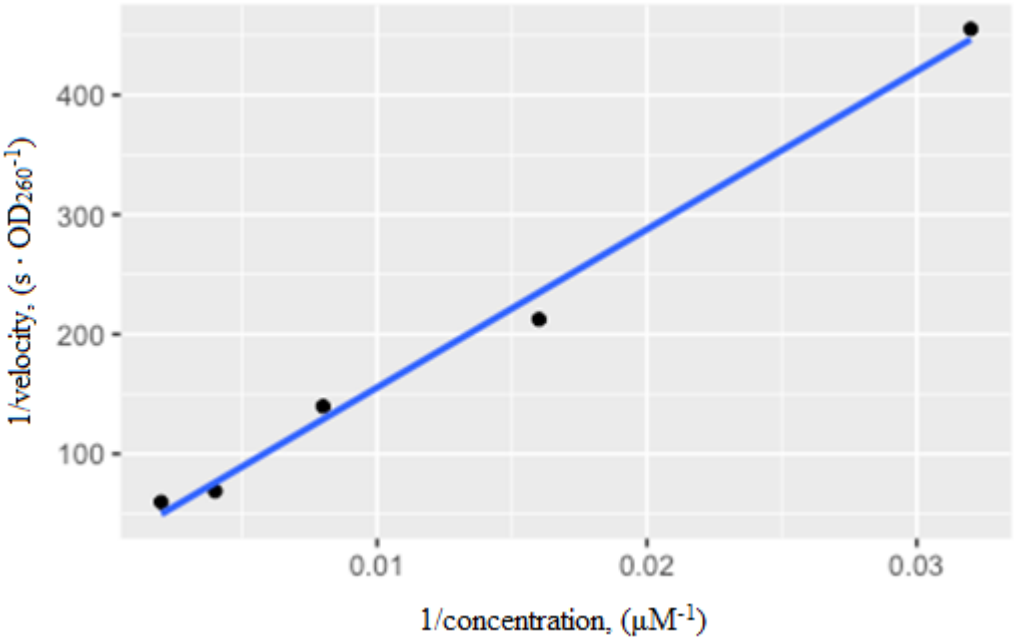

Figure 3.7 Lineweaver-Burke curve to obtain enzyme-substrate kinetics for ESBL and the Cep-glucose substrate

3.4.1. Lineweaver-Burke kinetic determination

Varying concentrations of Cep-glucose (500 μM, 250 μM, 125 μM, 62.5 μM, 31.25 μM) were incubated with 100 mU/ mL ESBL in triplicate (equating to an E_{tot} of 3.77 nM, assuming an average molecular weight of 35 kDa, and a specific activity of 5.87 U/ mg as reported by AG Scientific). Optical absorbance (OD_{260} corresponding to the C-N bond in the β-lactam ring[217]) was recorded every seven seconds over 15 minutes to observe a decrease in OD indicative of enzymatic hydrolysis of the Cep-glucose substrate resulting in a ring-opened cleavage product.

The graph above (Fig. 3.7) shows the Lineweaver-Burke plot of inverse velocity ($s \cdot OD_{260}^{-1}$) against inverse concentration (μM^{-1}). Velocity was computationally determined as the fastest change in OD_{260}; absolute values of the negative change (decrease) in OD were used in this calculation to obtain a positive velocity.

3.4.2 Mass spectroscopy on reaction products

Methods. Cep-glucose (**3**) (262 μg, 500 nmol, 1 mM final concentration) (Fig 3.8) was dissolved in 0.5 mL 0.1 M phosphate buffer (pH 6.5). ESBL (1 U/ mL final concentration) was then added and the reaction incubated at 25 °C. At 1 h and 16 h, a 150 μL aliquot was removed and purified through an Amicon Ultra centrifugal filter (regenerated cellulose, 3000 MWCO) in a benchtop centrifuge at 14,000 RCF for 15 min. The filtrate was collected and analyzed by LC-MS.

Results. LC-MS analysis of the reaction between Cep-glucose and ESBL revealed the presence of a ring-opened intermediate (**4** in Fig 3.8), both confirming Cep-glucose's function as a substrate for ESBL and thio-glucose as a poor leaving group. The following study was initially performed to confirm release of thio-glucose following ESBL-mediated ring opening. Though MS confirmed the presence of a weak signal indicative of thio-glucose, it also revealed the appearance of a strong signal corresponding to the mass of the ring opened intermediate with thio-glucose still attached, and, importantly, the disappearance of the initial Cep-glucose peak. Details of the experiments are described below.

Interestingly, though spontaneous elimination of thio-glucose appeared to produce minimal signal of the product in the initial observations, the presence of Ellman's reagent (DTNB) appeared to facilitate higher levels of thio-glucose release, as evidenced by DTNB capture to produce a mixed disulfide. (*Please note: Further experimental methods and LC-MS analysis detailing the elimination behavior of thioglucose and its capture in the presence of Ellman's reagent to produce the mixed disulfide are located in Appendix III.)*

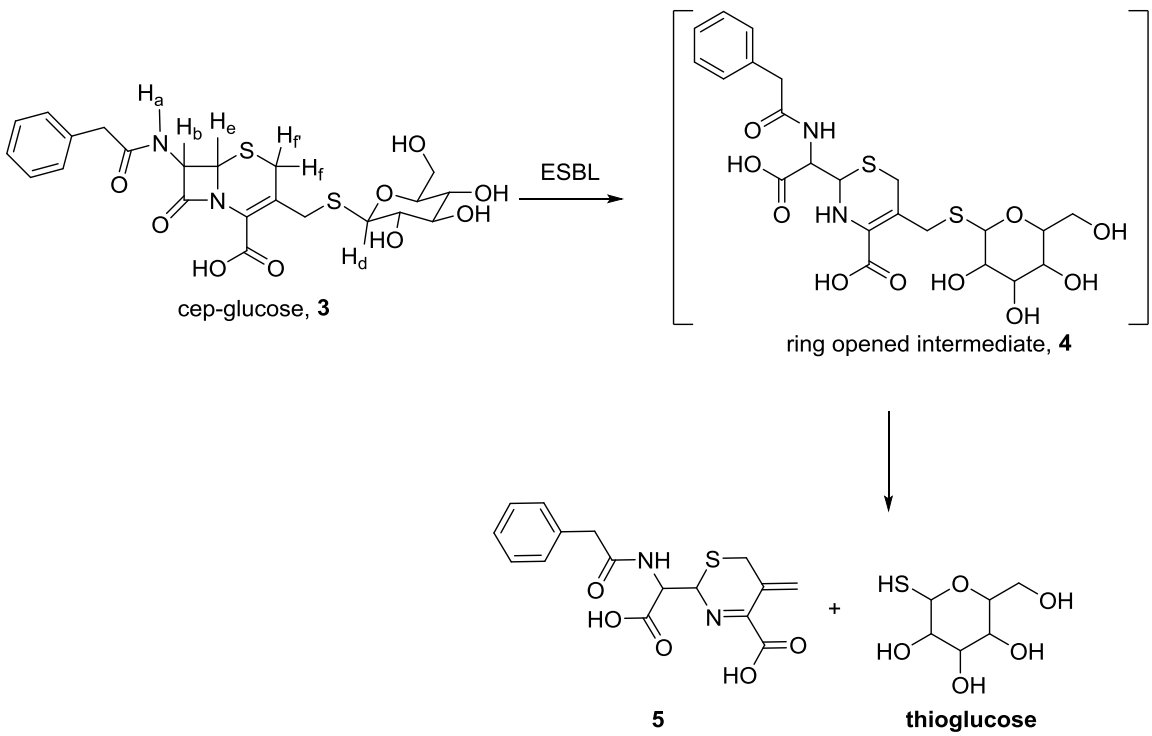

Figure 3.8. Biochemical schematic representing ESBL cleavage, formation of the ring-opened intermediate, and spontaneous release of thioglucose.

The chromatogram is similar for both the t = 1 h and 16 h samples, both showing two peaks with retention times 7.28 and 7.78 (Figs 3.9a and 3.10a) with a notable absence of any peak at 8.06 min which was previously assigned to cep-glucose (**3**) (See Appendix III, Fig A.3.3). The mass spectra for both the 7.28 and 7.78 min peaks give only one mass corresponding to the ring opened intermediate (**4**), appearing as [**4** – $H]^-$ with calculated *m/z* 543.1113. The two different retention times and identical masses are consistent with two isomers of **4**.

Free thioglucose is invisible by UV so is not observed in the chromatogram. However, upon analysis of the solvent front for the 1 h sample, a very weak signal corresponding to [thioglucose – $H]^-$ was observed in the mass spectrum (Fig. 3.9b).

The other product of thioglucose elimination, **5**, was not observed, likely due to its inherent instability. Similar results were obtained when the same experiment was run in 0.1 M phosphate buffer adjusted to pH 8.0.

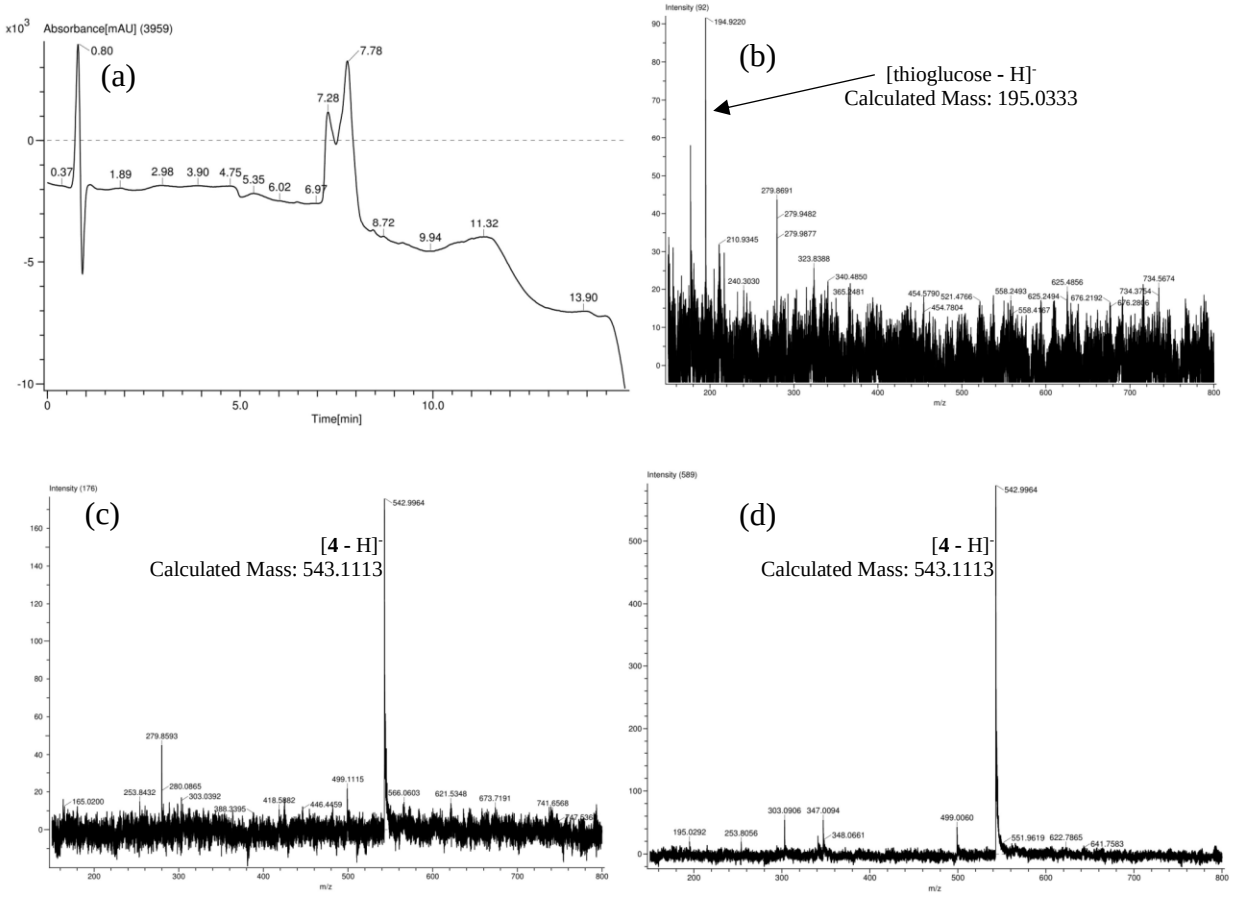

Figures 3.9a-d. LC-MS analysis of the reaction between cep-glucose and ESBL at t = 1h. a) Chromatogram showing two peaks at 7.28 min and 7.78 min. b) Mass spectrum corresponding to solvent front showing a very weak signal corresponding to thioglucose. c) Mass spectrum corresponding to the 7.28 min chromatogram peak showing only the ring opened intermediate **4**. d) Mass spectrum corresponding to the 7.78 min chromatogram peak showing only the ring opened intermediate **4**.

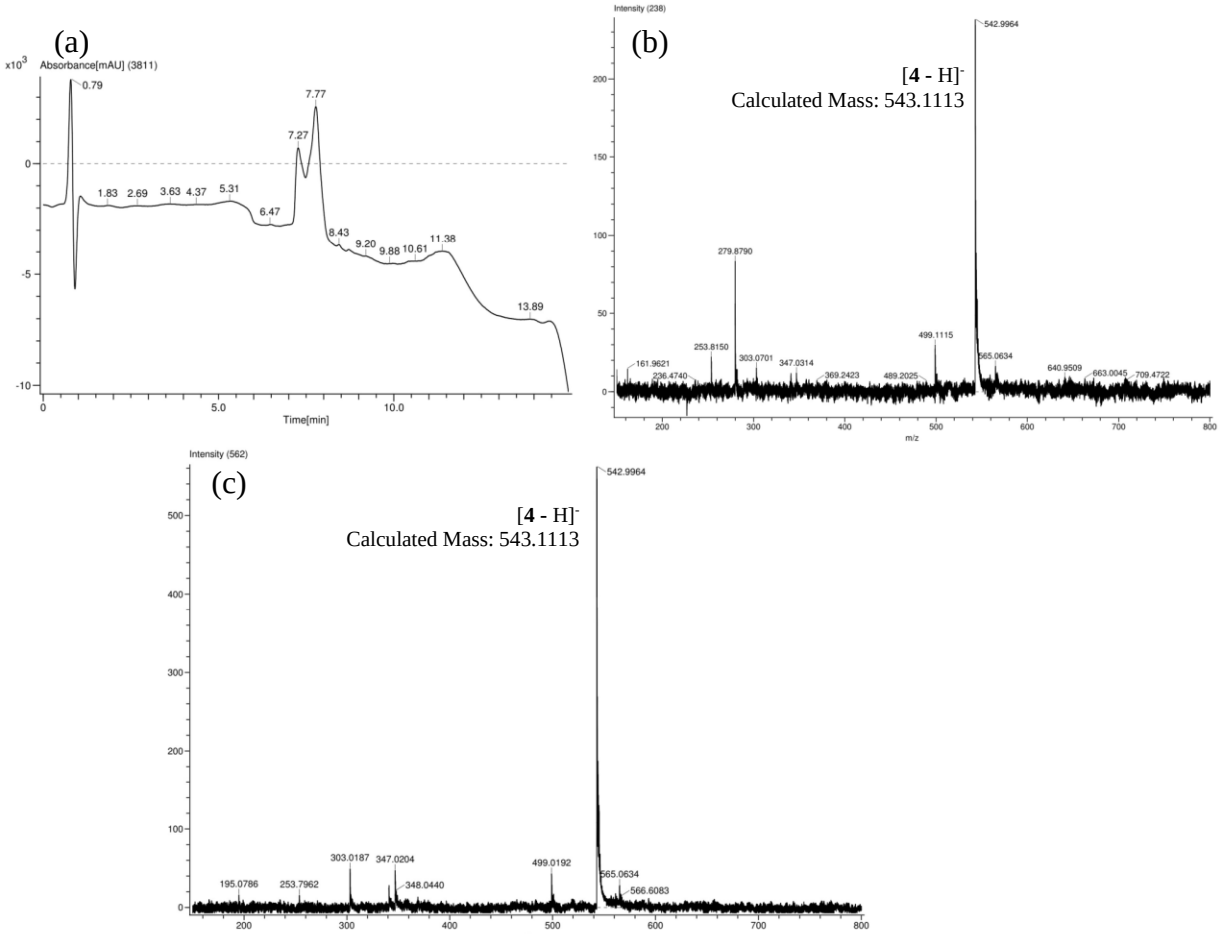

Figures 3.10a-d. LC-MS analysis of the reaction between cep-glucose and ESBL at t = 16h. a) Chromatogram showing two peaks at 7.27 min and 7.77 min. b) Mass spectrum corresponding to the 7.28 min chromatogram peak showing only the ring opened intermediate **4**. d) Mass spectrum corresponding to the 7.78 min chromatogram peak showing only the ring opened intermediate **4**.

3.4.3. Functional specificity studies.

Methods. (For detailed scheme of colorimetric chemical readout please see section 4.3.2.) In a 96-well standard clear microplate, two-fold dilutions of Cep-glucose substrate (625 μM to 39.0625 μM) and 250 μM DTNB (final concentrations) were diluted into 100 μL of 0.1 M PB (pH = 6.5). To each triplicate, either 200 μU/ mL of TEM-1 or ESBL was added, and optical absorbance (OD_{412}) was measured every 30 seconds for 30 to 45 minutes. Resulting were analyzed in MATLAB.

Specificity of substrate for ESBL. Kinetic studies using Ellman's reagent as a readout for thio-glucose release were performed to examine the cleavage of Cep-glucose as a substrate of different β-lactamase enzymes both classic, non-ESBL and ESBL. From the data shown, Cep-glucose is only cleaved by the enzyme blend containing ESBL (Fig. 3.12), and not by purified TEM-1 (Fig. 3.11), a non-ESBL classical β-lactamase. Therefore, Cep-glucose discriminates the presence of ESBL from non-ESBL-types.

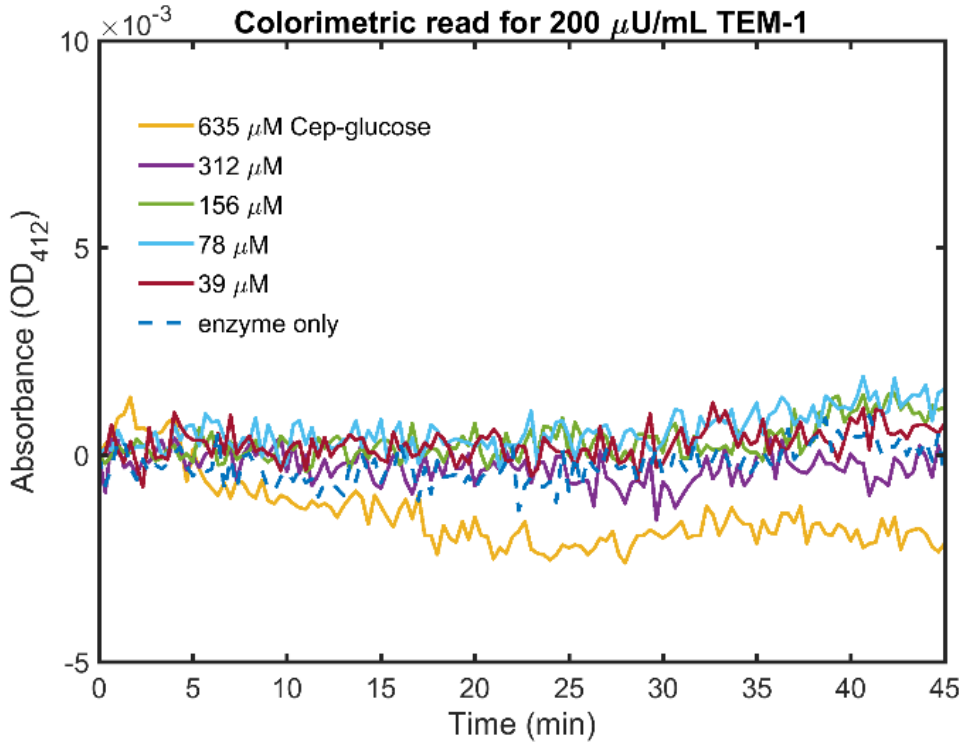

Figure 3.11. The Cep-glucose substrate is not cleaved by TEM-1, a non-ESBL. Varying concentrations of Cep-glucose substrate are diluted into 0.1 M PB (pH = 6.5) containing 250 μM DTNB. TEM-1 narrow spectrum beta-lactamase (final concentration 200 μU/ mL) is added just prior to reading using an absorbance plate reader. Absorbance change at 412 nm is monitored every 30 seconds over the course of 45 minutes to measure generation of TNB production resulting from thio-glucose released upon substrate cleavage. No discernable change is observed for any concentration tested. (Note the y-axis scale; zoomed plot provided to illustrate signals are only noise.)

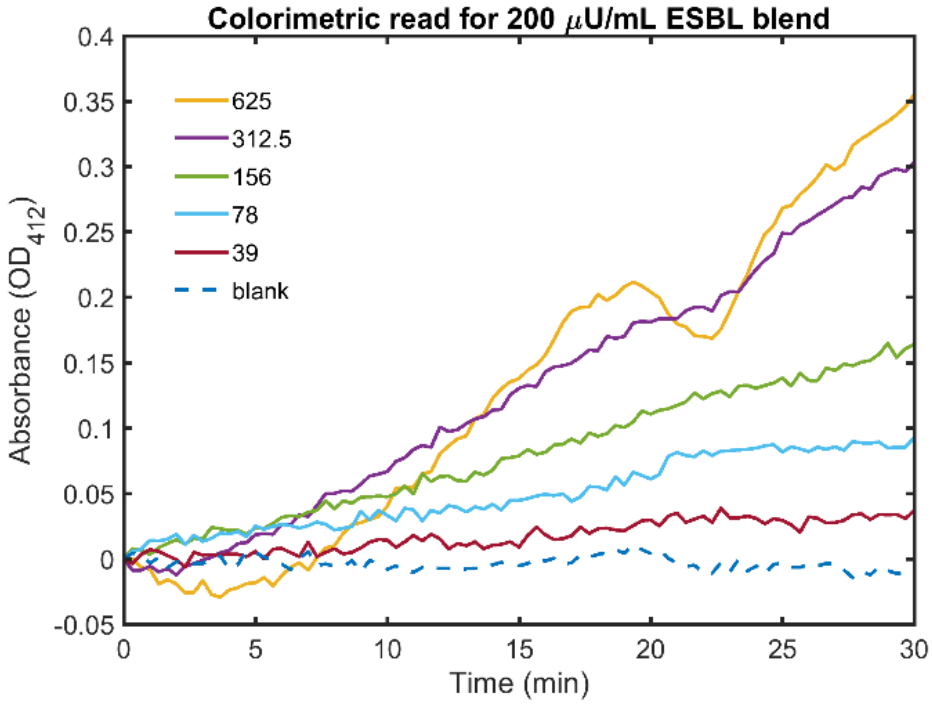

Figure 3.12. The Cep-glucose substrate is cleaved by the commercial ESBL blend. Varying concentrations of Cep-glucose substrate are diluted into 0.1 M PB (pH = 6.5) containing 250 μM DTNB. ESBL enzyme (final concentration 200 μU/ mL) is added just prior to reading using an absorbance plate reader. Absorbance change at 412 nm is monitored every 30 seconds over the course of 45 minutes to measure generation of TNB production resulting from thio-glucose released upon substrate cleavage. Increasing signals are observed with higher concentrations of cep-glucose substrate in a dose-response manner, indicating that cep-glucose is an ESBL substrate.

3.5. Synthesis schemes of SERS-active reporters

3.5.1. Cep-pNTP

Cep-pNTP full IUPAC name: 7-(2-phenylacetamido)-3-[(4-nitrophenyl)thiomethyl]-3-cephem-4-carboxylic acid.

Synthesis of Cep-pNTP was performed using exactly the same procedure as Cep-glucose, with the replacement of thio-glucose with the same molar equivalent of 4-

nitrothiophenol (pNTP, purchased from Sigma Aldrich). *(For details, please see synthesis of Cep-glucose in previous section 3.3.)*

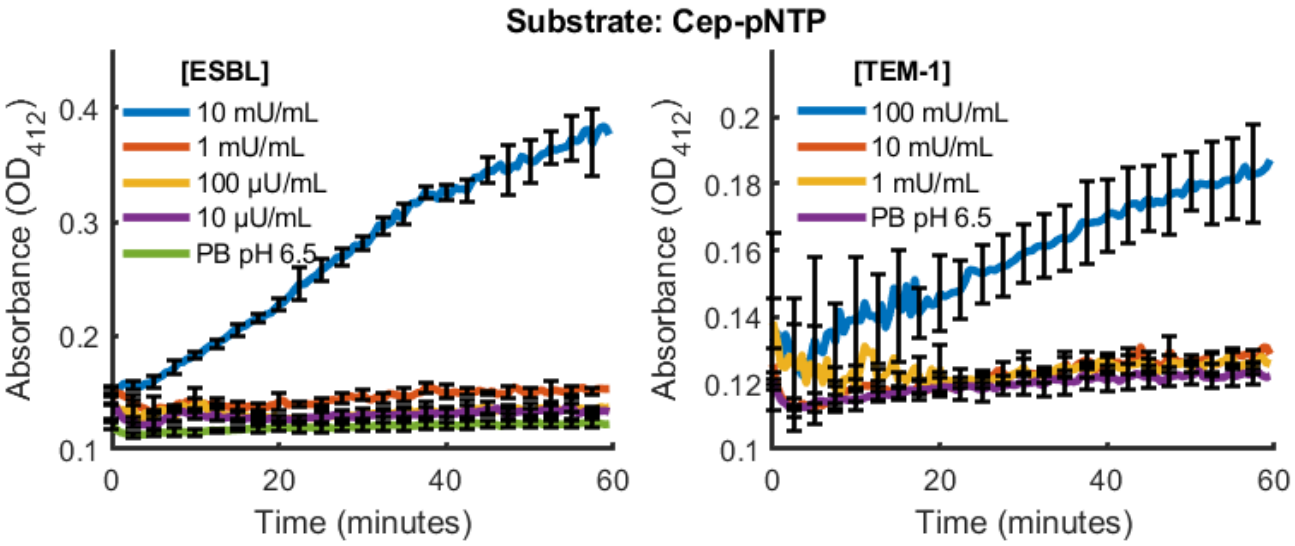

Figure 3.13. Plate reader absorbance kinetics monitoring Ellman's reagent as a function of time to verify the release of pNTP from Cep-pNTP in the presence of ESBL and TEM-1. 250 µM cep-pNTP with equimolar DTNB is prepared in 0.1 M PB (pH = 6.5) to which varying unit concentrations of either ESBL or TEM-1 are added and absorbance at 412 nm is monitored every 30 seconds over one hour. A signal increase is only observed at 100 mU/ mL TEM-1 whereas 10 mU/ mL ESBL produces a much higher absorbance signal. The comparatively lower activity of TEM-1 on Cep-pNTP and higher cleavage activity by ESBL indicate Cep-pNTP is more specific to ESBL than TEM-1. (Note the difference in y-axis scales.)

Functional verification & specificity of Cep-pNTP. Similarly to previous experiments in Chapter 4 with Cep-glucose, the liberation of a free thiol by hydrolysis of the beta-lactam ring should yield a reactive residue detectable by Ellman's reagent to produce a mixed disulfide and a colored TNB molecule whose absorbance peak can be measured at 412 nm. From this, we also observe that at equal unit concentrations, ESBL is much more effective at hydrolysis of Cep-pNTP than is TEM-1, whose signal is indistinguishable from the no enzyme control (PB pH 6.5 only) (Fig. 3.13). Upon verifying Cep-pNTP's biochemical behavior through our previously established

absorbance methods, we may substantiate that its readout activity by SERS rests on the basis of a hydrolytically functional molecule with a good leaving group.

3.5.2. Cep-diNTP

Cep-diNTP full IUPAC name: 7-β-thien-2-yl-acetamido-3-[(2,4-dinitrophenyl)thiomethyl]-3-cephem-4-carboxylic acid

Intermediate (Compound **2**) (6R,7R)-7-amino-3-{[(2,4-dinitrophenyl)thio]methyl}-8-oxo-5-thia-1-azabicyclo[4.2.0]oct-2-ene-2-carboxylic acid)

The synthesis of Cep-diNTP was based on the work of Quotadamo *et al.*[218] The rationale in using the improved synthesis was to achieve higher yield without the deprotection requirement as reported in the publication.

As shown in Figure 3.14, thiol (1,4-dinitrothiophenol, diNTP) was reacted with 7-aminocephalosporanic acid (7-ACA) (Compound **1**) in anhydrous acetonitrile (MeCN) in the presence of boron trifluoride to yield intermediate derivative Compound **2**. Derivative **2** was then directly reacted with 2-(thiophen-2-yl)acetyl chloride in anhydrous MeCN using potassium trimethylsilanolate as a base to yield Cep-diNTP.

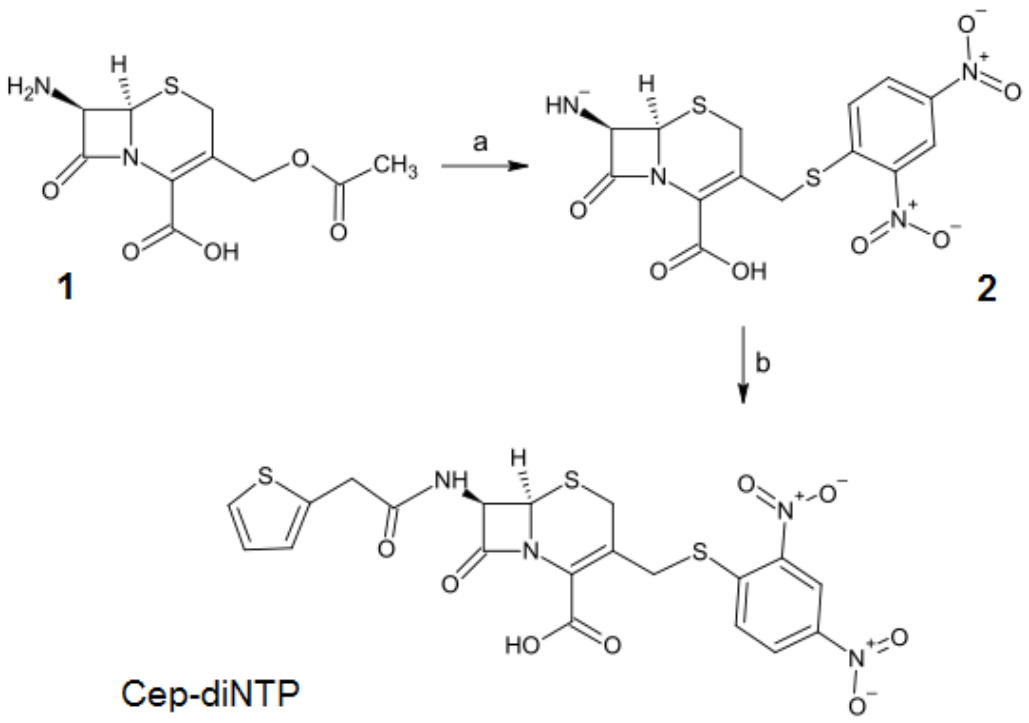

Figure 3.14. Synthesis scheme for Cep-diNTP. a) **1** (7-ACA, 1 equiv.), BF_3 (3 equiv.), MeCN, r.t., 2h; b) 2-thienylacetyl chloride (1 equiv.), potassium trimethylsilanolate (2 equiv.), MeCN, r.t. 1 h, then 50 °C, 2 h.

Functional verification. Cep-diNTP was verified as a substrate of ESBL and non-ESBL TEM-1 using a simple visual test. In 0.1 M PBS, 1 mM of purified Cep-diNTP substrate plus 250 μM DTNB was allowed to incubate with 10 U/ mL of ESBL or 100 U/ mL non-ESBL TEM-1 enzyme. Within one minute, it was observable by visual inspection that both ESBL and TEM-1 produced a highly visible yellow color change whereas the no-enzyme control did not, confirming Cep-diNTP to be a substrate for both ESBL and TEM-1 (Fig 3.15).

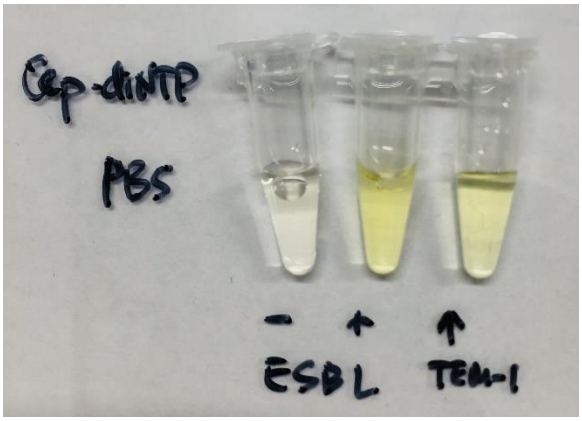

Figure 3.15. Showing visually observable color change upon addition of TEM-1 or ESBL in the presence of Ellman's reagent. All samples contain Cep-diNTP in 0.1 M PBS (pH 7.4). A no enzyme control (left) was compared to the addition of ESBL (middle) and TEM-1 (right); contrasting color changes were visible within 5 minutes.

3.6 Conclusions

Here we have detailed the synthesis of three new synthetic substrates and their design in functioning as different types of reporters of β-lactamase activity (see Chapters 4 and 5). We establish that the specificities can be fine-tuned to a degree in terms of specificity to β-lactamase thereby distinguishing different evolutions of the enzyme. We also characterize the reaction products spectrally (H-NMR, C-NMR, MS, IR) to verify their structure, and determine enzyme kinetics through direct optical measurement. Finally, we also establish the presence of an intermediate of Cep-glucose that persists after ring opening, and show its expulsion behavior is modified in the presence of DTNB.

3.6.1 Future work: Establishing chemistries for easier, higher yield production of more detection substrates with tuned specificity.

We utilize boron trifluoride in efforts to synthesize our Cep-diNTP substrate with a higher yield. Further research into procedures to replicate this method but for the

production of more detection substrates with different reporter moieties as well as different amide side chain determined specificities would be of high utility, especially in looking toward parallelization of array-format testing, or further multiplexing perhaps in a single or few samples.

3.6.2 Future work: Oxidation of the Cephem starting material.

Established procedures in the literature for the oxidation of the PMB-Cep-Cl starting material (either single or double) have shown increased stability[15] and higher yield of the Δ_2-Δ_3 isomer that allows reporter release[219] (shown in the schematic). Future work on our current substrates could be to modify the starting materials to study their stability behavior and synthetic yields, as outlined by Scheme 3.2.3 below.

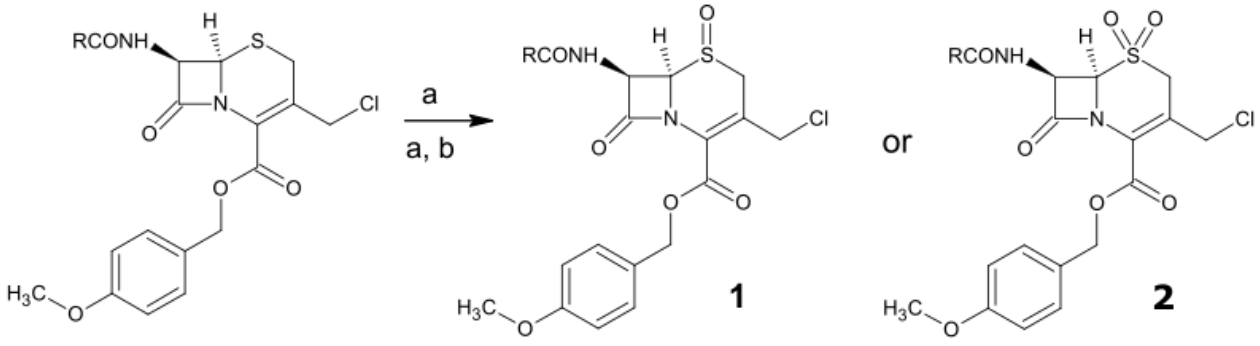

Figure 3.16. (Synthetic plan) Oxidation of the starting material with the use of *m*CPBA; a) *m*CPBA, DCM, 0°C 1 h, r.t. 4 h; b) mCPBA, DCM, 0°C 30 min, r.t. overnight. **1** is produced from (a) only, **2** from both (a) and (b).

Chapter 4: Cep-glucose, a trimodal detection substrate

4.1 Introduction

Bacterial resistance to β-lactam antibiotics continues to grow as their misadministration presents evolutionary pressure that drives bacteria to develop improved resistance enzymes. Known as extended-spectrum β-lactamases (ESBLs), these are capable of hydrolyzing advanced β-lactam antibiotics such as third- and fourth-generation cephalosporins. Phenotypic detection substrates can be used to rapidly identify a cultured patient sample within minutes prior to confirmation by more exhaustive but slower means, critically aiding in the antibiotic stewardship essential in maintaining the effectiveness of not only the cephalosporins but indirectly also the carbapenems, our last-resort β-lactams. To enhance the phenotypic detection arsenal, we have designed an ESBL detection substrate that releases a glucose molecule upon β-lactamase cleavage. Because many forms of detection for glucose exist, the substrate enables ESBL quantification via three modalities commonly found in the clinical laboratory: optical absorbance, for use with the most common microbiology platforms; fluorescence, for enhanced sensitivity; and electrochemistry, which offers the potential for integration into a handheld platform similar to a personal glucometer.

As fluorescence measurement is generally accepted to have higher sensitivities than chromogens, which rely on absorbance spectrophotometry, the development of fluorogenic ESBL substrates has expanded the phenotypic detection repertoire with the promise of lower limits of detection.[15–20] They include substrates that have been

designed to release well-characterized coumarins upon specific cleavage by advanced ESBLs including metallo-β-lactamases (MBLs), an improvement on substrates unable to distinguish β-lactamases with extended-spectrum profiles from narrow-spectrum β-lactamases.[21] Yet, as previously described methodologies require the specialization of a central microbiology lab facility, resistance testing away from equipped central labs, such as in disadvantaged regions, remains an underserved goal. Electrochemical readouts of a redox-active reporter have the potential to meet this paradigm, as demonstrated by the handheld personal glucose meter (PGM). Amperometric measurements of hydrolyzed Nitrocefin have also been reported in the literature, with the aim toward rapid detection of ESBL activity using disposable screen-printed sensors with small sample volumes to enable robust, field-portable instrumentation.[26] The description of multiple methods for resistance readout is promising as a multi-pronged approach to AMR detection, yet, each of these testing methods requires specific substrates, with each their own optimal readout modality. A single ESBL substrate possessing the versatility to enable different aforementioned readout techniques would democratize AMR testing access, as standard laboratories tend to have equipment for optical absorbance measurement, and more specialized, central laboratories possess fluorescence enabled equipment for sensitive detection (e.g., MicroScan Walkaway). Furthermore, though amperometric AMR detection is uncommon, establishing this methodology holds great promise toward the development of handheld, portable detection modules for use outside of equipped central lab facilities.

Toward the accommodation of a wide scope of previously described detection methodologies, we have developed a new cephalosporin-derived detection substrate (Cep-glucose) capable of multimodal detection by colorimetric, fluorescence, and electrochemical means. Key to this multimodal detection is the use of thio-glucose release as the detection method. Once liberated from the substrate, the reactive thiol moiety of this reporter molecule allows for the conceptualization of any thiol-sensitive chemistries into downstream detection. Further, as thio-glucose is a substrate for glucose oxidase (GOx), established electrochemical detection methods allow for the easy reimagination of PGMs into ESBL quantifying POC detection devices. These important features are further enhanced by the promise of lowered production costs as compared to commercially available substrates, thanks to the ease of synthesis through straightforward thiol chemistry for alkylation and production of Cep-glucose, making it potentially commercializable as a low-cost substrate. Here we demonstrate the use of this new substrate for the phenotypic detection of ESBL activity with colorimetric, fluorescence, and electrochemical readout.

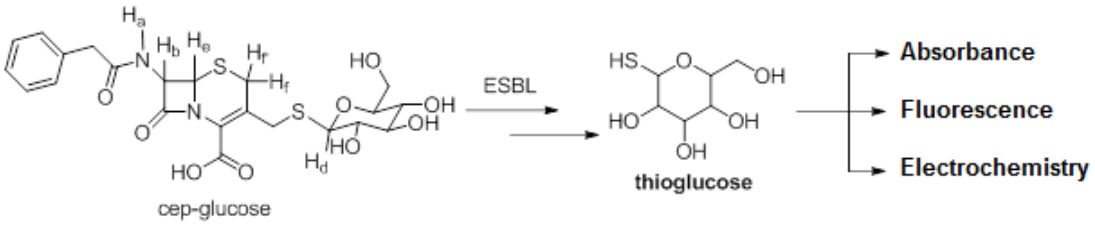

Figure 4.1 Our Cep-glucose detection substrate releases glucose as a trimodal reporter of ESBL-mediated resistance activity. The released thioglucose can act as a signaling molecule for downstream assay integration to enable multimodal readouts (absorbance, fluorescence, and electrochemistry).

4.2 Materials and Methods

4.2.1 Reagents and solutions.

Phosphate buffer (PB; 0.1 M; pH = 6.5) and all solutions were prepared with Milli-Q 18-MΩ water (Millipore purification system) and pH-adjusted with HCl. 4-Methoxybenzyl-3-chloromethyl-7-(2-phenylacetamido)-3-cephem-4-carboxylate was purchased from TCI America. 1-Thio-β-D-glucose was purchased from Cayman Chemical Company. Stock solutions of 50 mM Cep-glucose were prepared by dissolving the purified product in dimethylsulfoxide (DMSO) and aliquots were stored at -20 °C. Working dilutions were prepared by dissolving the stock solution in PB. TEM-1 β-lactamase enzyme was purchased from ThermoFisher Scientific. Extended-spectrum β-lactamase (ESBL) was purchased from AG Scientific (β-lactamase-BS), and has been tested to show hydrolytic activity against a broad range of β-lactam compounds including third, fourth, and fifth generation cephalosporins as well as carbapenems. Due to its reliable cleavage as determined by our enzyme kinetic characterization studies, this ESBL "blend" was used as a standard in this study, as specified ESBLs are not commercially available. 5,5'-Dithiobis-[2-nitrobenzoic acid] (DTNB, Ellman's reagent) was purchased from Sigma-Aldrich and a 100 mM solution was always freshly prepared in MilliQ water and diluted into PB to a final working concentration of 200 μM. Amplex red was purchased from Molecular Probes (Eugene, OR).

4.2.2 New ESBL detection substrate: Cep-glucose

Briefly, Cep-glucose was prepared as follows: 4-methoxybenzyl-3-chloromethyl-7-(2-phenylacetamido)-3-cephem-4-caboxylate (PMB-Cep-Cl) was dissolved in acetone and 1-thio-β-D-glucose was added to the reaction and allowed to stir at reflux for 4 hours. After solvent removal *in vacuo,* the aqueous layer was extracted with dichloromethane to yield the *para*-methoxybenzyl-protected Cep-glucose. Deprotection was performed using standard trifluoroacetic acid deprotection procedures to yield the Cep-glucose detection substrate. Full characterization of the Cep-glucose is presented in the supporting information. For ESBL detection experiments, Cep-glucose was prepared from frozen stocks less than six months old. Moderate degradation in performance for long-term storage and for storage at 4 °C are shown in Appendix IV.

4.2.3 Apparatus.

All electrochemical measurements were carried out on the Model 800B Series Electrochemical Detector (CH Instruments, Inc.) potentiostat interfaced to a PC system equipped with the CHI832B Electrochemical Analyzer version 9.02 software. Zensor TE100 (#ET077-40, EDAQ) screen-printed carbon paste electrodes possessing a Ag/AgCl reference electrode were used for replicates in cyclic voltammetric measurements (CV; scan rate of 100 mV s^{-1}), which were performed at room temperature with a working volume of 100 μL. CV peak heights were determined using eL-Chem Viewer, a freeware package available online (www.lchem.cz/elchemviewer.htm).[220] All spectral measurements (optical density, fluorescence) were performed using the SpectraMax M5 (Molecular Devices)

multiplate reader interfaced to a PC system equipped with the SoftMax Pro 7 software.

4.2.4 Colorimetric assay with Ellman's reagent.

Ellman's reagent reacts with free thiols to form a colored product (absorbance peak at 412 nm) and thus was used to detect the release of thio-glucose upon cleavage of our Cep-glu substrate. Measurements were carried out at room temperature in standard 96-well microplates in a 100 μL volume, with each well containing 200 μM Ellman's reagent and 250 μM Cep-glucose substrate in PB (pH = 6.5).

4.2.5. Fluorimetric assay with Amplex red reagent.

Each 100 μL volume of PB (pH 6.5) contained final concentrations of the following reagents: 10 μM Amplex Red, 0.5 U GOx, 100 μU HRP, and 250 μM Cep-glucose. Just prior to reading, experimental dilutions of ESBL or only PB were added in 10 μL volumes to 90 μL of the previously described solutions. Oxidation of Amplex Red to resorufin within experimental samples was measured at room temperature over the course of 60 minutes at 30 second intervals in standard 96-well flat bottom microplates using the kinetic fluorescent read setting on the microplate reader, with excitation at 530 nm and emission measurement at 590 nm.

4.2.6 Electrochemical assay via HRP enzyme inhibition by thiols

Electrochemical measurements were performed using carbon screen printed electrodes from Zensor (EDAQ). Experiments were performed in a 0.1 M phosphate buffer (pH 6.5) containing 0.5 M KCl to increase the stability of buffer solution against the Ag/AgCl reference electrode. 1.25 mM hydroquinone was used as a

mediator with 12 μM hydrogen peroxide. Each 100 μL reaction volume contained 1 U HRP, which was added after a 15 minute incubation of various dilutions of ESBL with 500 μM of our Cep-glucose substrate and pipetted to mix prior to measurement. CVs were run under a potential range of -0.4 to 0.6 V, a 100 mV/s sweep rate, with a sampling rate of 0.01 V. All samples were run in triplicate using new identical sensors as each replicate. An inhibitor calibration curve with thio-glucose as the inhibitor was produced to relate the current to released thio-glucose upon substrate cleavage following incubation (Appendix V).

4.3 Results and Discussion

4.3.1. Synthesis, verification, and characterization of Cep-glucose detection substrate.

The Cep-glucose molecule is presented in Scheme 4.1. As the state of research on detection of glucose and hydrogen peroxide is mature and reliable, we employed a thiolated form of glucose, 1-thio-β-D-glucose (thio-glucose), as the signaling molecule that is released upon hydrolysis of the substrate by ESBL. Importantly, as thiol chemistry would allow for a simple, one-step synthesis methodology followed by well-established acid-mediated deprotection protocols, we incorporated the thiolate in S_N2 displacement of the halogenated cephalosporin starting material, PMB-Cep-Cl. The starting material was selected based on prior synthesis methodology by van Berkel *et al.*,[219] who produced fluorogenic substrates for the detection of metallo-β-lactamases. Within this context, we expect that the starting

material, through the addition of specific side chains, can be generalized to producing detection substrates cleavable by ESBLs hydrolyzing later-generation (third and beyond) cephalosporins. As compared to Nitrocefin or CENTA, which are cleavable by enzymes that inactivate second-generation cephalosporins, our starting material has a benzyl group where CENTA and Nitrocefin have a thiophene, implying that our Cep-glucose molecule will be more selective. Following synthesis and purification, we verified the structure of our substrate through standard procedural analysis of spectral profiles to confirm the formation of a cephalosporin derivative covalently attached to thio-glucose (see: Appendix I).

Following synthesis of the new Cep-glucose molecule, we examined the adduct's activity as a biochemical substrate for ESBL. Cep-glucose was tested as a substrate for an ESBL blend as well as individual older-generation β-lactamase TEM-1, which are not considered as extended spectrum. The kinetic characterization of Cep-glucose hydrolysis (presented in the Supporting Information) was performed by continuously recording the absorbance variation at 260 nm, as described in previous literature.[171] Using the ESBL blend, I determined that the ESBL and Cep-glucose substrate have a Michaelis constant K_M of 572.65 μM and a catalytic constant k_{cat} of 43.9 s^{-1}, with catalytic efficiency k_{cat}/ K_M to be approximately 0.077 s^{-1} μM^{-1} (V_{max} = 0.1655 s^{-1}, MW estimated as 35 kDa). In contrast to more promiscuous substrates like CENTA and Nitrocefin that are cleavable by nearly all β-lactamases, the starting cephalosporin material is specific for ESBL and is thus not cleavable by narrow-spectrum β-lactamases TEM-1 *(Please refer to Subsection 3.4.3 for details*).

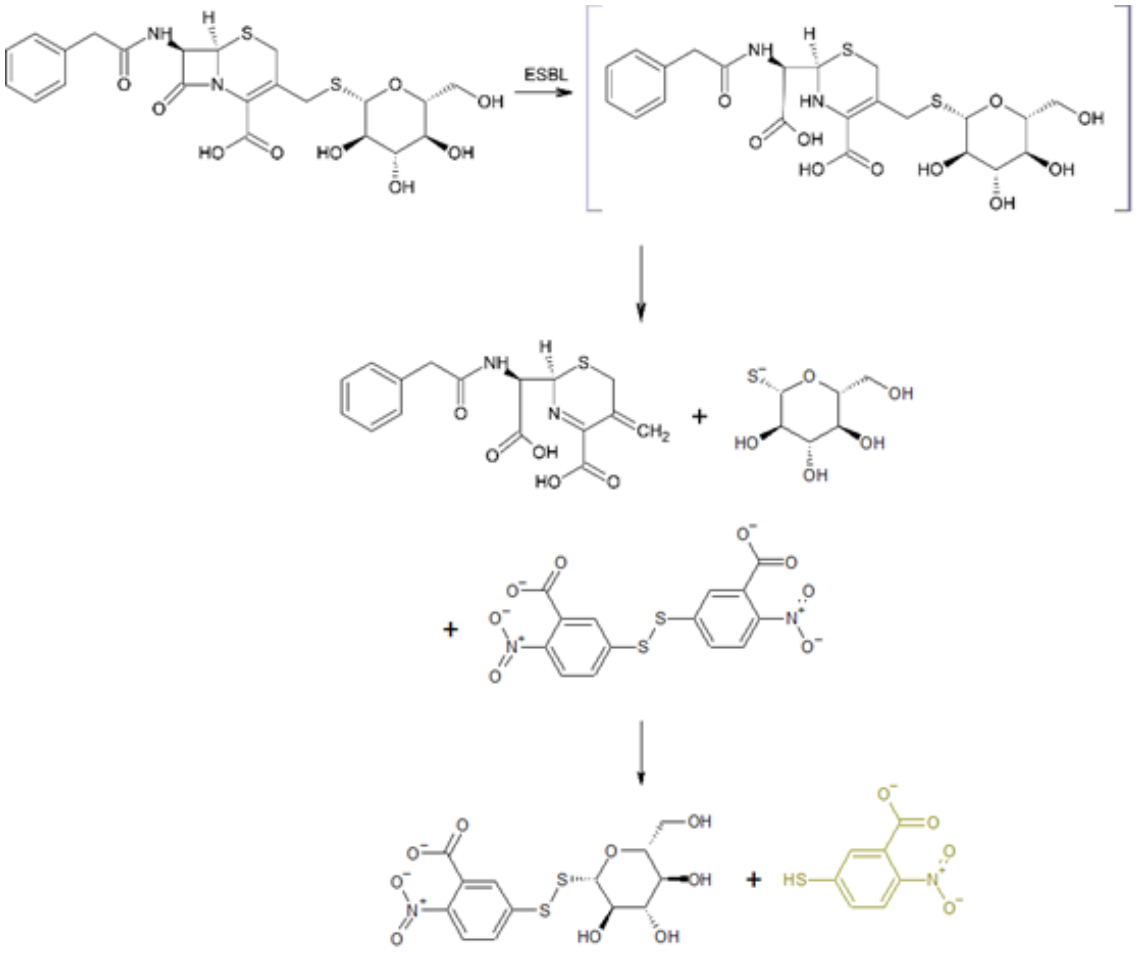

Figure 4.2 Schematic for the colorimetric detection of ESBL. ESBL cleavage of Cep-glucose detection substrate, ring opened intermediate, spontaneous release of thio-glucose and capture by DTNB resulting in production of a colored TNB molecule (yellow) measurable by absorbance colorimetry.

We designed our detection substrate to enable colorimetric readout via absorbance spectrophotometry in order to align with standard procedures and equipment found in clinical laboratories. The CENTA substrate directly releases the colored molecule 5-thio-2-nitrobenzoic acid (TNB) upon hydrolytic cleavage; similarly, we employed 5,5'-dithio-bis-[2-nitrobenzoic acid] (DTNB, also known as “Ellman’s reagent”), a symmetric molecule composed of two TNB halves linked by a disulfide bond, in our colorimetric readout scheme (Fig 4.2). When the β-lactam ring is hydrolyzed,

electronic rearrangement allows for the release of the attached thio-glucose, which may then participate in reactions enabling downstream readout modalities (Fig 4.1). As Cep-glucose releases thio-glucose upon cleavage by ESBL, which readily reacts with DTNB via its thiolate moiety to break the disulfide bond, it produces a mixed disulfide and colored TNB. The corresponding absorbance peak shift due to the resultant TNB can be measured at 412 nm.[11,221]

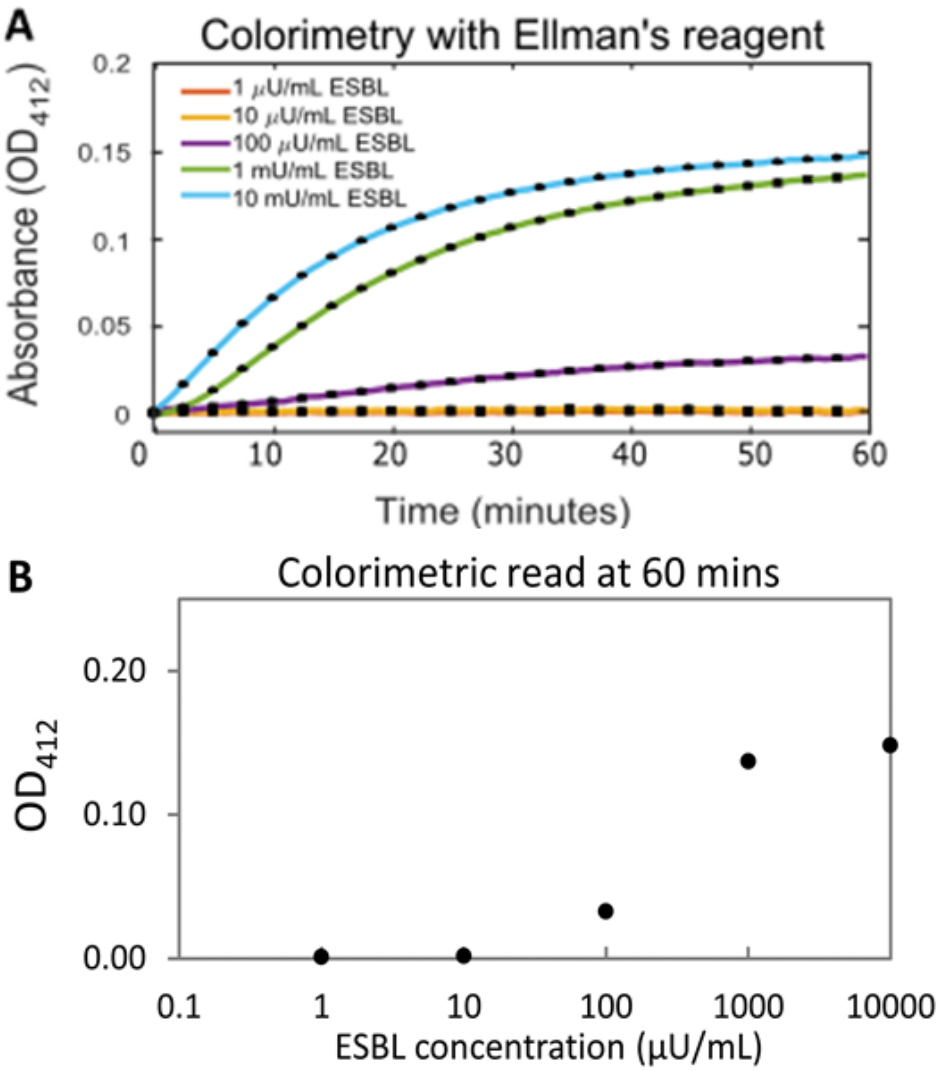

Figures 4.3.A&B. Colorimetric dose-response timecourse and endpoint detection of ESBL using the Cep-glucose substrate. A) Kinetic absorbance readout and B) endpoint signal quantification of DTNB production resulting from ESBL degradation of Cep-glucose yielding thio-glucose elimination and product capture. (Please note: error bars are plotted for experimental triplicates but are not visible due to their small values.)

To examine the detection performance of Cep-glucose as a colorimetric ESBL reporter, we incubated 250 µM Cep-glucose and 250 µM DTNB with varying unit concentrations (10 mU/mL to 1 µU/mL) of ESBL in 100 µL of 0.1 M phosphate buffer (pH 6.5 at RT), and monitored the absorbance peak over the course of 60 minutes (Figs 4.3.A&B). Relying on optical density readout, we were able to easily distinguish a concentration of 100 µU/mL from lower amounts. The limit of detection was calculated to be approximately 19 µU/mL ESBL (approximated to be 70 pM assuming an average enzyme molecular weight of 35 kDa and a specific activity of 5.87 U/mg as provided by the vendor), corresponding to three standard deviations above the background signal, or OD_{412} of 0.07.

4.3.2 Fluorimetric detection.

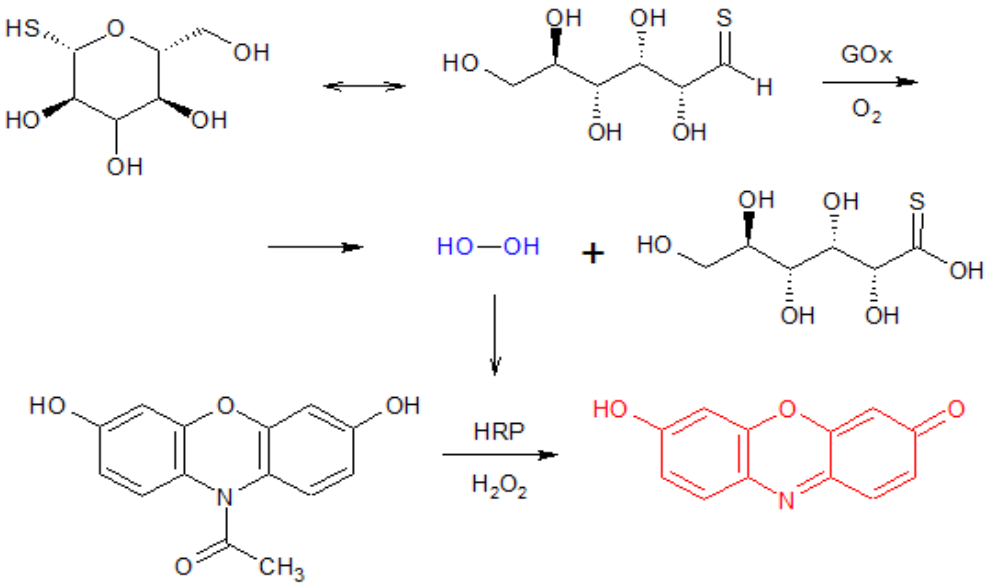

Figure 4.4. Schematic for the fluorimetric detection of ESBL. Released thio-glucose is a substrate for GOx,, and produces hydrogen peroxide in the presence of oxygen. HRP in solution may then use the produced hydrogen peroxide to oxidize Amplex red into resorufin, which is measurable by fluorescence monitoring (excitation/ emission peaks at 563 nm/ 587 nm).

With the intent of achieving lower limits of detection, we investigated the incorporation of our Cep-glucose substrate in a biochemical scheme to allow for measurable fluorometric readout. To accomplish this, we utilized thio-glucose's ability to serve as a substrate for glucose oxidase (GOx), producing 1-thio-β-D-gluconic acid and H_2O_2[222] (Fig 4.4). For our fluorogenic molecule, we chose *N*-acetyl-3,7-dihydroxyphenoxazine (Amplex red) as it has been well-characterized as a stable and sensitive reporter of H_2O_2, producing highly fluorescent resorufin (excitation maximum at 563 nm, emission maximum at 587 nm) in an irreversible enzyme-catalyzed oxidative reaction mediated by HRP.[223] Various concentrations of ESBL (1 μU/mL to 10 mU/mL) were incubated with 250 μM Cep-glucose substrate and 10 μM Amplex red in the presence of 0.5 U GOx and 100 μU HRP in a 100 μL volume of 0.1 M PB (pH 6.5) at room temperature, and the generation of an emission signal was continuously recorded at 590 nm with excitation at 530 nm over the course of one hour (Figs 4.5.A&B). With the fluorometric assay, we estimate the limit of detection to be 0.98 μU/mL ESBL, which generates a signal that is larger than three standard deviations above the background signal. Though the fluorometric read-out provides higher sensitivity than the colorimetric read-out, one aspect of the assay design prevents the difference from being much greater. HRP, which catalyzes the conversion of Amplex red to fluorescent resorufin, is inhibited by free thiols.[224]

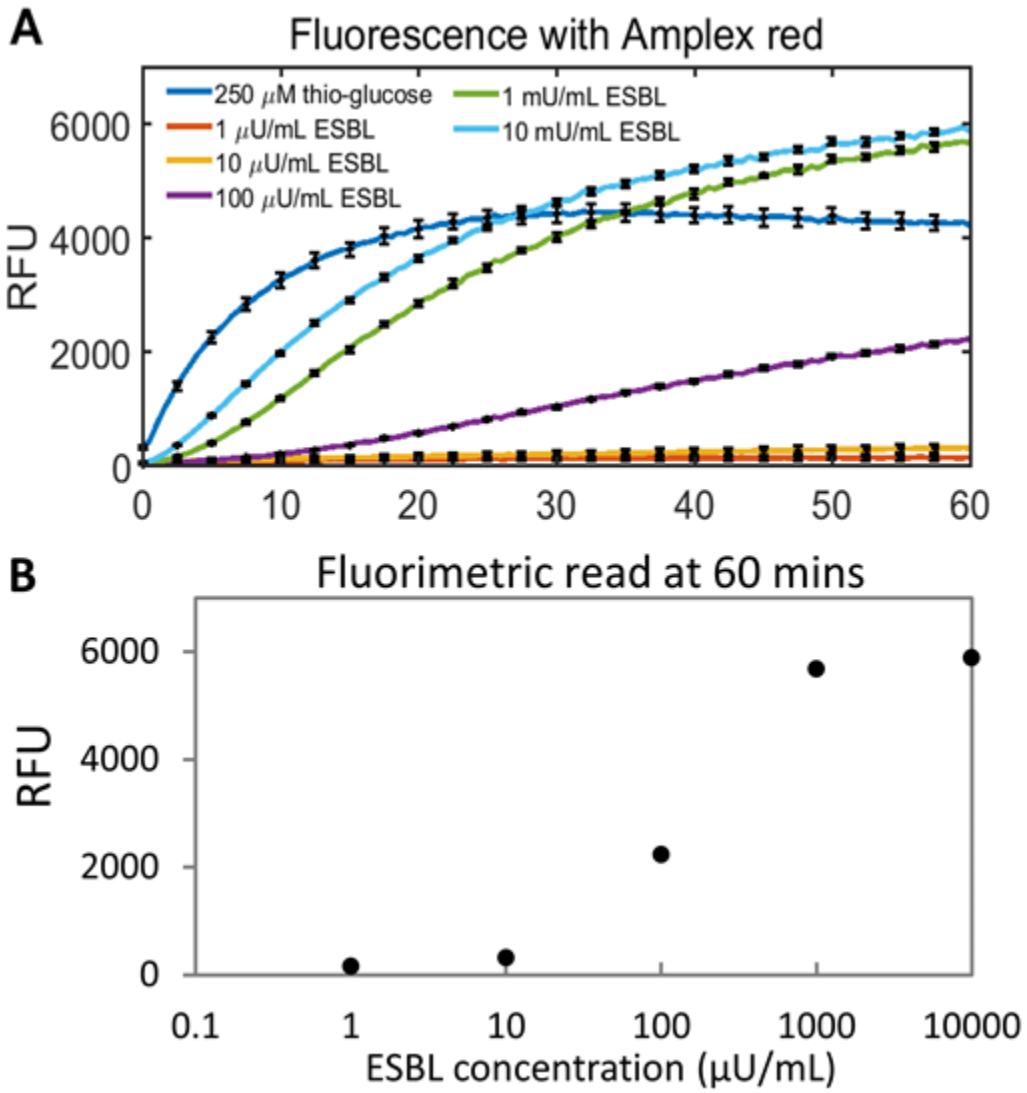

Figs. 4.5.A&B. Fluorimetric dose-response timecourse and endpoint detection of ESBL using the Cep-glucose substrate. A) Kinetic fluorescence readout and B) endpoint signal quantification of the oxidation of Amplex red into resorufin from released thio-glucose, degraded into byproducts including hydrogen peroxide by GOx. (Please note: error bars are plotted for experimental triplicates but are not visible due to their small values.)

4.3.3 Electrochemical detection by sulfide inhibition.

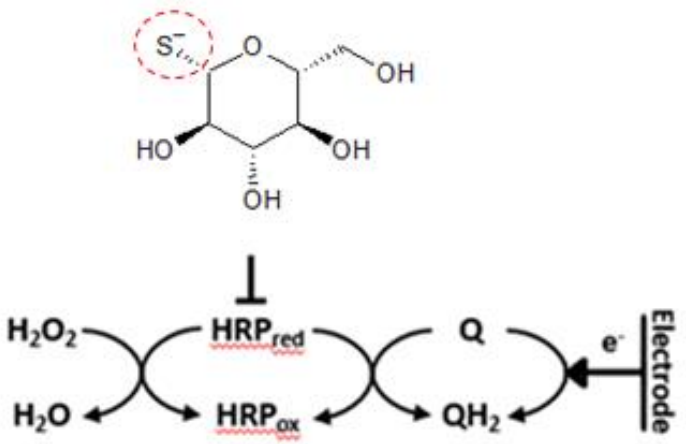

Figure 4.6. Assay scheme for HRP-inhibitory electrochemical detection. Released thio-glucose is also a reactive free thiol that inhibits HRP activity, thereby decreasing redox activity that can be monitored by electroanalytical methods.

Previous reporting of ESBL-producing *E. coli* strains through the amperometric detection of Nitrocefin cleavage,[26] and methods of non-glucose target detection through engineered glucose generation schemes led us to explore Cep-glucose's potential in expanding ESBL detection beyond the central lab by utilizing electrochemical methods. Though thio-glucose generated from Cep-glucose cleavage can in theory serve as a source of electrochemically active H_2O_2, we found that employing the sulfide detection scheme based on the sulfide inhibition of HRP previously described by Savizi *et al.* provided an electrochemical method with better performance (Fig 4.6).[224] This scheme utilizes the inhibitory effect of thiols on HRP to decrease its participation in a redox cycling scheme that produces current via a hydroquinone (HQ) mediator. We expect that the release of thio-glucose from the cleavage of Cep-glucose by ESBL would provide a source of inhibitory free thiols,

and sought to demonstrate a dose-dependent current decrease with respect to ESBL. Varying amounts of ESBL were incubated for 15 minutes under identical conditions and HRP was added just prior to cyclic voltammetry measurement (time points up to 60 minutes were tested, however no improvement in detection sensitivity was observed). The depth of the oxidation peak was measured (Figs. 4.7.A&B), showing a decrease in oxidation current for increasing concentrations of ESBL. A limit of detection of approximately 66 μU/mL was calculated (3σ above background). We produced a calibration curve measuring varying known amounts of thio-glucose (Appendix V). Back calculations using this calibration curve indicate an estimated release of 147±3.3 μM thio-glucose after incubation of Cep-glucose with 10 mU/mL ESBL.

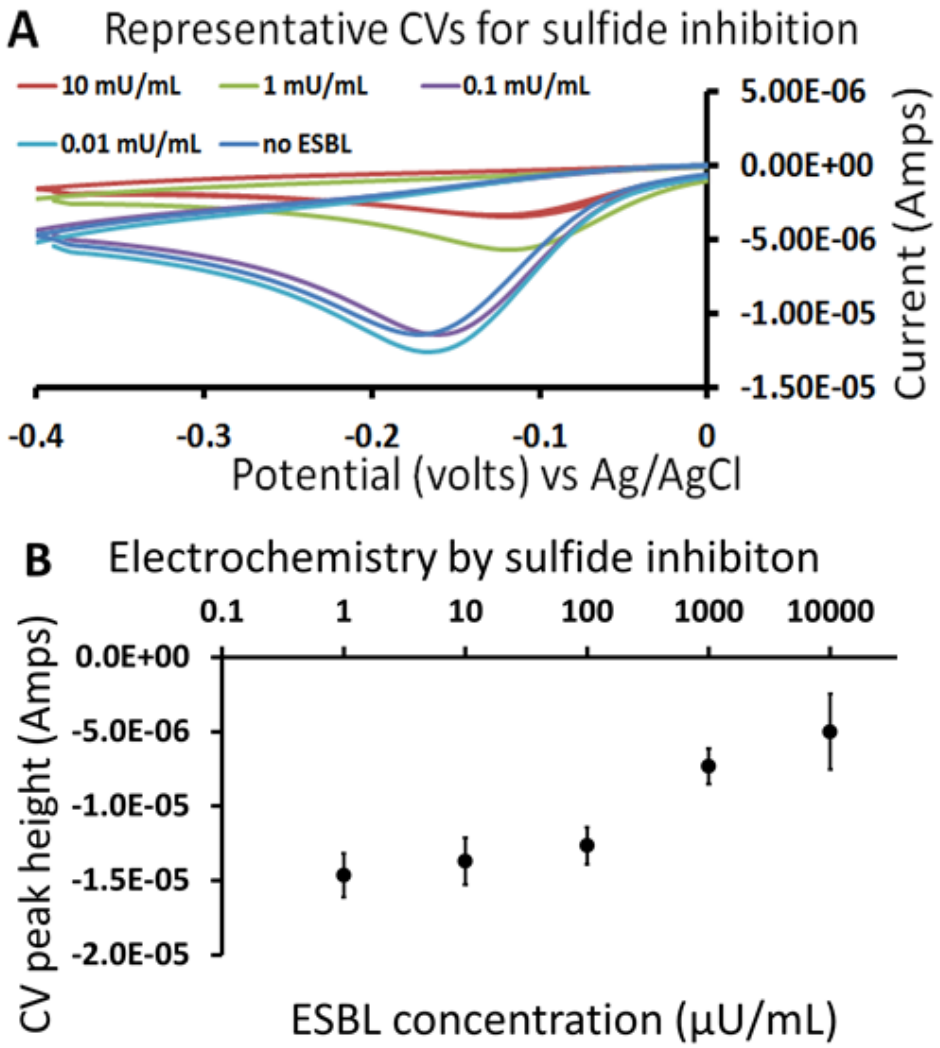

Figures 4.7.A&B. Electrochemical detection of ESBL using Cep-glucose substrate. A) Representative CVs showing inhibition peaks for varying concentrations of ESBL. As the potentiostat cycles through the set voltage limits a negative current peak corresponding to greatest thiol inhibition of redox activity occurs. B) Peak heights are quantified and plotted to show sigmoidal behavior typical of biosensing.

4.3.4 Electrochemical detection of ESBL using Cep-glucose in a commercially available personal glucose monitor (PGM)

Methods. The Cep-glucose detection substrate was prepared from a 19.5 mM stock in deuterated DMSO, diluted into 0.1 M phosphate buffer (pH = 8.5) to a final concentration of 3 mM. 1 µL of a 1 KU/ mL stock of the ESBL blend (AG Scientific) was added to 24 µL of the 3 mM Cep-glucose solution (final concentration 40 U/ mL ESBL) and allowed to incubate at 25ºC for 5 minutes. From this, a 2 µL aliquot was taken and pipetted onto a square of Parafilm®, a generic glucose oxidase based test strip (TruePoint, OK Biotech) was inserted into a OneTouch® Ultra2® blood glucose monitor (PGM) adjusted to calibration setting 49 (as directed on the TruePoint box), and the reservoir tip was touched to the aliquot allowing the sample to wick up into the test strip and held in place until a reading was displayed on the PGM. This process was repeated for the thio-glucose calibration control and the no ESBL negative control. The experiment was also performed for the following pH ranges: 9.0, 9.5, 10.0, 10.5, 11.0, 11.5.

Results. All pH values tested gave consistent results similar to pH 8.5 (but contributed to greater error range ± 5 mg/ dL) for the ESBL-positive experimental condition, with no ESBL registering in the PGM as “ERROR 4” or “low glucose”, and with the addition of 40 U/ mL ESBL registering just above the 20 mg/ dL displayed limit of detection. The 2.5 mM thio-glucose positive calibration control (used to compare the performance of thio-glucose to D-glucose for which the PGM is designed to detect)

had consistently lower readings than what would be expected from an equimolar sample of D-glucose.

Experimental condition (pH 8.5)	**Result on PGM display (mg/ dL)**	**Approx. molar equivalent (mM)**
2.5 mM thio-glucose	35 ± 2 mg/ dL	2 mM
40 U/mL ESBL 3 mM Cep-glucose	25 ± 3 mg/dL	1.5 mM
No ESBL 3 mM Cep-glucose	"low glucose, below 20 mg/ dL" ("ERROR 4" displayed)	< 1 mM

Table 4.1. Experimental and control results of PGM detection of ESBL with Cep-glucose. (Error for each experiment calculated from conditions performed in triplicate using new test strips.)

Discussion. Thio-glucose released from the Cep-glucose substrate upon ESBL cleavage can accumulate in high enough concentrations to register a reading within the working range of a commercially available PGM. Though higher pH ranges do not appear to impact detection performance, if the entirety of the 3 mM Cep-glucose substrate is hydrolyzed to release the equivalent concentration of thio-glucose, the PGM would be expected to display a reading in the 50 mg/ dL range. However, the consistently lower readings present a loss of approximately half the expected signal, indicating there is much room for improvement. Additionally, as free thio-glucose is also lower-performing than expected with approximately a quarter signal loss

(expected reading for 2.5 mM glucose is 35 mg/ dL), it may be an inherent property of thio-glucose as a poor substrate for glucose oxidase. Other strong considerations are the limiting rate of thio-glucose release from the ring-opened Cep-glucose intermediate, and if the released free thiol exerts any inhibitory effects in the TruePoint test strips that would impact electrochemical readout.

4.3.5 Detection of ESBL-producing *E. coli*.

SHV-4 ESBL-producing *E. coli* (strain J53-2 pUD21, *ATCC* product number *BAA-200*) were initially streaked onto tryptic soy agar (Difco) plates containing 10 µg/mL ceftazidime as a selection agent and allowed to incubate overnight at 37 ºC to produce single colonies. From this, one colony was selected and allowed to grow overnight (16 hours, shaking at 37 ºC) in liquid tryptic soy broth (10 mL volume) containing 10 µg/mL ceftazidime. CFU dilutions were prepared directly in PBS from the turbid culture. In a 96-well microplate, various conditions were prepared in 100 µL total volume of 0.1 M PBS (pH = 7.4): bacteria only, bacteria with 250 µM Ellman's reagent, and ten-fold dilutions of bacteria (including a no bacteria control) with 250 µM Cep-glucose detection substrate and 250 µM Ellman's reagent. Samples were incubated in the microplate at 25 ºC and absorbance measurements at 412 nm were taken at 2 hours and 4 hours using a microplate reader.

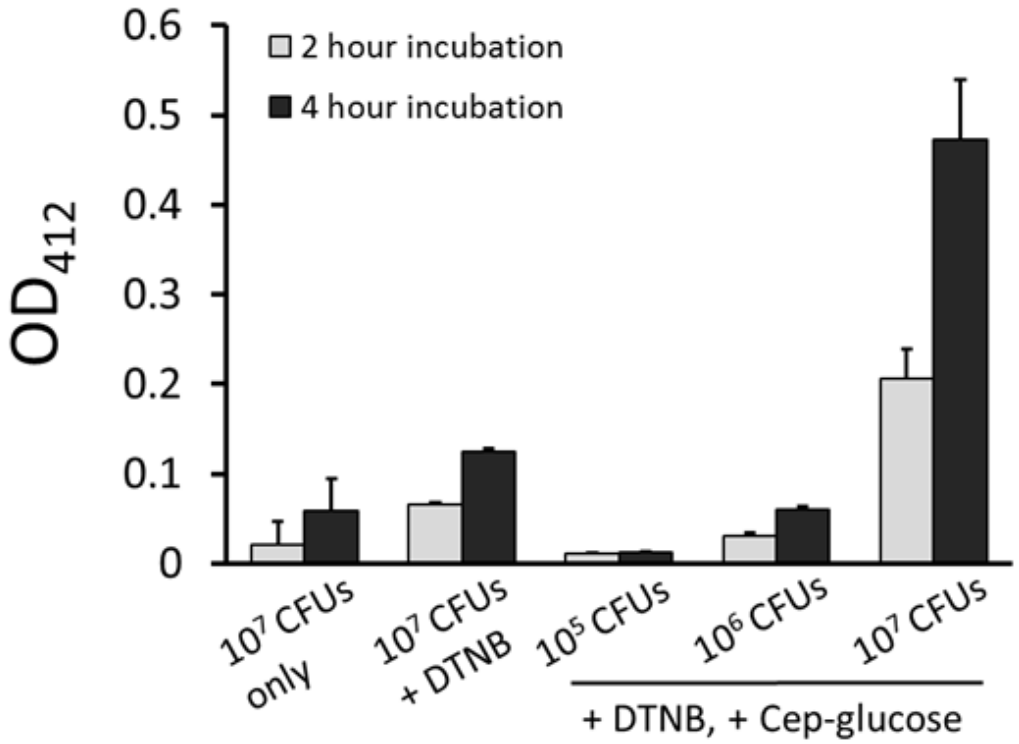

Figure 4.8. Colorimetric signal change for Cep-glucose with cultured *E. coli* that produces SHV-4 ESBL. As compared to 0 CFUs (used as background subtraction), 10^7 CFUs with Cep-glucose and Ellman's reagent generated an easily measurable signal. 10^7 CFUs with and without Ellman's reagent (no Cep-glucose) were also included as negative controls. (Error bars were calculated from triplicates; experiment was reproducible.)

Results. Within two hours of direct incubation of 10^7 CFUs *E. coli* with the Cep-glucose detection substrate and DTNB, an increase in absorbance readout was observed as compared to the no Cep-glucose + DTNB control included to calibrate for any background chromogenicity (i.e., thiolates arising as metabolic byproducts); additionally, an increase in absorbance signal was observed after four hours. No discernable absorbance readout was observed for any lower CFU dilutions (Fig 4.8).

Discussion. The signal magnitude for 10^7 CFUs after 2 hours is similar to the signal level that accumulates for 10 mU/ mL of the commercial ESBL blend. However, it is

unclear how the onset of observable ESBL activity with live cells compares with our previous experiments using the commercial ESBL enzyme blend. Considerations to take into account are the Cep-glucose substrate's diffusion behavior across the outer membrane into the periplasmic space where β-lactamases are localized. On a chemical level, this behavior may be impacted by Cep-glucose's possession of many more hydroxyl groups as compared to previously established chromogenic substrates. Furthermore, the two-step disulfide exchange with DTNB to produce color may require diffusion of the TNB chromogen or released thio-glucose back out of the cell to contribute to readout. Exploration of sample preparation steps to include lysis by either chemical (detergents) or mechanical (sonication) means could help elucidate methods for improving detection performance at lower CFUs.

4.4 Conclusion

In this study we have shown that our new detection substrate Cep-glucose can enable three different readout modalities (colorimetric, fluorimetric, amperometric) for the detection of varying levels of ESBL spanning at least three orders of magnitude. Our colorimetric detection scheme using Ellman's reagent allows for use of common absorbance spectrophotometry techniques. Our fluorescence detection scheme using Amplex red, despite greater assay complexity, provided lower limits of detection for greater sensitivity. Additionally, we engineered an amperometric means of detection to illustrate the possibility of antibiotic resistance testing outside of the central laboratory.

4.4.1. Future work: Optimizing HRP activity.

Protein engineering of the HRP enzyme to be less susceptible to inhibition by thiols could provide a more robust enzyme for more efficient oxidation of Amplex red to resorufin and thus increase the sensitivities measured by fluorimetric readout. Alternatively, development of a synthetic protocol to achieve Cep-glucose adduct by way of an oxygen moiety in place of the sulfur as the C-3 position alkyl halide could produce a normal glucose molecule that undergoes more efficient oxidation by GOx, as well as eliminating the release of HRP-inhibitory thiols into solution, thereby resulting in an overall improvement in assay performance.

4.4.2 Future work. Detection using commercial personal glucose meter.

Optimization studies of either the assay (to increase release of thio-glucose from the Cep-glucose ring open intermediate through studies in buffer elements that may increase concerted expulsion of the leaving group) or the electrochemical detector ("hacked" glucometer for lower limits of detection) could result in sensitivities allowing for readout of glucose release by way of a portable glucose meter.

Chapter 5: Cep-pNTP and Cep-diNTP, SERS-active reporters

5.1 Introduction

Previously we have described one detection substrate capable of reporting ESBL activity. However, given the various classes of β-lactamase as well as the ever-expanding sub-classes as new permutations appear, it would be of great advantage to have a collection of reporter substrates corresponding to various β-lactamases from classical non-ESBL types to ESBL types, metallo-β-lactamases, and carbapenemases. Even more advantageous would be the capability of assaying for these different resistance enzyme evolutions in a single sample with a single measurement. Cep-glucose and the currently developed chromogenic substrates (Nitrocefin, etc.) are unable to do this; however, as Raman spectroscopy is capable of single-sample multiplexing due to its narrow band optical properties, creation of a suite of detection substrates that release Raman-active reporter molecules—each with a unique optical fingerprint—would provide a resistance detection toolkit of immense benefit. Moreover, our use of sulfur/ thiol chemistry for the assembly and disassembly of our reporter molecule is compatible with surface-enhanced Raman spectroscopy (SERS), which utilizes metal nanostructures for signal enhancement. Thus, we investigated the synthesis of new ESBL sensing molecules for use with SERS.

Here we will overview a basic explanation of the physics behind the theory of Raman scattering, its enhancement on appropriate nanometal surfaces, and how this allows for multiplex spectral monitoring of ESBL resistance using our reporter substrates.

5.1.1. Raman spectroscopy.

Photons from incident light can interact with a molecule in different ways. The vast majority of interaction is in the form of an elastic scattering event, in which the molecule absorbs the energy, is raised to a virtual state (a temporarily stable vibrational mode), and emits the energy with no net change, falling back to its ground state in what is known as Rayleigh scattering. In a much rarer phenomenon, the excited molecule may fall back to a vibrational (real phonon) state higher than its ground state, emitting energy that is less than that of the incoming photon; this is known as Stokes shifted Raman scattering. In yet an even rarer third phenomenon, if the molecule is already in a vibrational energy (excited phonon) state when it is excited by another incident photon to a virtual energy state, it releases more energy than that of the incident photon in relaxing back to its ground state, a behavior known as anti-Stokes Raman scattering. Because anti-Stokes scattering is so rare, typical Raman measurements are only performed using Stokes shifted light (Fig. 5.1).

Raman scattering behavior is highly dependent on and unique to the molecule's underlying arrangement, thereby giving it a spectral signature "fingerprint". It is also independent of virtual energy state, only depending on wavenumber to describe its Raman shift (the difference in energy between initial and final vibrational states).

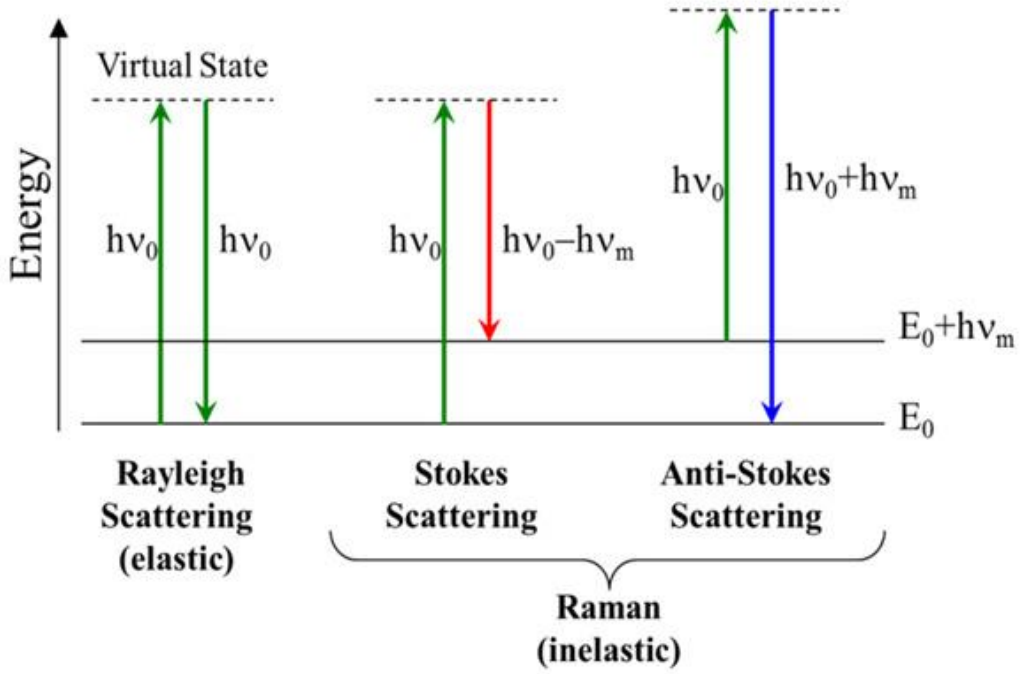

Figure 5.1. Jablonski diagram representing quantum energy transitions for Rayleigh and Raman scattering.

Raman scattering can also use any frequency of light, only requiring a monochromatic source (laser). This gives it a key advantage over IR spectroscopy as it can employ a wide range from UV to IR. Still, shorter wavelengths are more conducive to higher Raman scattering intensity as the power of scattering is proportional the fourth exponent of the light's frequency (power $\propto \nu^4$). Raman scattering is typically performed in the mid-visible to IR range in order to mitigate interference by the inherent fluorescence of a molecule which is also more intense at shorter wavelengths, but also maintain the power afforded by shorter frequencies. Another important advantage of Raman spectroscopy is its narrow-band nature as compared to fluorescence methods: bleed-over due to spectral overlap is not as prominent in Raman as in fluorescence, which is ultimately conducive to greater potential in multiplexing.

The most effective identification of analytes using Raman spectroscopy is achieved with pure samples, or when the analyte's spectral behavior is represented by the most dominant portion of the recorded spectral range (i.e., the analyte is a particularly Raman-active molecule). However, Raman by itself is not particularly sensitive for most applications. As Raman was initially confined to high purity concentration samples, the enhancement discovery from SERS increased the effectiveness of Raman spectroscopy as an analytical technique by many orders of magnitude.

5.1.2 Surface enhancement.

Surface enhancement is carried out through the use of noble metal nanostructures. In these materials the Raman signal is enhanced by many orders of magnitude.[225–228] This enhancement due to two phenomena known as surface plasmon resonance (SPR) and chemical effects, the former of which is responsible for the majority of enhancement effects.[229–231] Research advancing the enhancement properties of SERS through the engineering of nanostructures has led to the attainment of detection and identification on the single molecule level.[231–233] A phenomenon known as "localized surface plasmon resonance (LSPR)" enables the generation of SERS enhancement on the surfaces of metal nanostructures. LSPR occurs when the oscillations of free surface electrons ("plasmons") replete on the surfaces of appropriately-sized nanostructures couples with the excitation wavelength of incident light that is on the same order as the oscillations, generating "resonance". LSPR accounts for the vast majority of total SERS enhancement factor (10^4 to 10^8); the lesser part of the

enhancement factor ($\leq 10^4$) is attributed to chemical enhancement which arises from direct bond coordination with the metal surface.

In the current work, silver nanoparticles (AgNPs) are used as SERS surface materials thanks to their high resonance as compared to other noble metals such as copper, nickel, platinum, and aluminum.[234] (Note that due to their similar resonance characteristics, gold nanoparticles can just as easily be employed in these studies. Both gold and silver based nanoparticles with diameters smaller than 5 nm exhibit high surface enhancement properties. However, gold has better stability properties than silver, giving it a longer shelf life and greater commercial potential.)

The enhancement effect of SERS can be described by the following equation:

$$\text{Enhancement} \propto \left(\frac{1}{a+d}\right)^{12},$$

where a is the average molecular radius of the nanoparticle and d is the analyte's distance from the metal nanostructure surface. As evidenced by the distance relationship in this equation, critical to the effectiveness of SERS is the proximity of the analyte to the metal nanostructure surface.[235–237] The above equation describes the diminishment of enhancement effects as to the twelfth power of total distance $a+d$. As a result, adsorption of target analytes to the metal surface is an advantageous strategy for the effective detection of rarer species in a sample volume (low concentration analyte). Further, as the rapid diminishment of SERS begins at the

unitary nanometer scale (i.e., over 50% decrease in enhancement at 2 nm from the surface), infeasibilies arising in the detection of bulkier biomolecules in the nanometer range constrain SERS based detection to small molecules as the ideal substrate class due to their diminutive size range.

Advantages of SERS as a bioanalytical technique. Compared with UV-vis absorption spectroscopy and infrared spectroscopy, SERS gives a fingerprint vibrational information of the adsorbates on the metal surfaces, and the added advantage of its enormous enhancement factor of up to 10^{14}, which brings the limit of detection down to the level of single molecules.[232,238,239] SERS is additionally suitable for aqueous environments thanks to the transparency of water that allows the use of laser light as in Raman spectroscopy. This makes SERS based detection ideal for our biological matrix based assays, or in idealized aqueous media containing buffer salts. Thanks to its increased sensitivity, surface enhancement makes Raman ultimately a more feasible means as an analytical technique, and can be considered on par with fluorescence spectroscopy but superior multiplexing density.[232,240,241] SERS is additionally advantageous over fluorescence in its label-free nature as it directly detects a molecular fingerprint without any additional treatment necessary. In comparing SERS to other highly sensitive spectroscopic techniques such as mass spectrometry, especially when paired with chromatographic separation methods (LC, GC) which provides extremely high resolution, the advent of portable SERS has now made this spectroscopic technique field accessible, giving SERS a distinct advantage

for lower resource or remote settings away from a centralized laboratory with specialized equipment.

5.1.3 Multiplexing.

The basis for our SERS multiplexing is the release of different SERS-active small molecule reporters from the cephalosporin-derived detection substrate upon interaction with β-lactamase. The SERS-active small molecules were chosen based on several characteristics: (1) their strong nucleophilicity as thiolates participating in Sn2 displacement organic synthetic reactions to produce our detection substrates; (2) their possession of an aromatic nitro group which has a large scattering cross-section due to the symmetric nitro stretch; and (3) their possession of a released thiol moiety when released, aiding in reaction with the AgNP surface to form a thiolate adlayer.[237,242,243]

We based our choice of *para*-nitrothiophenol (pNTP) as it is very well established in the literature as a SERS active molecule with good adsorption properties.[244] Additionally, the synthesis of a second detection substrate releasing 2,4-dinitrothiophenol (diNTP) was also based on its successful detection as reported in the literature.[245,246]

In order to confirm that the two SERS-active reporter molecules had spectra that were sufficiently narrow-band without indistinguishable overlap, SERS measurements were made on pNTP and diNTP separately, then overlaid as shown below in Fig. 5.2.

As observed from these spectra, ratios will be compared between the distinguishing peaks as follow in Table 5.1.

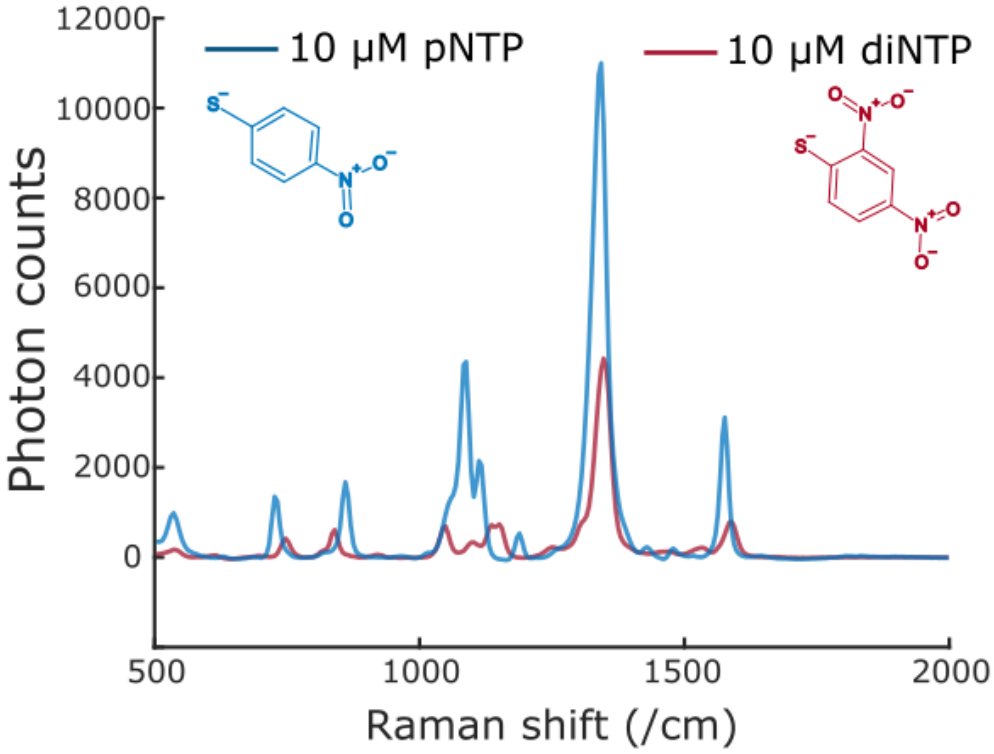

Figure 5.2. Comparative SERS spectral overlay of pNTP and diNTP to identify distinguishing peaks between the two reporter substrates (both at 10 µM).

	Wavenumber (photon count)		
pNTP	726 (1348)	860 (1672)	1088 (4350)
diNTP	747 (415)	839 (607)	1150 (734)
Peak ratio	**3.248**	**2.755**	**5.926**

Table 5.1. Comparative signature peak ratios for pNTP and diNTP SERS-active reporters. Calculated ratios between identified peaks and count values to be used as an initial standard metric representative of 1:1 molar ratio release of SERS-active reporters in a single sample on a single sensor.

5.1.4. Schemes for ESBL and non-ESBL distinguishing substrates.

Our detection substrates have been designed with different SERS-active molecules as leaving groups (via C-3 position alkylation) that serve as specific reporters corresponding to differing amide side chains (at the C-7 position amino group). The presence of the benzyl group on Cep-pNTP is designed to behave similarly to cephalosporin antibiotics that have a similar or identical side chain, which are often a feature of the second-generation cephalosporins (e.g., Cefaclor) and can thus be generalized to be indicative of resistance toward them. Figure 5.3 depicts preferential cleavage of Cep-pNTP by ESBL, thus liberating the pNTP thiolate, allowing it to participate as a SERS-active molecule.

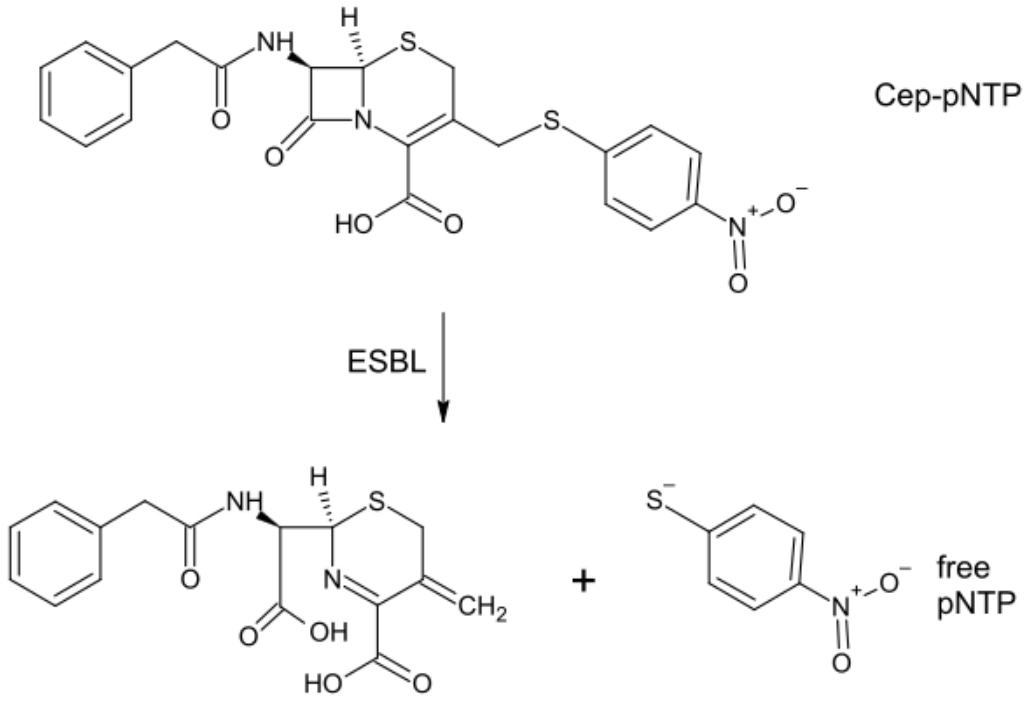

Figure 5.3. Cep-pNTP substrate which represents a second-generation cephalosporin is hydrolyzed by ESBL (but not non-ESBL enzyme TEM-1).

Under the same rationale as the detection substrate just described, Cep-diNTP was designed with a C-7 amide side chain possessing a thiophene group. The presence of this thiophene is found in many first-generation cephalosporins (e.g., Cefalotin), and is expected to be hydrolyzable by classical, non-ESBL enzymes such as TEM-1. In fact, Cep-diNTP is structurally identical to Nitrocefin, a substrate of TEM-1, with the exception of the sulfide moiety as the C-3 position alkyl halide. (Again, the purpose of attachment by the sulfur is to enable the release of the diNTP SERS-active reporter upon intramolecular rearrangement leading to halide expulsion, upon β-lactam cleavage.) As shown in Figure 5.4, the Cep-diNTP substrate is expected to be hydrolysable by both classical TEM-1 and ESBL thanks to its extended-spectrum of activity.

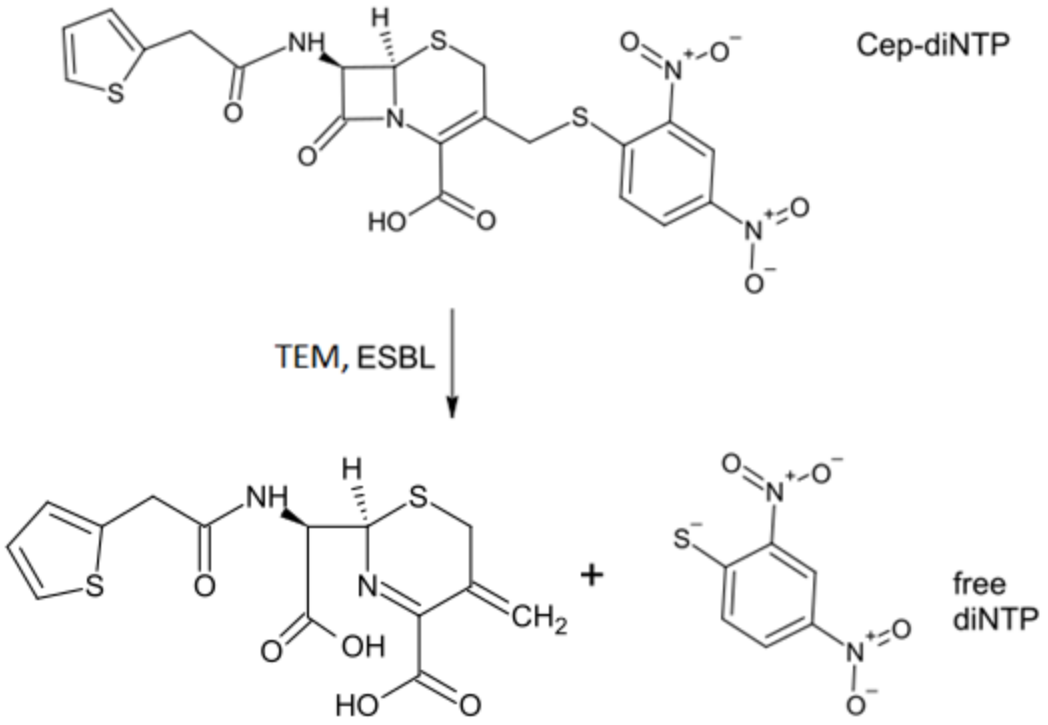

Figure 5.4. Cep-diNTP substrate can be hydrolyzed by both a non-ESBL classical β-lactamase (TEM-1) and ESBL.

5.2 Experimental

5.2.1 Absorbance colorimetry.

Ellman's reagent reacts with free thiols to form a colored product (absorbance peak at 412 nm) and thus was used to detect the release of thio-glucose upon cleavage of our Cep-glu substrate. Measurements were carried out at room temperature in standard 96-well microplates in a 100 μL volume, with each well containing 250 μM Ellman's reagent and 250 μM of the Cep-pNTP or Cep-diNTP substrate in PB (pH = 6.5).

5.2.2 Measurement by SERS

SERS paper sensors printed with silver nanoparticles were purchased from Metrohm and cut into 5 mm x 5 mm squares prior to use. SERS measurements were performed using a portable Raman system consisting of a 785 nm diode laser (Innovative Photonic Solutions, Monmouth Junction, NJ), QE65000 Raman spectrometer (Ocean Optics, Dunedin, FL), and fiber optic probe (Integrated Photonic Solutions, Monmouth Junction, NJ). Laser power is set to approximately 15 mW. Each spectrum is collected using a 1 second CCD exposure for 3 accumulations (averaged). Spectra are averaged across 5 spots (in a configuration like the value 5 on a six-sided die). Data were analyzed in MATLAB using custom in-house code adapted from the literature.[247]

5.2.3 Multiplex detection of ESBL and non-ESBL with SERS

Samples consisted of 250 μM of each detection substrate (Cep-pNTP, Cep-diNTP) in 100 μL 0.1 M PBS (pH = 7.4), to which either final concentrations of 10 mU/ mL ESBL, 1 U/ mL TEM-1 (non-ESBL), or no enzyme was added and allowed to

incubate for 10 minutes, after which 2 μL volume aliquots of the sample were pipetted onto the sensor. After 15 minutes of air dry time, SERS measurements were made.

Dose-response experiments were performed in the same way, except with 100 μM substrate in 0.1 M phosphate buffer (pH = 8.0) and an incubation time of 1 h, after which a 4 μL sample volume was pipetted onto the sensors, and given 25 minutes of dry time prior to measurement.

5.3 Results

5.3.1 Dose-response behavior of SERS-active reporter release.

In our first step of directly establishing SERS-based detection, we first must observe that Cep-diNTP is also a cleavable substrate of ESBL. To do this, we incubate it with ESBL under the same conditions as previously described, and observe an increase in SERS signal while remaining conscious of baseline (no ESBL background) considerations. In Fig. 5.5, we can see that Cep-diNTP is a ready substrate for ESBL, and in its presence produces the same peaks as previously observed with diNTP in solution alone.

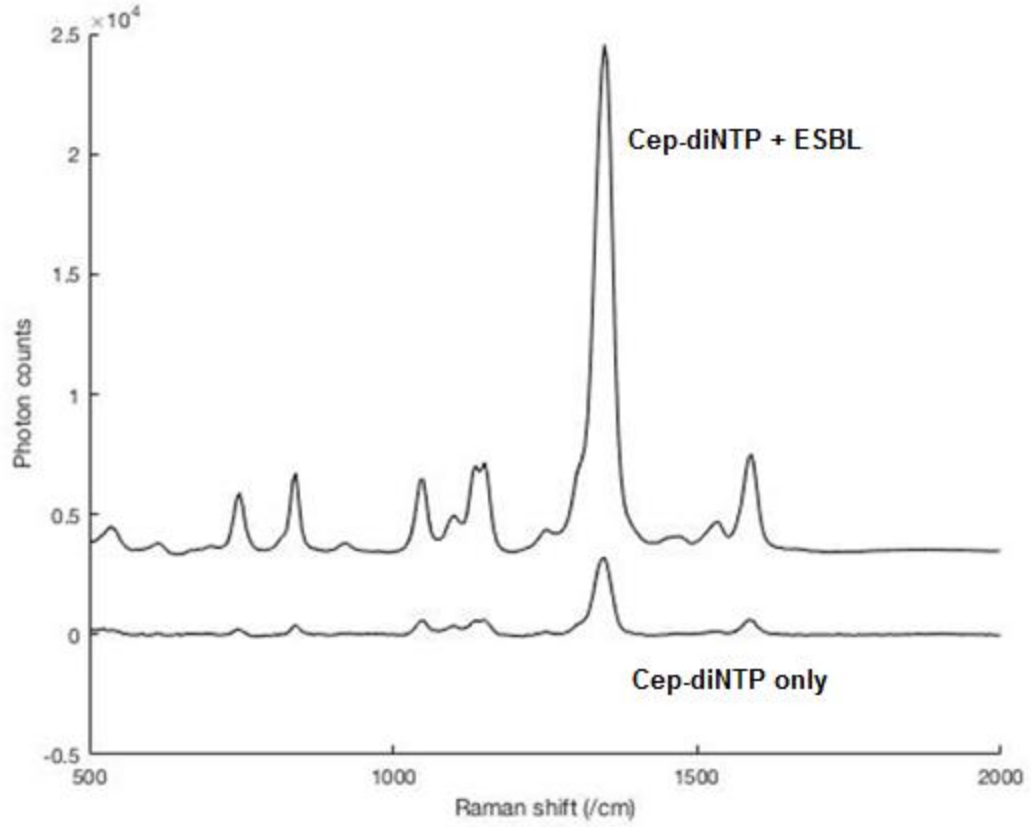

Figure. 5.5. Cep-diNTP is cleaved by ESBL (10 mU/mL) and releases diNTP. Higher photon counts are observed in the presence of ESBL, indicative of the SERS activity resulting from diNTP binding to the SERS substrate surface; minimal signal is observed with Cep-diNTP alone.

Using our Cep-pNTP substrate, we can observe a dose-response behavior as it produces spectra of greater peaks with increasing concentrations of ESBL, indicating the release of more pNTP reporter. The spectra display identifying peaks that are in accordance with the previously shown spectra of pNTP in solution (Fig. 5.2 overlay). We can easily visualize this dose-response behavior (Fig 5.6) through use of the diagnostic SERS peak at 1340 cm^{-1}, which from Fig. 5.2., can be seen as the most prominent (strongest) to yield highest sensitivities when monitoring pNTP for ESBL detection. (NB: The strong 1340 cm^{-1} peak is shared by both diNTP and pNTP, only allowing for its use as a diagnostic peak if substrates are assayed separately.

Therefore, subsequent single-sample multiplexing instead utilizes peaks that are unique to either reporter, as indicated in Tables 5.1 & 5.2.)

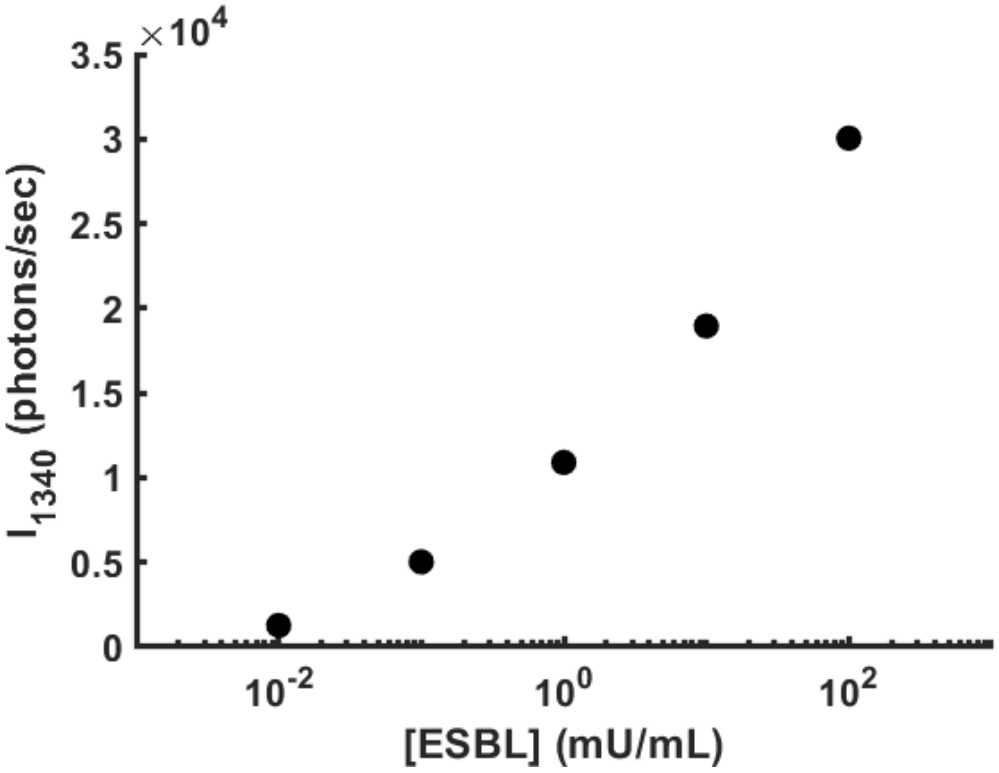

Figure 5.6. Dose-response behavior of Cep-pNTP substrate with increasing amounts of ESBL concentration (0.01 mU/mL ESBL to 100 mU/mL in 10-fold dilutions). Data points represent spectral peaks at 1340 cm^{-1} and are normalized to the no ESBL control. (Please note: plots represent experiments performed in triplicate with error bars present but not seen due to their small values.)

5.3.2 Comparative spectra for multiplex analysis.

Here we introduce both substrates combined in solution to incubation with either no enzyme, ESBL, or TEM-1 (non-ESBL). Depicted in Figure 5.7, our three different samples represent cases where there is ESBL present, non-ESBL enzyme present, and no enzyme present. As expected, the ESBL is able to hydrolyze both Cep-diNTP and Cep-pNTP, producing a mixed spectral plot, as shown in Figure 5.8.

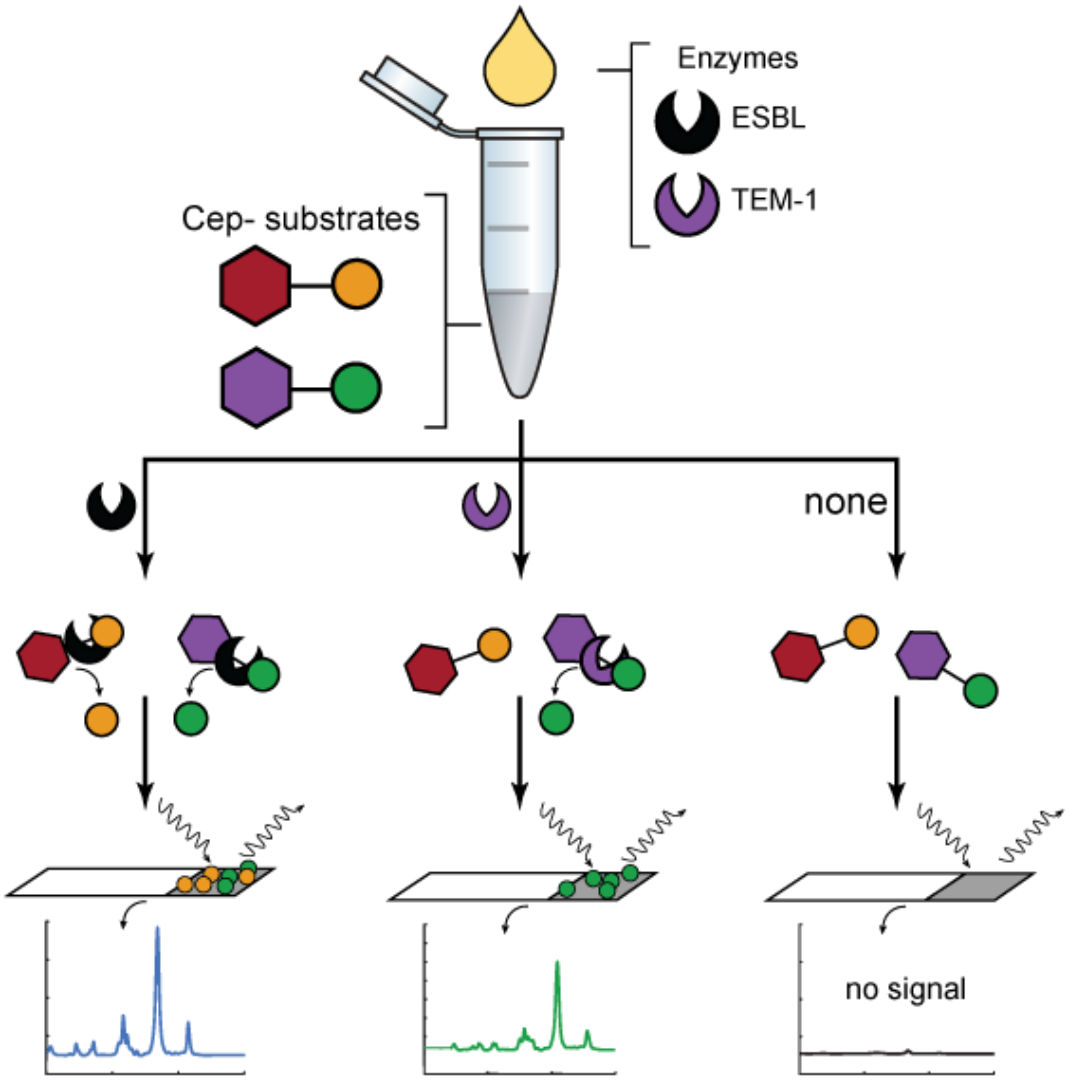

Figure 5.7. SERS can distinguish ESBL from non-ESBL TEM-1 through use of Cep-pNTP and Cep-diNTP substrates. SERS-active reporters in combination give different spectral readouts corresponding to three cases: presence of ESBL (left), non-ESBL (middle) or no β-lactamase in the sample.

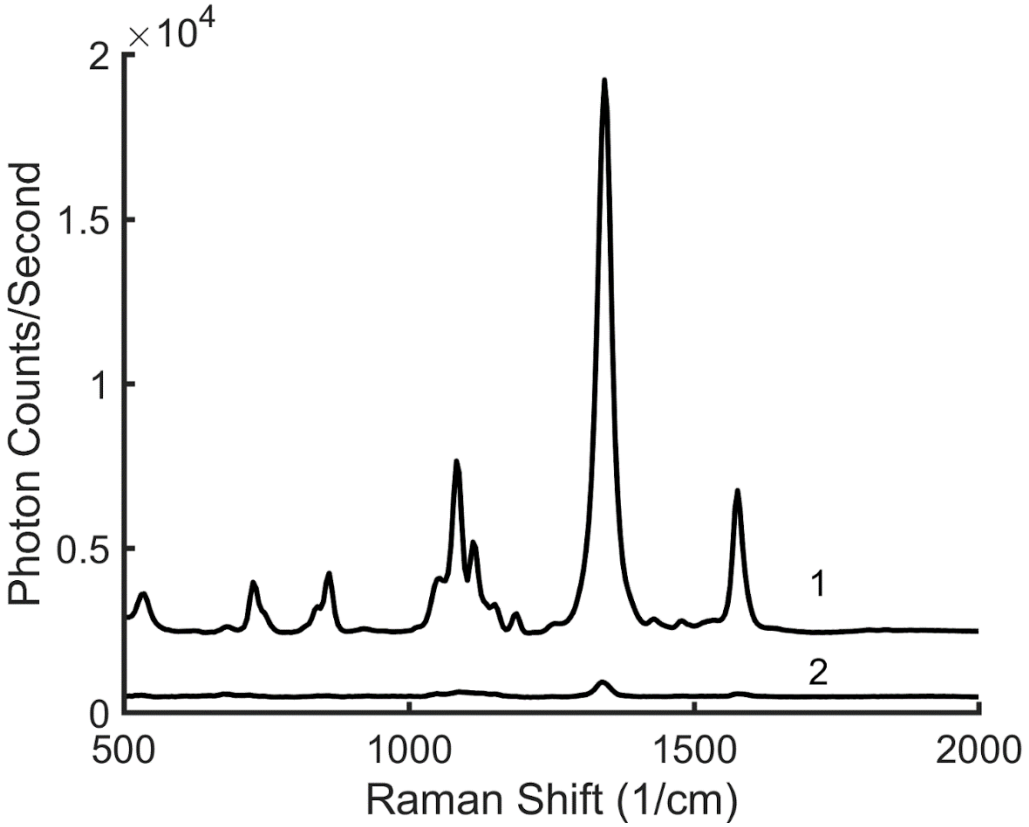

Figure 5.8. SERS spectra from both substrates with ESBL. Plot [1] **ESBL** (10 mU/mL) incubated with 0.25 mM of both substrates (Cep-pNTP, Cep-diNTP) in PB for 10 minutes. [2] is both substrates alone. These spectra are analyzed with those from Fig. 5.9 to demonstrate distinguishing ability.

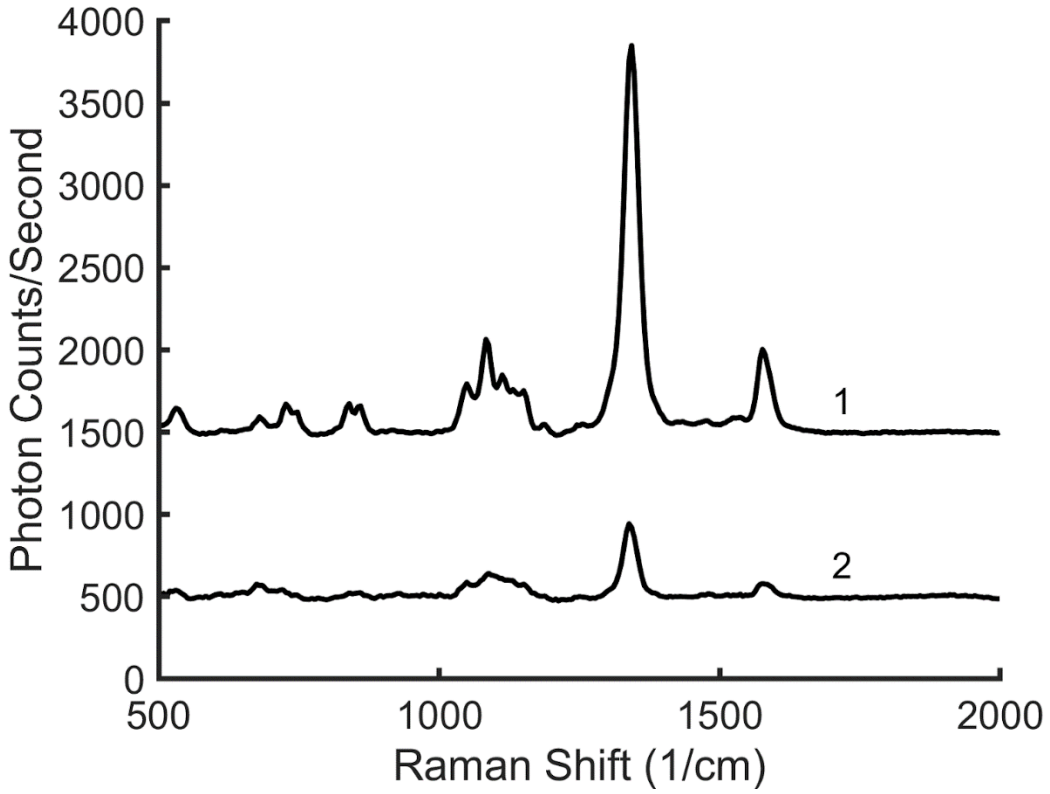

Figure 5.9. SERS spectra from both substrates with TEM-1 non-ESBL. Plot [1] is 1 U/mL of **TEM-1** classical β-lactamase enzyme with 0.25 mM of both substrates (Cep-pNTP, Cep-diNTP) in PB for 10 minutes. [2] is both substrates alone. These spectra are analyzed with those from Fig. 5.8 to demonstrate distinguishing ability.

We then add classical β-lactamase TEM-1 (non-ESBL) to an equal molar mixture of both substrates (Cep-pNTP, Cep-diNTP). Here in Fig. 5.9, we observe a different spectral readout in comparison to the previous plot (Fig. 5.8).

By calculating the ratios of the comparative signature peaks as outlined above in Table 5.1, we can distinguish the presence of ESBL versus TEM-1 in the full reaction that includes equal starting concentrations of Cep-pNTP and Cep-diNTP. Here we can observe the peak ratios to determine the relative presence of reporter corresponding to preferential cleavage behavior of ESBL versus TEM-1. From

calculated values in Table 5.2, we see the addition of TEM-1 into an equimolar substrate combination produces lower peak ratios (signatures of pNTP divided by diNTP), across all three diagnostic peaks at unique wavenumbers, indicating the greater presence of diNTP as the Cep-diNTP is preferentially hydrolyzed by the non-ESBL. With the addition of ESBL, we observe peak ratios generally closer to the values obtained with equimolar diNTP and pNTP shown in Table 5.1, with the implication that ESBL cleaves both substrates while TEM-1 cleaves the Cep-diNTP substrate more efficiently. Further characterization by enzyme kinetic studies would help elucidate this behavior.

	Peak ratios (photon counts of pNTP/diNTP)		
Wavenumbers	726:747	860:839	1088:1150
TEM-1	1.390	0.9195	2.087
ESBL	2.815	2.378	6.422

Table 5.2. Ratiometric calculations of diagnostic peak heights corresponding to pNTP and diNTP reporters following enzymatic cleavage. Compared to ratios in Table 5.1, the lower ratios of samples containing TEM-1 seen here indicate increased hydrolytic activity on Cep-diNTP (due to a larger denominator); samples containing ESBL have a ratio more similar to that of Table 5.1, suggesting ESBL acts on both substrates with minimal preferential behavior.

5.4. Conclusion

Here we have shown SERS to be a viable methodology for the multiplex detection of different β-lactamase enzymes within the same sample using a single sensor. Future work could characterize the behavior of enzyme-substrate kinetics in greater detail in

an attempt to better understand the ratiometric behavior of SERS reporters in multiplex detection of β-lactamase enzymes possessing different activity spectrums.

In continuing toward the creation of a suite of SERS reporter substrates, we can begin by the inclusion of commercially available ESBL substrates (Fig. 5.10) such as CENTA, an established chromogenic substrate, or ceftriaxone, a third-generation antibiotic that also happens to have a releasable thiol moiety that is also SERS active. From here, we may continue to synthesize more reporter-releasing substrates with varying amide side chains to tune specificities to different families of β-lactamases. At this point, we would implement a more sophisticated processing strategy for signal analysis of resultant SERS spectra, such as principal component analysis (PCA), or linear discriminant analysis (LDA).

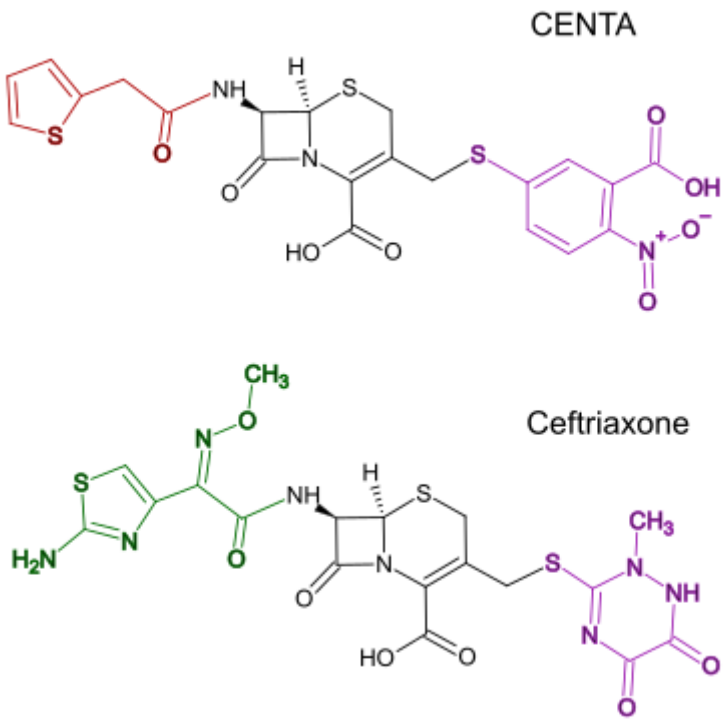

Figure 5.10. Two commercially available substrates that may serve as SERS reporters. SERS-active groups are labeled in magenta. CENTA is a first-generation cephalosporin with the corresponding side chain shown in red; ceftriaxone is a third-generation, with the corresponding side chain shown in green.

Chapter 6: Conclusion

6.1: Summary of findings

In the previous reports, we have established the chemical synthesis and characterization of detection substrates capable of reporting β-lactamase enzymatic activity. In this toolkit, we present Cep-glucose, a completely novel ESBL detection substrate, that releases glucose as a reporter that can be coupled into biochemical assay schemes enabling readout by three different modalities (absorbance colorimetry, fluorescence, electrochemical). We then elect the use of SERS as a readout modality with multiplexing capability, and detail the synthesis and behavior of two more previously undescribed detection substrates that can distinguish ESBL from non-ESBL in a single sample, single sensor format. Furthermore, we validate the great potential of our engineered assays by demonstrating successful performance with live bacterial cultures, as well as demonstrating drug resistance readout using unmodified store-bought personal glucose meters.

6.2: Contributions to the field and potential impact

6.2.1. Potential for direct impact on patient outcome

As our work directly detects the resistance activity conferred by the most common survival strategy employed by microbes associated with nosocomial infection, it lays the foundation for direct testing of patient clinical samples. Especially important in the interrogation of a clinical sample is multiplex detection, as the same pathogen is likely to produce a variety of beta-lactamases; therefore, the multiplex strategy offered by SERS offers a critical starting basis for expansion into practical use.

Though not directly addressed by this work as it also requires populational studies to assess accuracy rates, it is clear the application of our previously described assays to real clinical samples would yield results regarding bacterial susceptibility to cephalosporin treatment, directly informing the course of patient care, and therefore also health outcomes.

6.2.2. Potential impacts on public health

Antibiograms provide overall antimicrobial susceptibility profiles in order to serve as a treatment guide for regional hospital or healthcare systems. CLSI recommends the compilation of aggregate data at least annually with a minimum of 30 test isolates within the period analyzed. As our work aims to provide a diagnostic tool that is a rapid, post-culture test for resistance enzymes that is both inexpensive and can be performed in a standard lab, integration of our tool into the antibiogram workflow can speed compilation efforts by acting as an initial confirmatory test for clinical specimens regarding cephalosporin susceptibilities. This speed has the potential added benefit of facilitating more frequent antibiogram updates in order to more closely track cephalosporin resistance trends on the population scale especially as it pertains to this most commonly prescribed antibiotic class. Follow-up confirmatory tests can focus on any “hot spots” of resistance emergence to better allocate efforts in high-throughput susceptibility screenings for more efficient use of more resource-intense methodologies performed at central laboratories.

6.2.3. Supporting higher accessibility to healthcare

As our work has demonstrated resistance readout methodologies requiring simpler tools with lower technical expertise requirements than gold standard testing, we expect that it would make AST more commonplace. As optical plate readers are a standard unit of lab equipment, patient samples need not be shipped to central testing laboratories prior to days-long turnaround for results. Portable SERS instruments also brings additional multiplex capability to resistance testing outside of the central laboratory. If established as an AST methodology, even more isolated populations with the potential for bottlenecking of bacterial genetics can be profiled to trace the origins of resistance dissemination.

Our electrochemical testing proof-of-concept lays the real potential for finer adaptation of our Cep-glucose based ESBL assay for use with highly portable and commercially available personal blood glucose monitors (PGMs) that have been FDA approved for home use, making AST as quick and readily available as hourly blood-sugar testing for type 1 diabetics. Viability of PGMs as an AST method would follow a two-pronged approach: the further optimization assay conditions to maximize the release of glucose in our Cep-glucose scheme, and the customization of PGMs to have lower limits of detection for increased sensitivity.

Overall, the methodologies described in this work aim to lower the barrier of access to AST by implementing less time and labor-intensive assay strategies aimed at detection of the most common bacterial resistance strategy to the most commonly prescribed class of antibiotics.

6.3: Future work

6.3.1. Studies with mock matrices

Systematic testing the robustness of our assays in controlled matrices to include potential interferents (e.g., residual glucose, hydrogen peroxide, contaminating proteins, ions, reductants, oxidizers, etc.) would provide a first necessary step in adapting the assays for use in the clinic.

6.3.2. Studies with live bacteria

As all standard phenotypic detection methodologies are performed post-culture, our assays should be performed with various other strains of live bacteria from resistant isolates to confirm feasibility in clinical use.

6.3.3. Studies with clinical human samples.

Once the prior two future work goals are completed, robustness testing using real clinical samples from human patients on a population level would provide the necessary reliability data to determine precision, accuracy, etc. required prior to FDA approval.

6.3.4. Furthering SERS based multiplex detection

As discussed in Chapter 5, the synthesis of a suite of detection substrates each with unique SERS reporters (leaving group) that correspond to different cephalosporin generations (amide side chain) would provide an ultimate single-sample, single-sensor screen for cephalosporin resistance. Additionally, development of multiplex spectral analysis by way of signal processing methods could be then implemented in a

software format to automate analysis for easier user interpretation. Ultimately, this would pair with a sample workflow that integrates patient sample application into a single-package device, thus providing a powerful tool for resistance analysis beyond the central laboratory.

6.3.5. Ultra-convenient and pervasive resistance detection

Similar to creation of a suite of SERS-active reporter substrates, side chain modifications could provide a suite of glucose-releasing ESBL detection substrates for detection using the PGM. Because of its high portability and FDA approval, PGM repurposing for AST holds a huge potential for the sensing of specific resistance mechanisms, in our case the hydrolytic activity of ESBL. Studies to compare different levels of resistance corresponding to MIC would be useful in validating PGM performance; accordingly, as PGMs have already been optimized to report quantifiable levels of glucose in blood, the amount of resistance activity can in theory be quantified from a given patient sample, particularly pertaining to cases of sepsis. Immobilization of glucose oxidase and catalase in collection tubes could provide a streamlined sample preparation strategy to reduce background glucose levels. In considering other sample types, new sample prep methods could be engineered, custom test strips be designed, and custom glucometers could be adapted for dedicated use in the clinic or bedside. In the hospital, attachment of a device containing the Cep-glucose substrate to standard tubing equipment could be a potential strategy to monitor for the presence of ESBL producing organisms. Overall, enabling drug resistance detection in PGMs holds immense potential for simple and widespread AMR monitoring.

Appendices

Appendix 1. Verification spectra for PMB-Cep-glucose (Compound **1** and **2**).

Prepared by Dr. Shweta Ganapati, University of Maryland College Park (Chemistry & Biochemistry).

Cephem **1**: IR (ATR, cm^{-1}): 3327(w, br), 2981 (s), 1776 (m), 1717 (m), 1669 (w), 1516 (s), 1512 (m), 1454 (m), 1382 (m), 1248 (m), 1161 (m), 1030 (m), 907 (m), 823 (w), 7569 (m), 730 (s).^{1}H NMR (600 MHz, $CDCl_3$): 7.44 (d, *J* = 8.9, 1H), 7.28 - 7.20 (m, 7H), 6.83 (d, *J* = 8.6, 4H), 5.71 (dd, *J* = 4.7, 8.9, 1H), 5.17 (d, *J* = 11.7, 1H), 5.10 (d, *J* = 11.7, 1H), 4.97 (d, *J* = 9.9, 1H), 4.90 (d, *J* = 4.7, 1H), 4.28 (d, *J* = 13.7, 1H), 3.81 - 3.72 (m, 5H), 3.56 – 3.27 (m, 12 H), 2.96 (d, *J* = 13.7, 1H). ^{13}C NMR (150 MHz, $CDCl_3$): δ 172.0, 164.8, 162.3, 160.2, 134.4, 131.0, 129.6, 129.0, 128.0, 127.5, 126.8, 124.1, 114.3, 86.0, 79.8, 78.4, 72.8, 71.1, 68.6, 63.2, 59.7, 58.1, 55.5, 53.6, 43.5, 33.7, 31.1, 26.4. High-Res MS (ESI): *m/z* 669.1554 ($[M + Na]^+$), calculated for $C_{30}H_{34}N_2O_{10}S_2Na^+$ 669.1553.

Summary: The ^{1}H NMR shows coupling between H_a 7.44 ppm (d, *J* = 8.9, 1H) and H_b 5.71 ppm (dd, *J* = 4.7, 8.9, 1H), H_b 5.71 ppm (dd, *J* = 4.7, 8.9, 1H) and H_e 4.90 ppm (d, *J* = 4.7, 1H), $H_{c'}$ 5.17 ppm (d, *J* = 11.7, 1H) and H_c 5.10 ppm (d, *J* = 11.7, 1H), and $H_{f'}$ 4.28 ppm (d, *J* = 13.7, 1H) and H_f 2.96 ppm (d, *J* = 13.7, 1H), labeled in Figure 1. The splitting patterns of these peaks and their integrals are consistent with these assignments. Both systems, Hc', Hc and Hf', Hf have large coupling constants, 11.7 Hz and 13.7 Hz, respectively, due to germinal coupling. All the correlations inferred from coupling constants in the ^{1}H NMR spectrum are also observed in the COSY data shown in Figure 3. The COSY data also shows that proton H_d, the anomeric proton,

4.97 ppm (d, J = 9.9, 1H) correlates to its vicinal proton (C2) on the thioglucose ring, and its coupling constant of 9.9 Hz indicates that the two protons are axial to each other. Accordingly, the anomeric configuration is β.

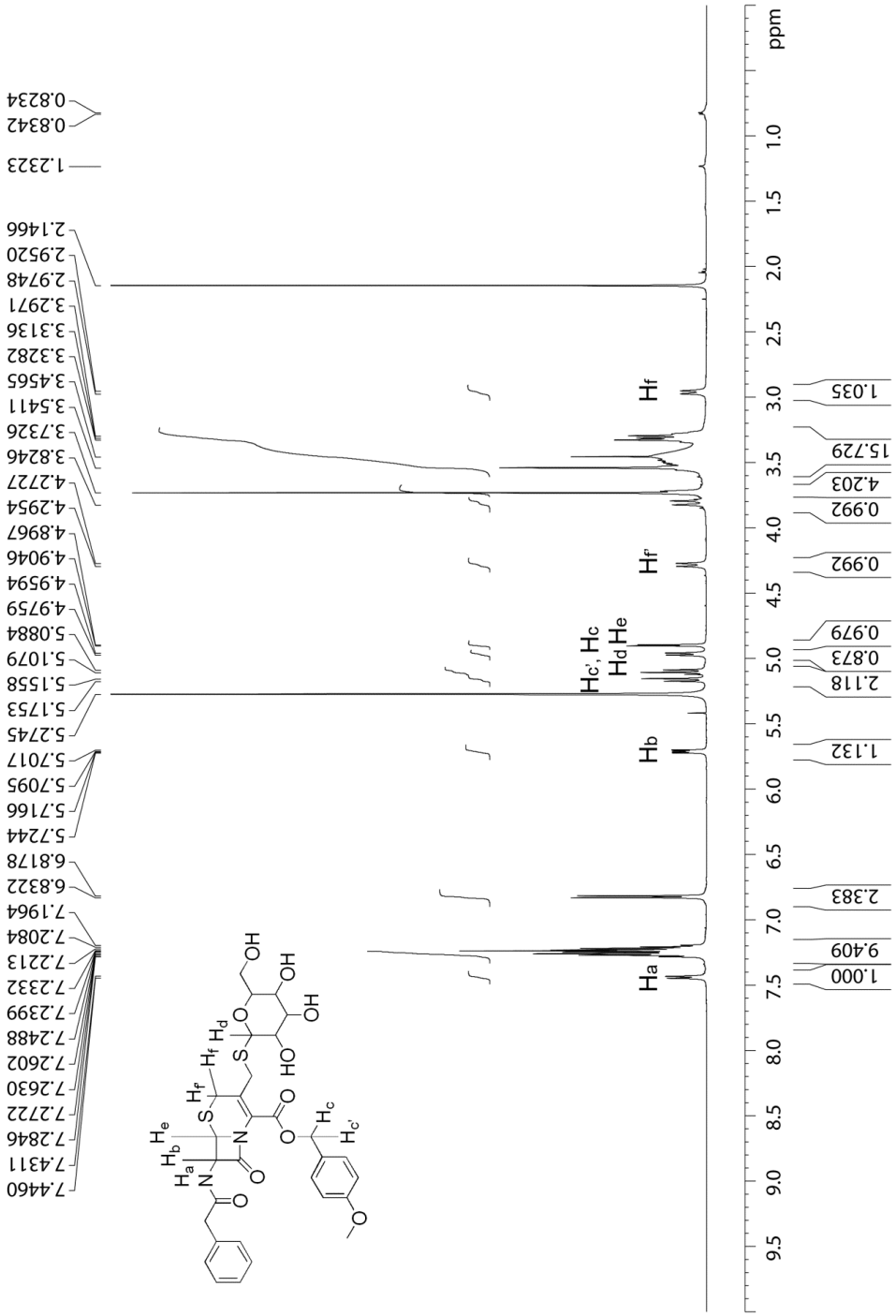

Figure A.1.1. ^{1}H NMR spectrum (600 MHz, $CDCl_3$) recorded for **1**.

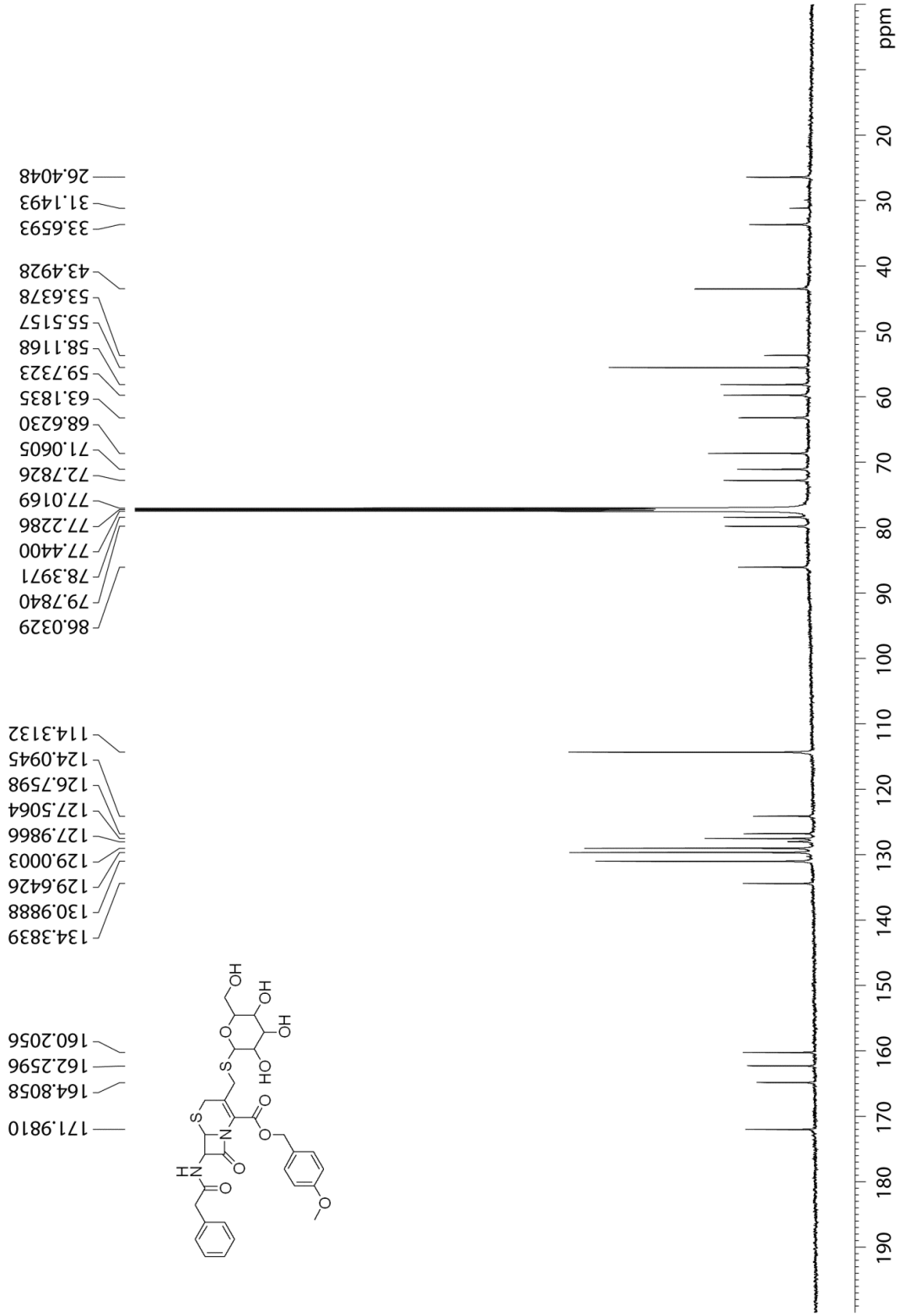

Figure A.1.2. ^{13}C NMR spectrum (150 MHz, $CDCl_3$) recorded for **1**.

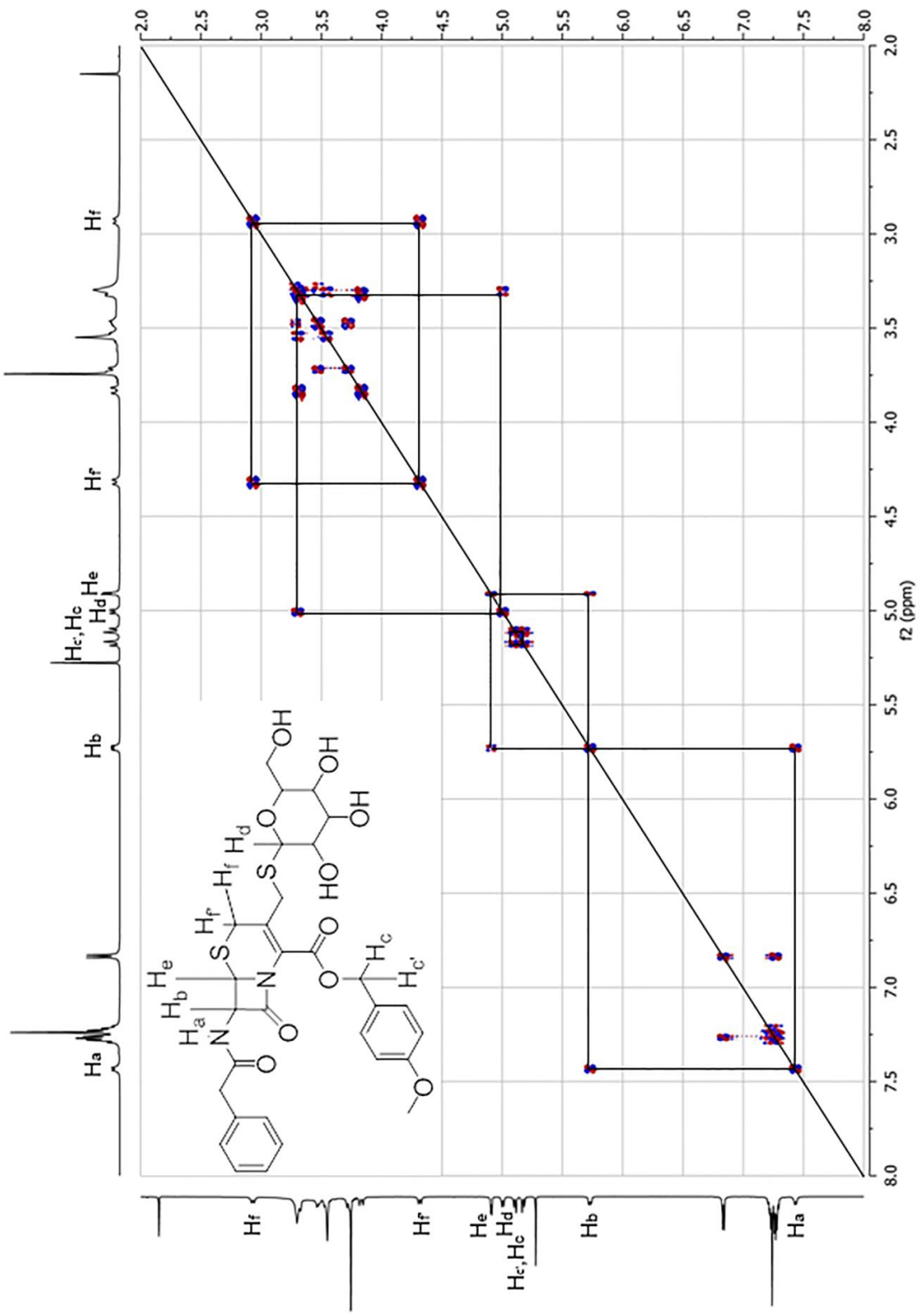

Figure A.1.3. COSY spectrum (600 MHz, $CDCl_3$) recorded for **1**.

Cephem **2**: ^{1}H NMR (600 MHz, CD_3CN): 7.37 (d, *J* = 8.0, 1H), 7.34 – 7.25 (m, 7H), 6.92 (d, *J* = 8.6, 2H), 6.28 (br s, 1H), 5.48 (br s, 1H), 5.42 (dd, *J* = 3.8, 8.0, 1H), 5.19 (d, *J* = 3.8, 1H), 5.11 (s, 2H), 4.19 (d, *J* = 9.7, 1H), 3.78 (s, 3H), 3.74 – 3.02 (m, 14 H). ^{13}C NMR (150 MHz, CD_3CN): δ 172.2, 168.5, 165.6, 161.0, 136.4, 131.6, 131.4, 131.1, 130.4, 130.2, 129.6, 128.5, 127.9, 122.0, 119.4, 118.4, 115.0, 84.9, 81.3, 79.3, 79.2, 73.6, 71.3, 68.5 62.8, 61.8, 56.0, 54.2, 50.4, 43.3, 35.7.

Summary: All NMR data for cephem **2** was collected in CD_3CN instead of $CDCl_3$ as the peaks were better resolved in CD_3CN. The ^{1}H NMR shows coupling between H_a 7.37 ppm (d, *J* = 8.0, 1H) and H_d 5.42 ppm (dd, *J* = 3.8, 8.0, 1H), and H_d 5.42 ppm (dd, *J* = 3.8, 8.0, 1H) and H_e 5.19 ppm (d, *J* = 3.8, 1H), labeled in Figure 4. The splitting patterns of these peaks and their integrals are consistent with these assignments. These correlations are also observed in the COSY data shown in Figure 6. The COSY data also shows that protons H_b 6.28 ppm (br s, 1H), and H_c 5.48 ppm (br s, 1H), are coupled to each other, Figures 6 and 7. Interestingly, these protons are broad singlets in the ^{1}H NMR spectrum, presumably with very small coupling constants. These protons are connected through 3 carbon atoms and show long range W-coupling due to the conformation of the cephalosporin ring system. In cephem **2**, protons H_f 5.11 ppm (s, 2H) correspond to a sharp singlet which does not correlate with any other protons. This singlet peak is in contrast to protons in the same position in cephem **1**, $H_{c'}$ 5.17 ppm (d, *J* = 11.7, 1H) and H_c 5.10 ppm (d, *J* = 11.7, 1H) which are diastereotopic. The correlation of anomeric proton H_g 4.19 ppm (d, *J* = 9.7, 1H) to its vicinal proton (C2) on the thioglucose ring is observed from the COSY data, Figure 6. Proton H_g in cephem **2** is upfield shifted by 0.8 ppm as compared to proton H_d 4.97 ppm (d, *J* = 9.9, 1H) at

the same position in cephem **1**. However, their coupling constants with the corresponding vicinal protons on the thioglucose rings are comparable (9.7 Hz and 9.9 Hz respectively), indicating that the anomeric conformation is β in both compounds.

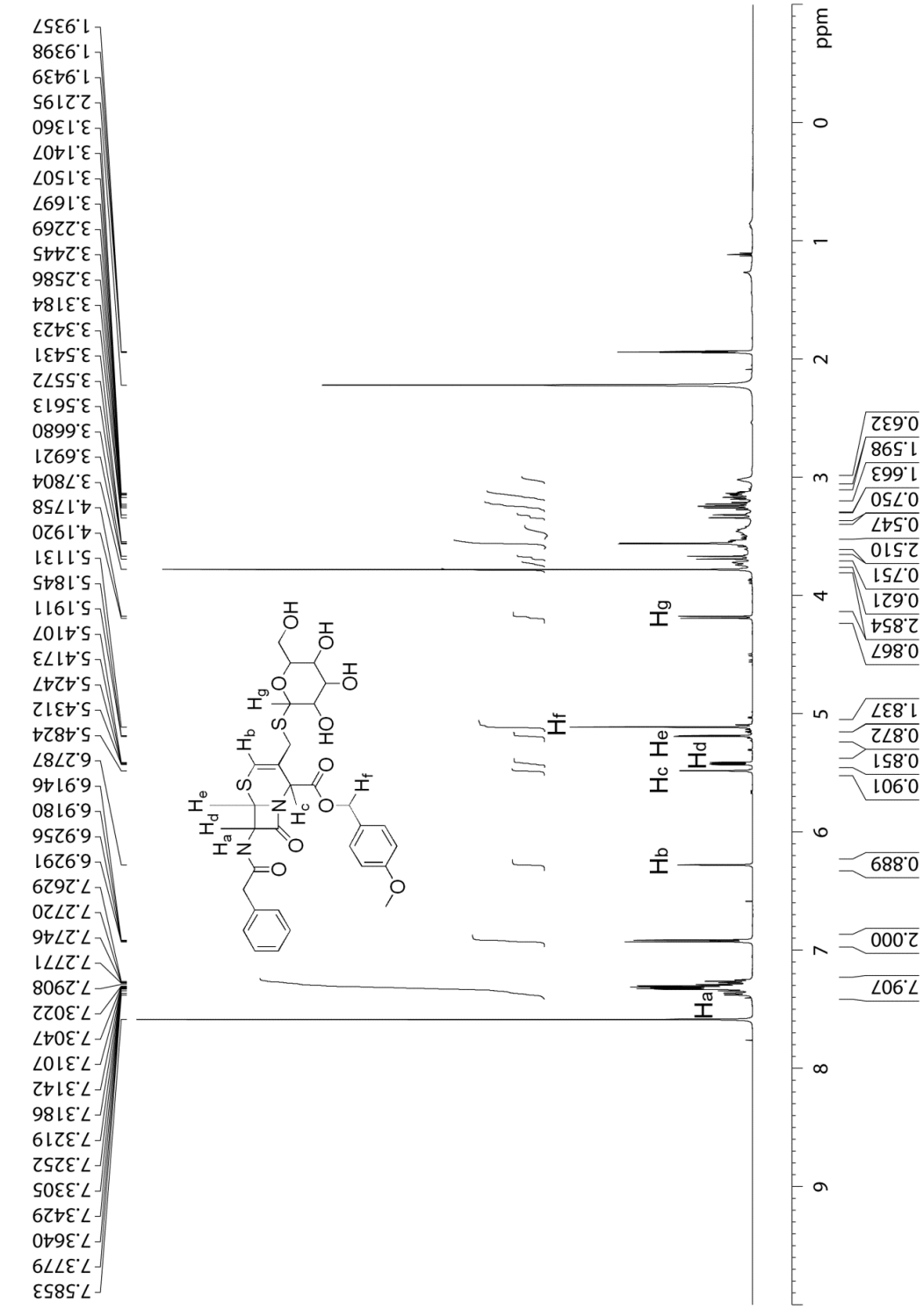

Figure A.1.4. ^{1}H NMR spectrum (600 MHz, CD_3CN) recorded for **2**.

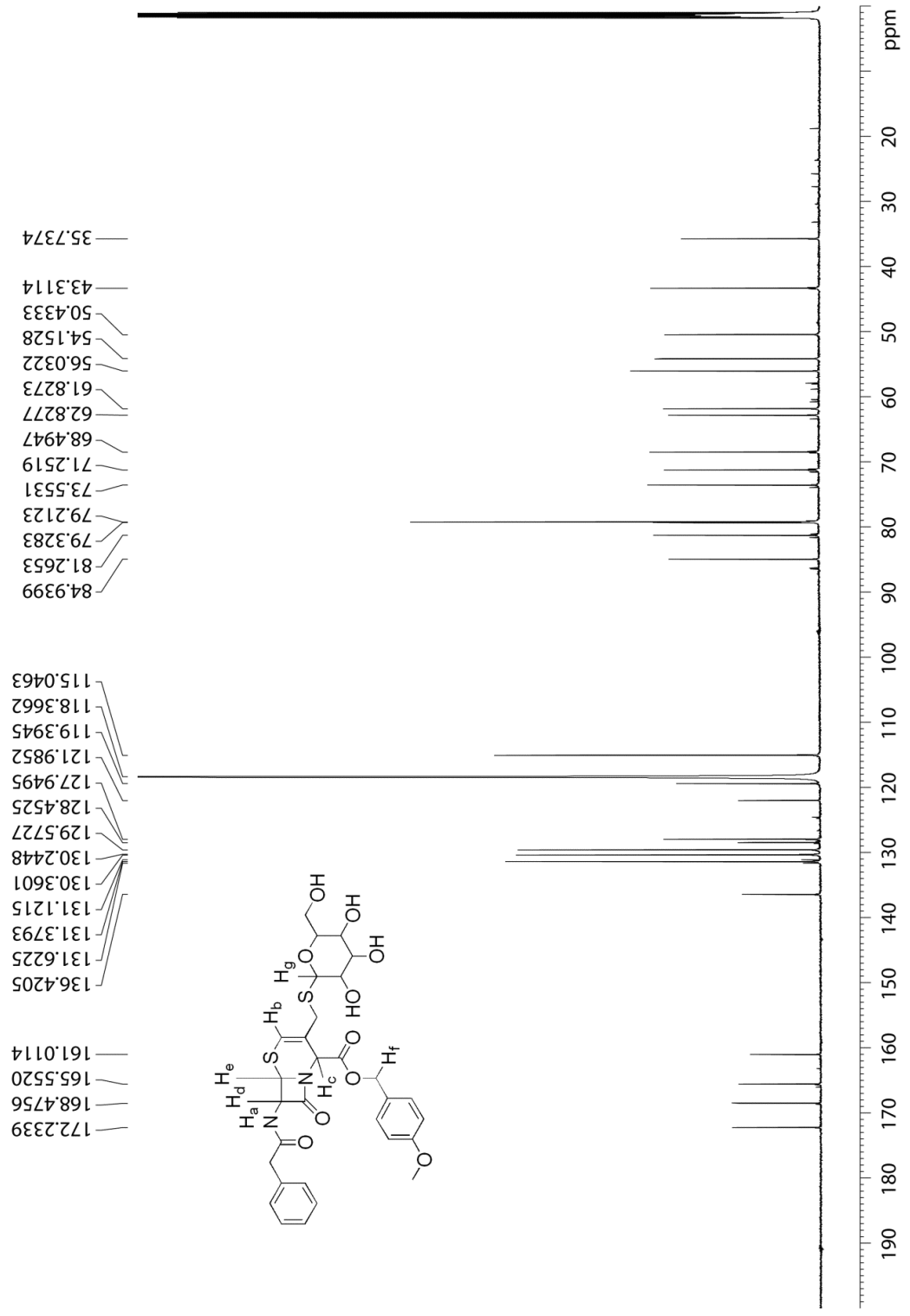

Figure A.1.5. ^{13}C NMR spectrum (150 MHz, CD_3CN) recorded for **2**.

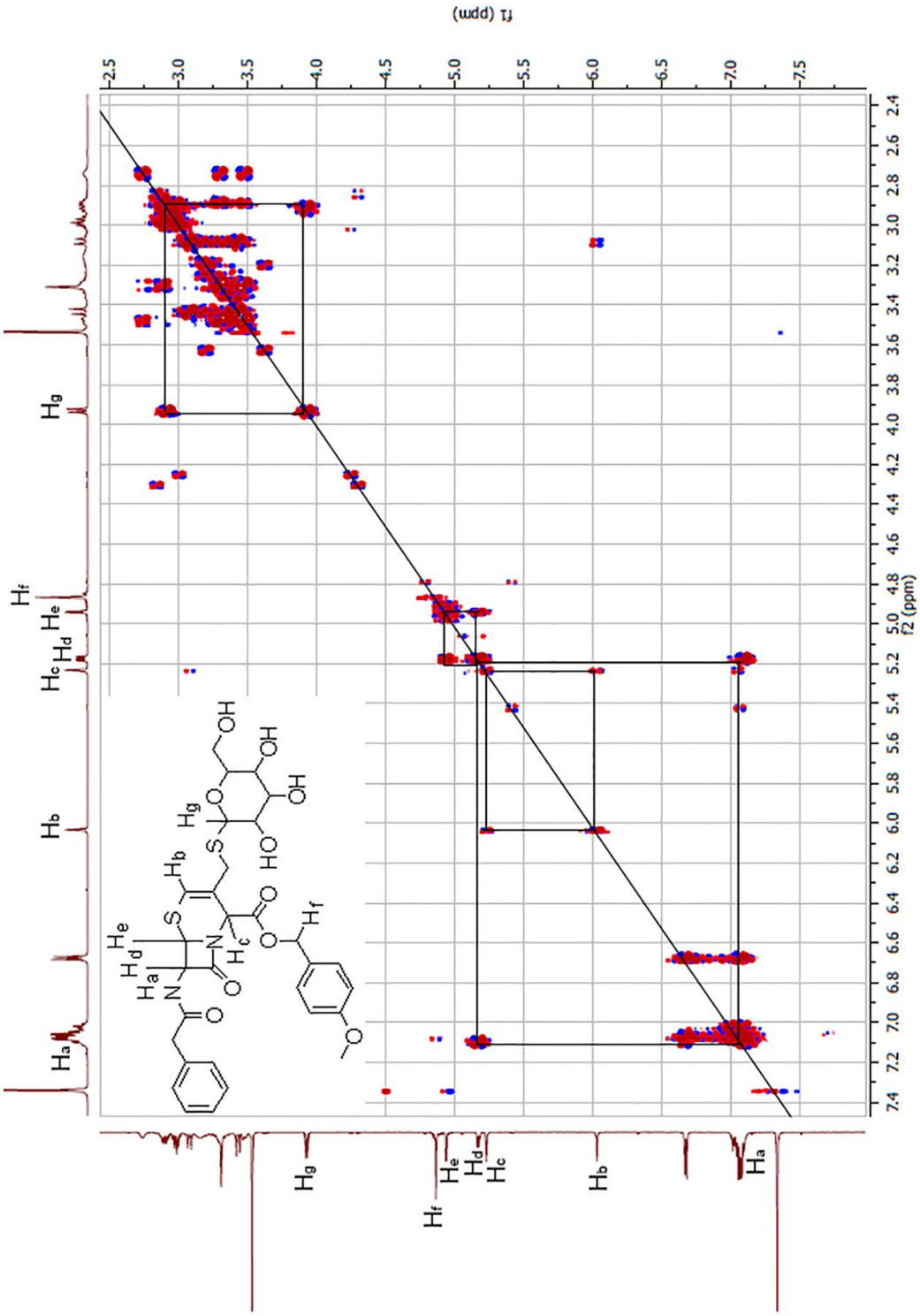

Figure A.1.6. COSY spectrum (600 MHz, $CDCl_3$) recorded for **2**.

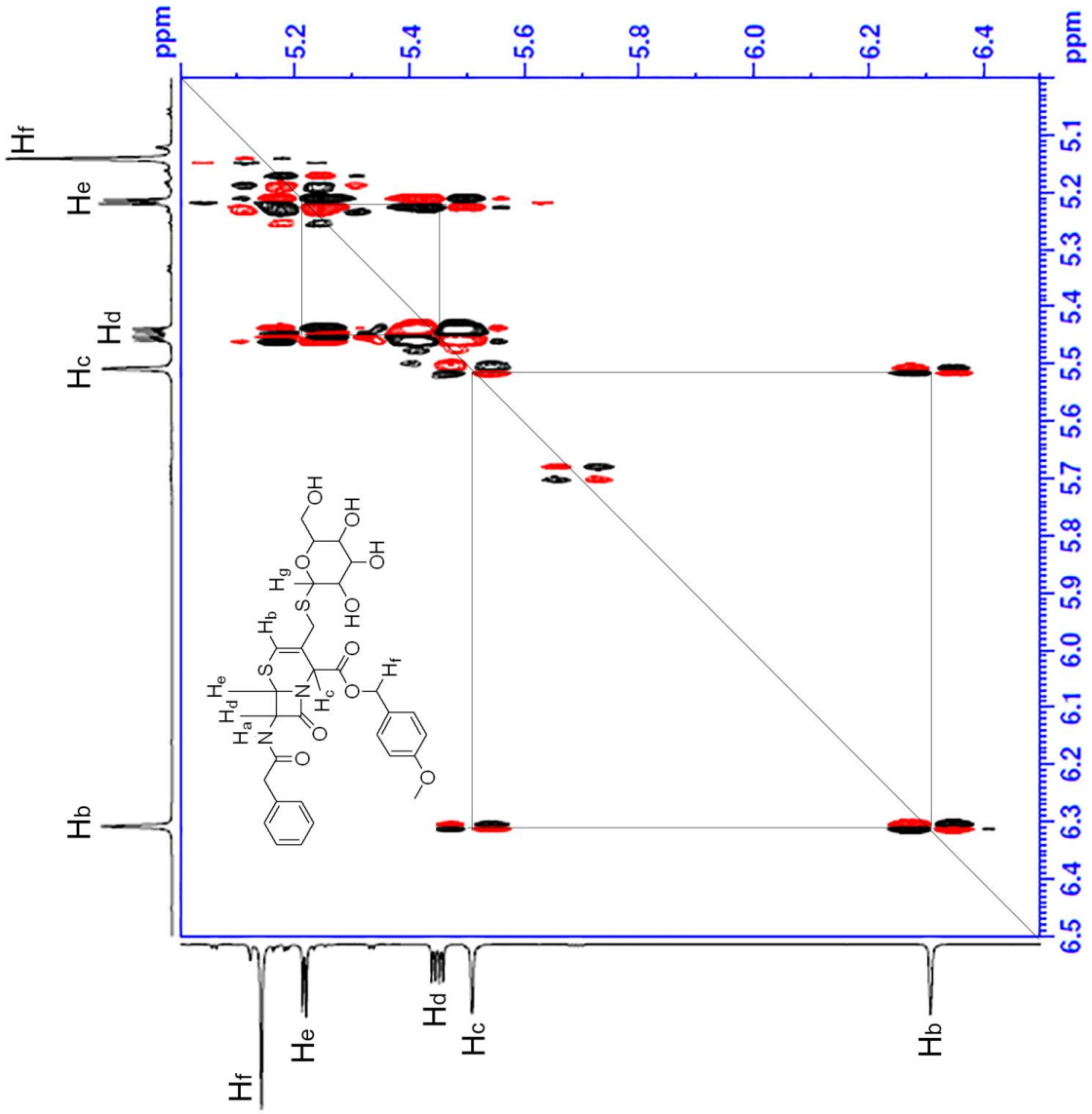

Figure A.1.7. COSY spectrum (600 MHz, $CDCl_3$) recorded for **2** showing correlation between H_b and H_c.

Appendix 2. Verification spectra for Cep-glucose (Compound **3**).

Prepared by Dr. David Watts, University of Maryland College Park (Chemistry & Biochemistry).

^{1}H NMR (600 MHz, 22 ^{o}C, DMSO-d_6), δ: 13.44 (bs, 1H), 9.08 (d, *J* = 8.3 Hz, 1H), 7.33 – 7.25 (m, 4H), 7.22 (tt, *J* = 6.9, 1.8 Hz, 1H), 5.63 (dd, *J* = 8.3, 4.7 Hz, 1H), 5.06 (d, *J* = 4.7 Hz, 1H), 4.19 (d, *J* = 9.7 Hz, 1H), 3.94 (d, *J* = 13.6 Hz, 1H), 3.76 (d, *J* = 17.8 Hz, 1H), 3.66 (d, *J* = 11.9 Hz, 1H), 3.59 – 3.52 (m, 2H), 3.52 – 3.42 (m, 3H), 3.17 – 3.08 (m, 2H), 3.08 – 3.01 (m, 1H), 3.00 – 2.94 (m, 1H). Glucose alcohol protons appear at 3 – 5.5 ppm but are too broad to integrate.

HRMS, ESI (-): *m/z* 525.0150 ([**3** - H]$^-$), calculated for $C_{22}H_{25}N_2OS_2^-$ 525.1007.

Summary: ^{1}H-NMR shows coupling between H_a 9.08 ppm (d, *J* = 8.3 Hz, 1H) and H_b 5.63 ppm (dd, *J* = 8.3, 4.7 Hz, 1H), as well as H_b 5.63 ppm (dd, *J* = 8.3, 4.7 Hz, 1H) and H_e 5.06 ppm (d, *J* = 4.7 Hz, 1H), labeled in Figure A.2.1. These assignments are supported by COSY NMR (Fig A.2.3). $H_{f'}$ 3.94 ppm (d, *J* = 13.6 Hz, 1H) was assigned based on an identical *J* coupling value and similar chemical shift to the analogous proton in **1** while COSY data shows that the coupled geminal proton H_f is overlapping with other peaks at 3.46 ppm. Importantly, in the spectrum of **3**, all the protons associated with the *p*-methoxy benzyl protecting group are missing while the lactam protons H_b and H_e are still present (Fig A.2.2) with similar *J* coupling and chemical shifts, suggesting the lactam remains intact. Additionally, the anomeric C-H_d proton 4.19 ppm (d, *J* = 9.7 Hz, 1H) still has a large *J* coupling value indicating β configuration

of the glucose moiety is retained. Finally, the new carboxylic acid proton appears as a broad singlet at 13.44 ppm while the alcohol protons on the thio-glucose fragment appear as a very broad unintegrateable resonance (3 – 5.5 ppm), likely due to fast exchange with residual H_2O.

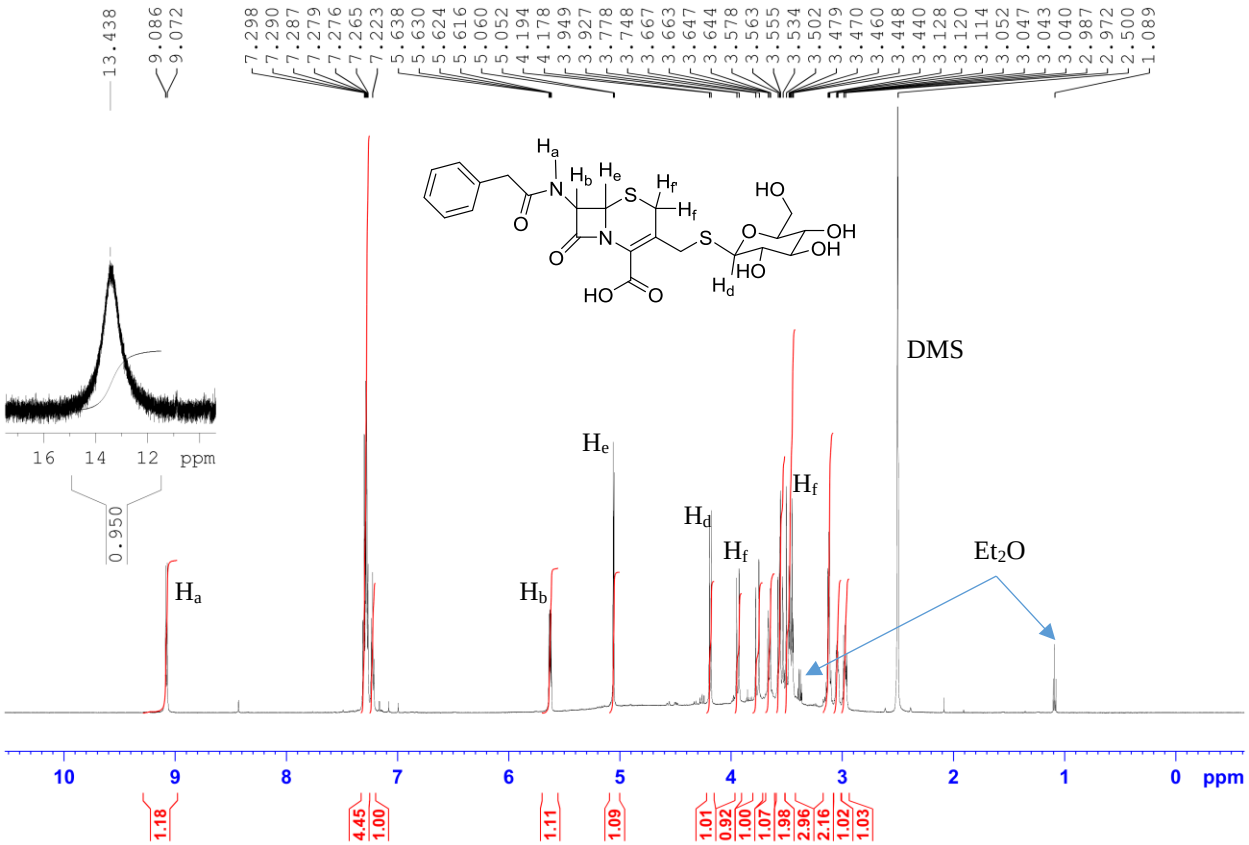

Figure A.2.1. ^{1}H-NMR spectrum (600 MHz, DMSO-d_6) recorded for **3**.

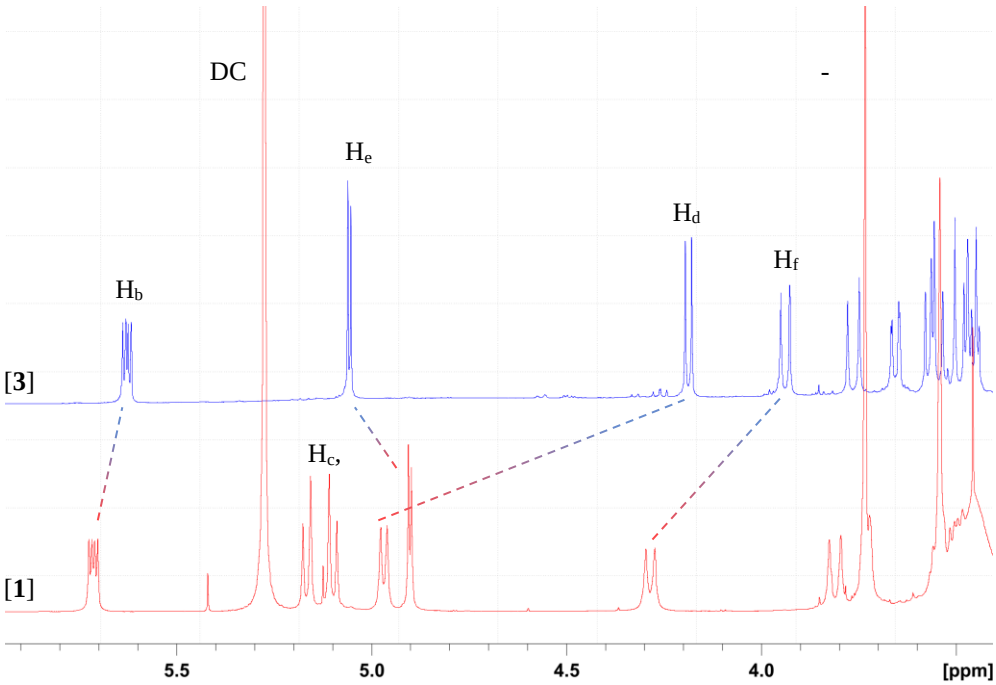

Figure A.2.2. Comparison of the 3.5 – 6 ppm range in the ^{1}H-NMR spectra of cep-glucose, **3**, (blue trace, 600 MHz, DMSO-d_6) and PMB-cep-glucose, **1**, (red trace, 600 MHz, $CDCl_3$). Of note is the absence of the protecting group methylene protons H_c and $H_{c'}$ and methoxy group OCH_3 (3.73 ppm) in the spectrum of cep-glucose, **3**, while the lactam protons H_b and H_e are retained.

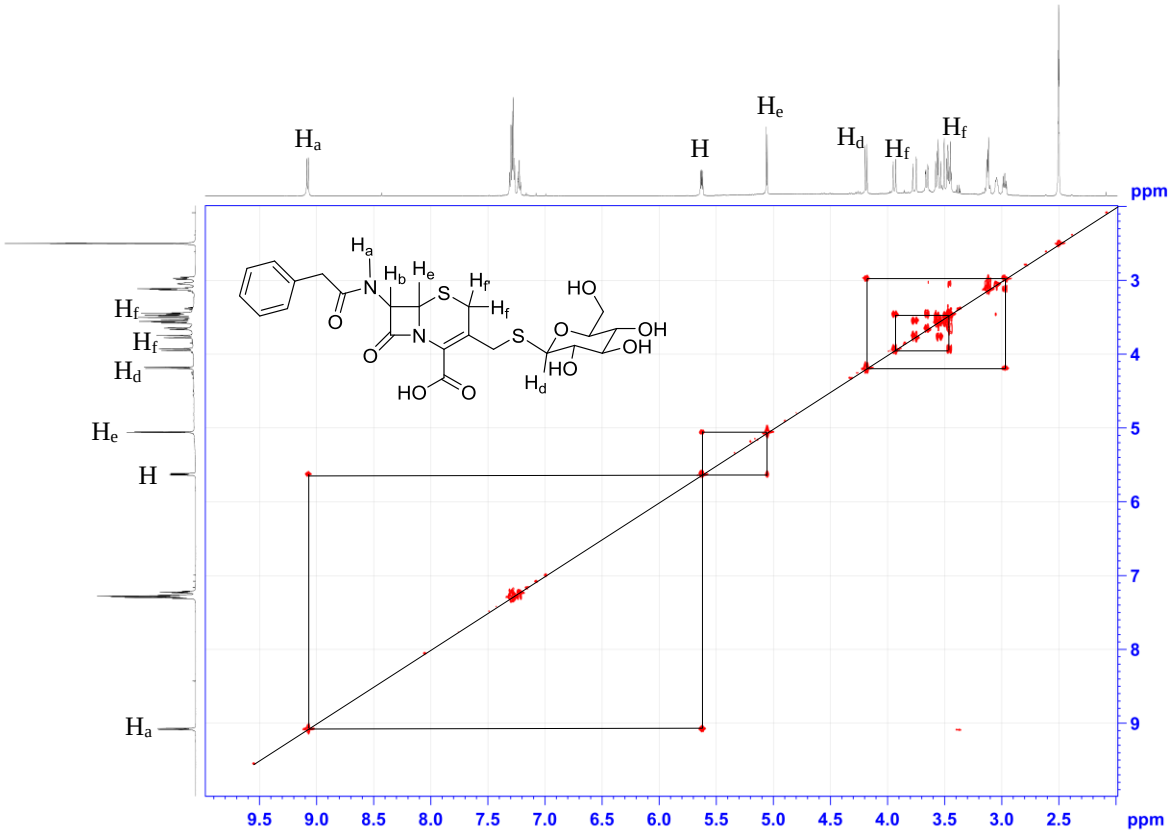

Figure A.2.3. COSY NMR spectrum (600 MHz, DMSO-d_6) recorded for cep-glucose, **3**.

Appendix 3. LC-MS experimental data for PMB-Cep-glucose and Cep-glucose

Prepared by Dr. David Watts, University of Maryland College Park (Chemistry & Biochemistry).

LC-MS Conditions:

For all LC-MS experiments, an injection volume of 5 µL was used and the mobile phase consisted of 0.1% formic acid solution (A) and methanol (B). The separation was performed on an Agilent 1100 as follows: the concentration of solvent B started at 10 % from 0 to 2.0 min, linearly increased to 75 % at 7.0 min, increased to and kept at 100 % from 9.0 to 12.0 min, then decreased to and kept at 10 % from 13.0 to 15.0 min. A reverse-phase Imtakt Cadenza-C_{18} column (2.0·50mm, particle size 3 µm) was used, and the flow rate was set to 0.25 ml/min. Chromatograms were produced using a 190 – 400 nm UV detector.

The HPLC was fed into a Jeol AccuTOF ESI mass spectrometer operating in negative mode with a needle voltage set to -2100 V and 250 °C vaporizing temperature. A spectral window of 150 – 800 *m/z* was monitored.

LC-MS of PMB-cep-glucose (1):

A sample of PMB-cep-glucose (**1**) (267 µg, 4 nmol, 2 mM final concentration) was dissolved in 0.2 mL MeOH and analyzed by LC-MS. Only one peak in the chromatogram was observed (Fig S*****). The mass spectrum showed masses belonging to $[\mathbf{1} - H]^-$, $[\mathbf{1} + HCOO]^-$, $[\mathbf{1} + COOCF_3]^-$ (Fig S*****). Formate comes from HPLC mobile phase solution (A) while the trifluoroacetate is a contaminant possibly

originating from the deprotected cep-glucose product (**3**) which had been analyzed prior to this sample on the same column.

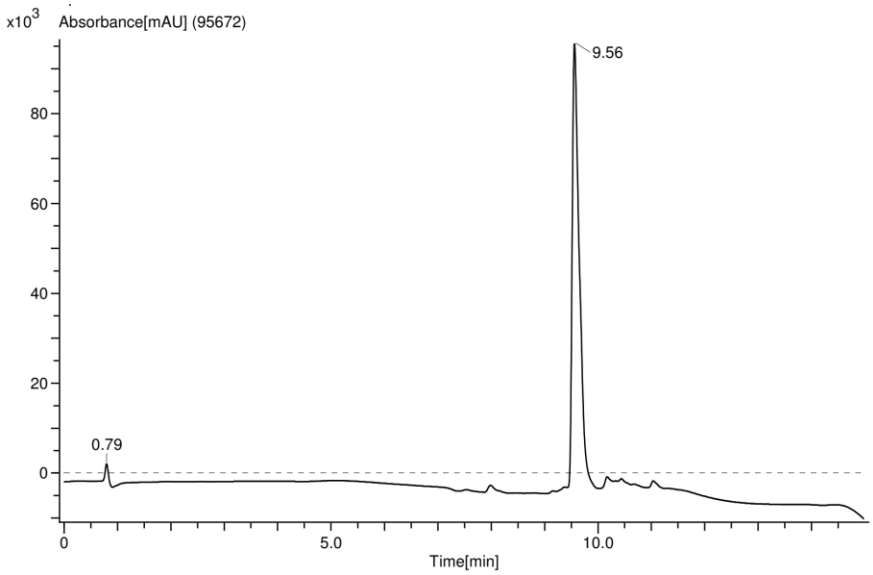

Figure A.3.1. Chromatogram of PMB-cep-glucose (**1**) showing a retention time of 9.56 min.

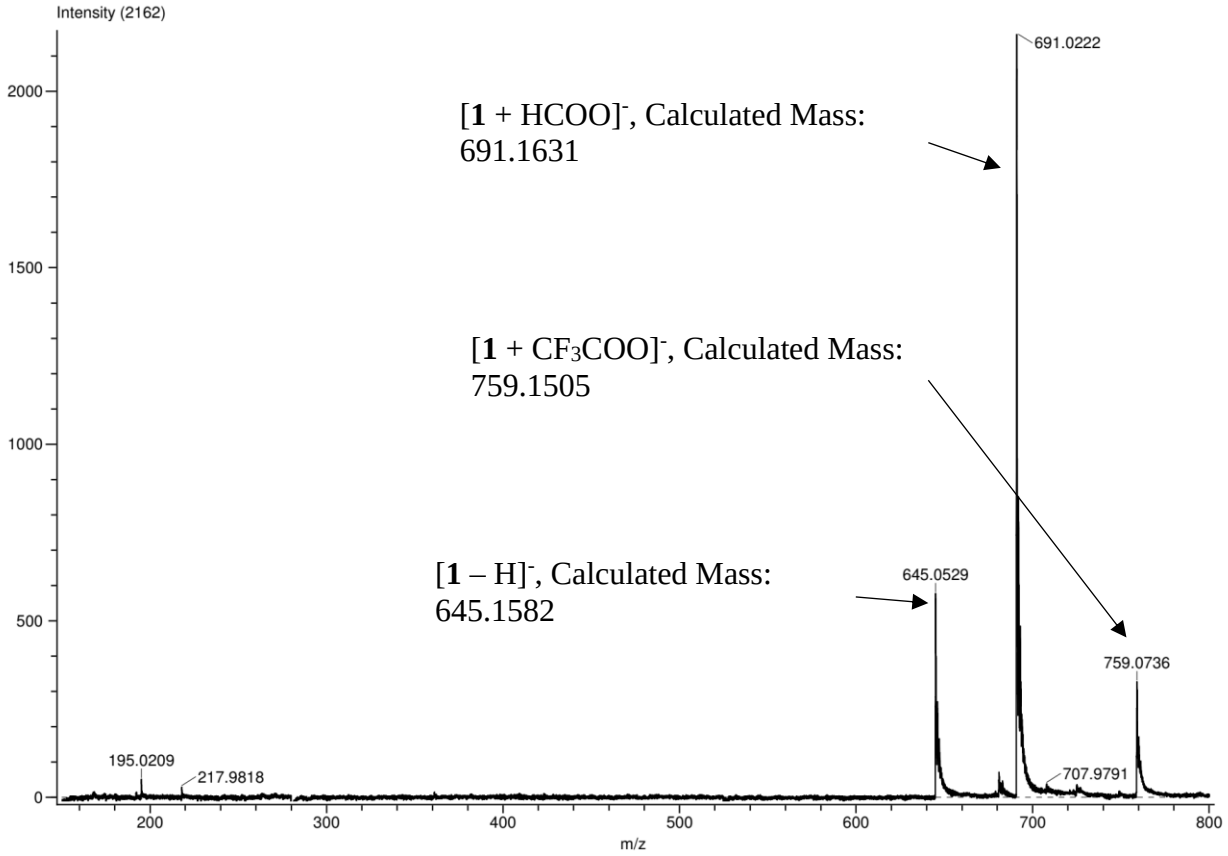

Figure A.3.2. Mass spectrum of the 9.56 min chromatogram peak showing PMB-cep-glucose (**1**) upon eluting from the HPLC column.

LC-MS of cep-glucose (3):

A sample of cep-glucose (**3**) (157 μg, 300 nmol, 1 mM final concentration) dissolved in 0.15 mL 0.1 M phosphate buffer (pH 6.5) was analyzed by LC-MS. Only one peak in the chromatogram was observed with a retention time of 8.06 min (Fig A.3.3). The mass spectrum of this peak shows only one major species, belonging to [**3** – H]$^-$ (Fig A.3.4).

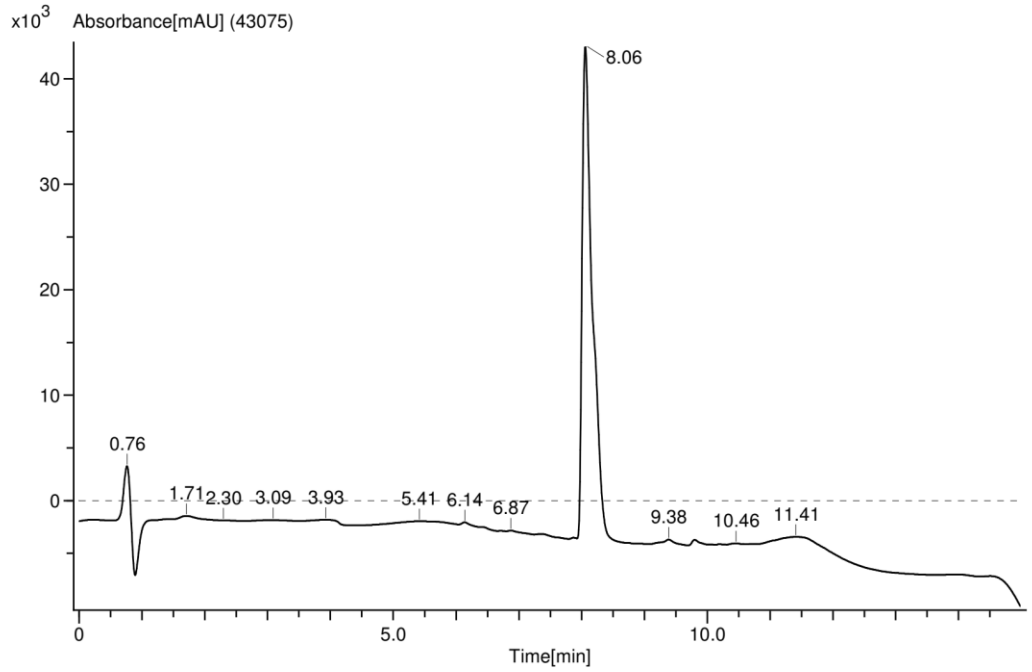

Figure A.3.3. Chromatogram of cep-glucose (**3**) showing a retention time of 8.06 min.

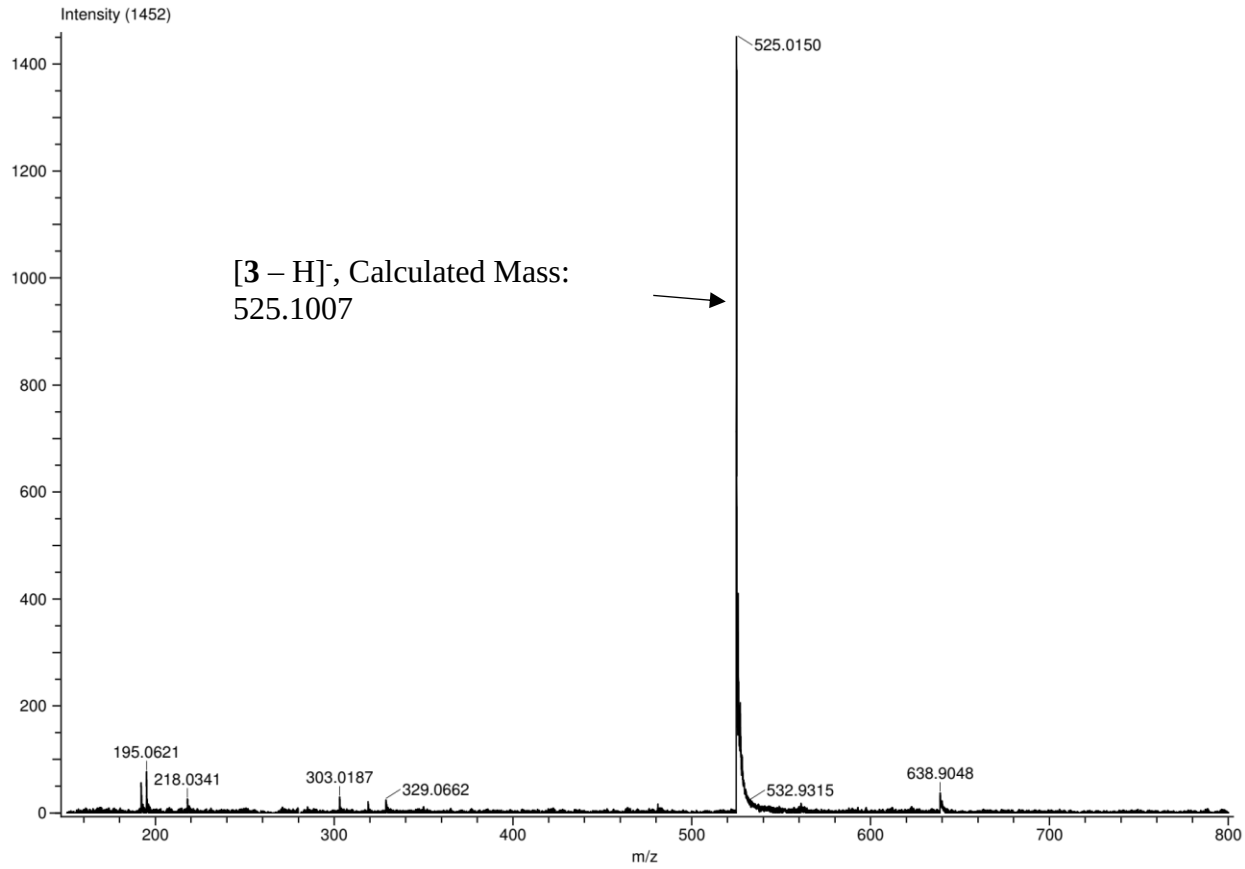

Figure A.3.4. Mass spectrum of the 8.06 min chromatogram peak showing cep-glucose (**3**) upon eluting from the HPLC column.

Using Ellman's reagent to visualize thioglucose release by LC-MS:

In order to visualize the release of thioglucose by LC-MS, Ellman's reagent (dithio nitrobenzoic acid, DTNB) was used. DTNB absorbs in the UV region and therefore both the reagent itself and its derivatives are observed in the chromatogram. Secondly, due to the presence of a carboxylic acid moiety on both aryl rings, DTNB and its derivatives are easily ionized and observed in negative mode by ESI-MS.

LC-MS analysis of cep-glucose (**3**) in the presence of Ellman's Reagent:

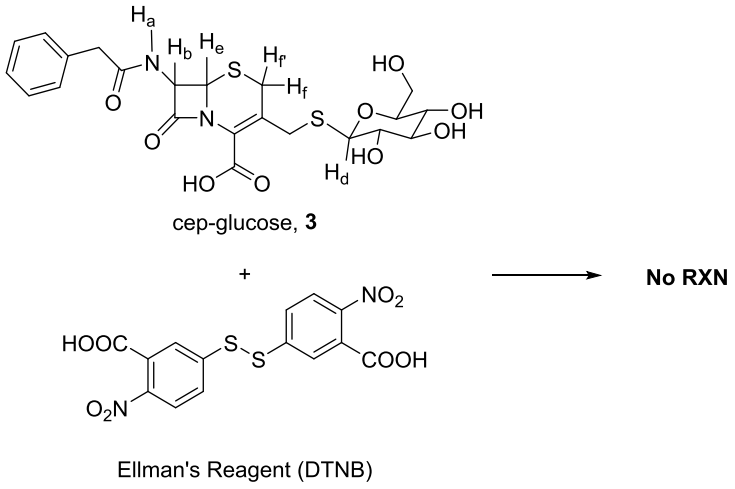

Cep-glucose (**3**) (1 mM final concentration) was combined with DTNB (1 mM final concentration) in 150 µL of 0.1 M phosphate buffer (pH 7). After incubating at 25 °C for 60 min, the reaction mixture was analyzed by LC-MS. The chromatogram showed three peaks (Fig A.3.7.a) with retention times 0.92, 8.07, and 9.41 min. Nothing was observed in the mass spectrum for the peak eluting at 0.92 min (Fig A.3.7.b) and so it was assigned as the solvent front. The 8.07 min peak, with identical retention time to pure cep-glucose (**3**), indeed only showed [**3**-H]$^-$ in the mass spectrum (Fig A.3.7.c). The 9.41 min peak was found to belong to DTNB (Fig A.3.7.d). No mass belonging

to the mixed disulfide originating from the reaction of free thioglucose with DTNB was observed.

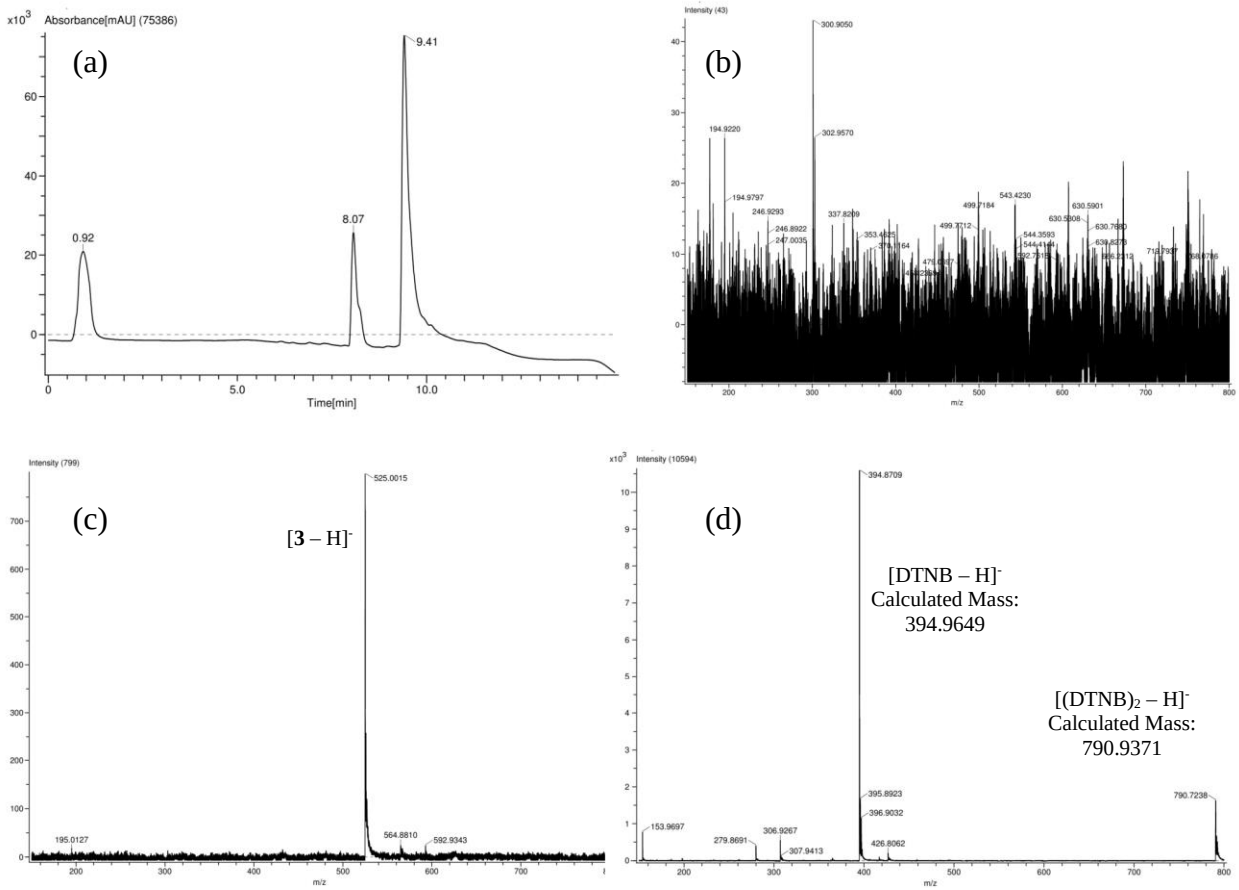

Figure A.3.7. LC-MS analysis of the mixture of cep-glucose (**3**) and Ellman's reagent. a) Chromatogram showing three different peaks assigned as the solvent front (0.92 min), cep-glucose (**3**) (8.07 min), and Ellman's reagent (DTNB) (9.41 min). b) Mass spectrum of the 0.92 min eluent, solvent front. c) Mass spectrum of the 8.07 min eluent showing cep-glucose (**3**) d) Mass spectrum of the 9.41 min eluent showing Ellman's reagent (DTNB).

LC-MS analysis of cep-glucose in the presence of Ellman's Reagent:

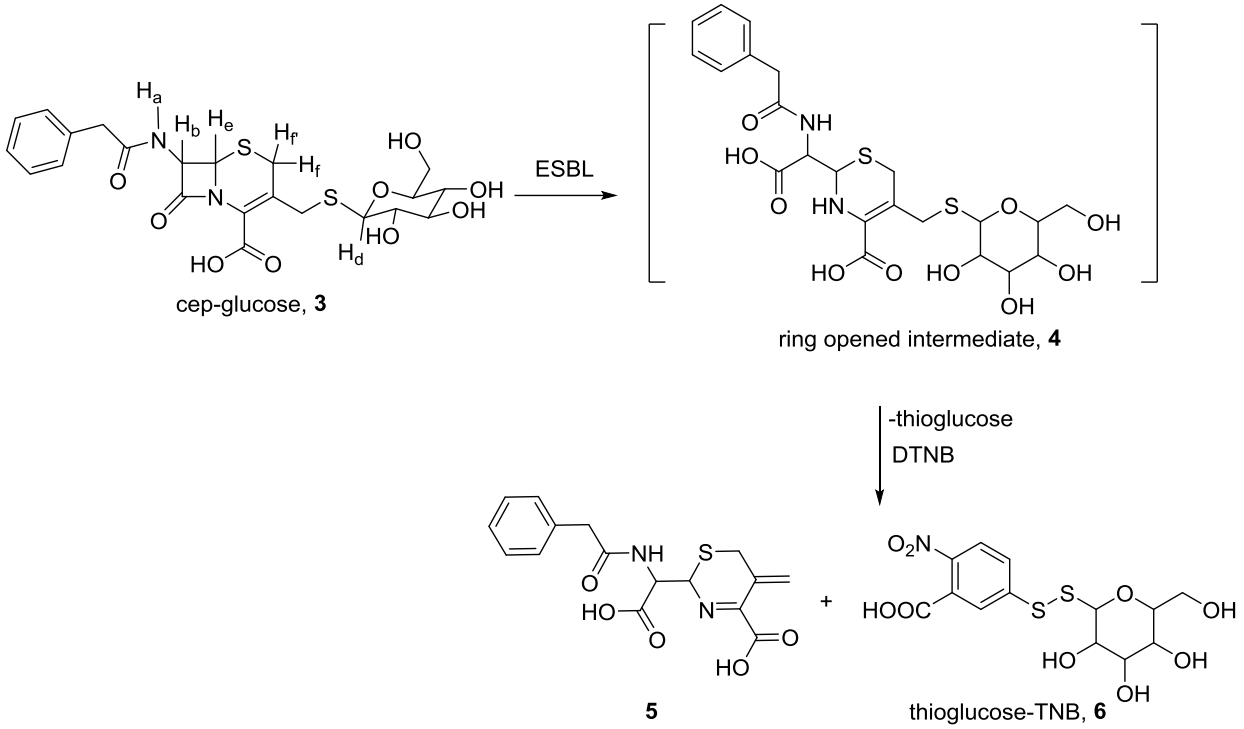

Cep-glucose (**3**) (1 mM final concentration) was prepared in 150 µL 0.1 M phosphate buffer (pH 7.0) along with DTNB (1 mM final concentration). ESBL (1 U/ mL final concentration) was then added and the reaction mixture incubated at 25 °C for 1 h. To remove ESBL, the whole volume (150 µL) was purified through an Amicon Ultra centrifugal filter (regenerated cellulose, 3000 MWCO) in a benchtop centrifuge at 14,000 RCF for 15 min. The filtrate was collected and analyzed by LC-MS. Analysis of the chromatogram (Fig A.3.8.a) shows that the peak corresponding to cep-glucose (**3**) (retention time = 8.07 min) has disappeared and a new peak with a retention time of 7.07 min has appeared. Analysis of the mass spectrum of the new 7.07 min peak shows that it is comprised of two major species: the ring opened intermediate **4** (appearing as [**4** – H]$^-$, *m/z* 392.0115), and the mixed disulfide thioglucose-TNB (**6**) (appearing as [**6** – H]$^-$, *m/z* 543.1113) resulting from the interception of free thioglucose by Ellman's reagent (DTNB). Further analysis shows

that **4** arrives at the spectrometer slightly earlier than **6** (Figures A.3.8.b and A.3.8.c). Because it is in excess, unreacted DTNB is also observed in the chromatogram (retention time = 9.39 min) (Fig A.3.8.d). The other product of thioglucose elimination, **5**, was not observed.

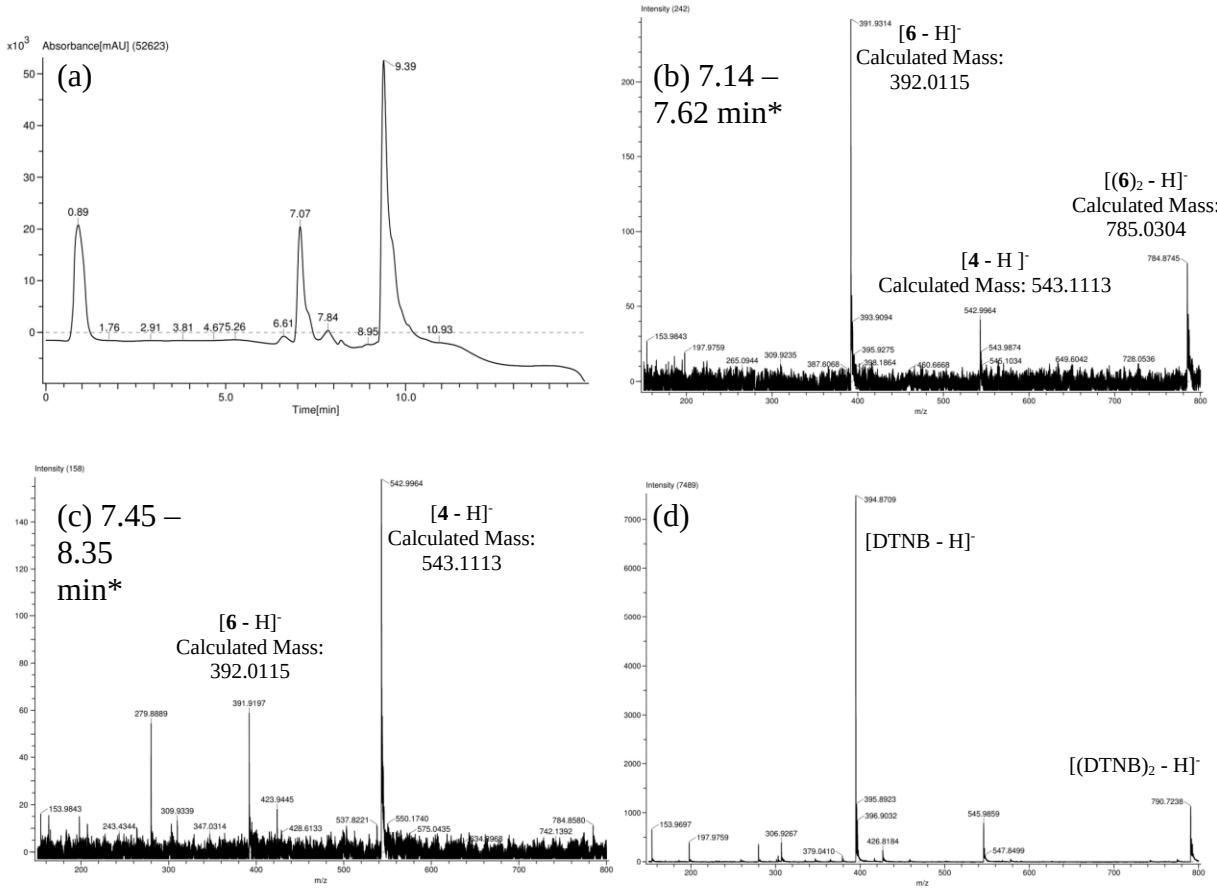

Figure A.3.8. LC-MS analysis of the reaction of cep-glucose (**3**) and ESBL in the presence of Ellman's reagent (DTNB). a) Chromatogram showing three peaks assigned as the solvent front (0.89 min), product mixture (7.07 min) and DTNB (9.39 min). b) Mass spectrum of eluent corresponding to the 7.07 min chromatogram peak, arriving at the mass spectrometer at 7.14 – 7.62 min. c) Mass spectrum of eluent corresponding to the 7.07 min chromatogram peak, arriving at the mass spectrometer at 7.45 – 8.35 min. d) Mass spectrum of eluent corresponding to 9.39 min peak. *Times recorded in the mass spectrum are higher than in the chromatogram due to the time it takes the eluent to travel from the HPLC to the spectrometer.

Appendix IV. Stability of Cep-glucose in aqueous solution.

The figures below detail performance of the Cep-glucose detection substrate alongside commercially purchased CENTA as they are kept in an aqueous preparation of 0.1 M phosphate buffer at +4°C for 1, 7, and 14 days post-preparation (Figs. A.4.1, A.4.2, A.4.3, respectively). Solutions are brought to r.t. and Ellman's reagent (diluted to 250 μM final concentration from 100 mM stock prepared in DMSO) is added prior to experimental use.

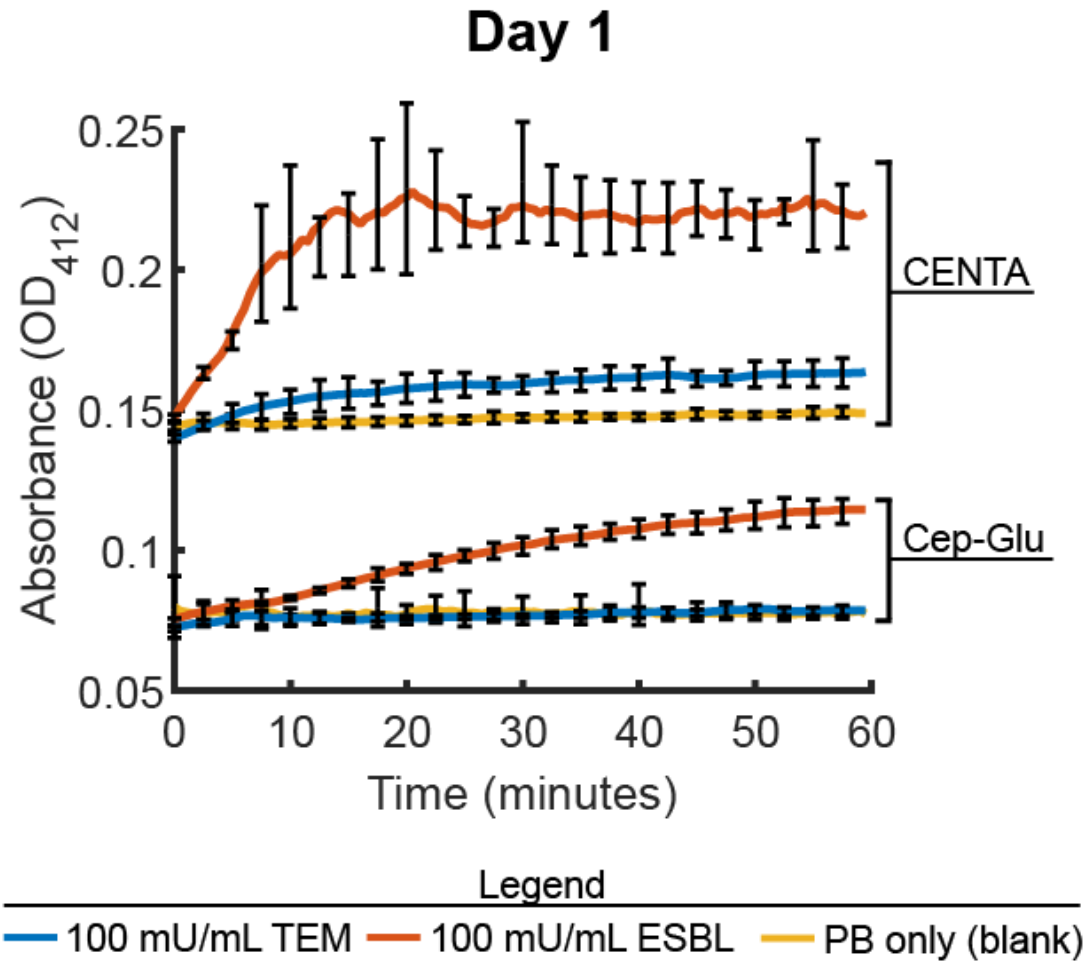

Fig. A.4.1

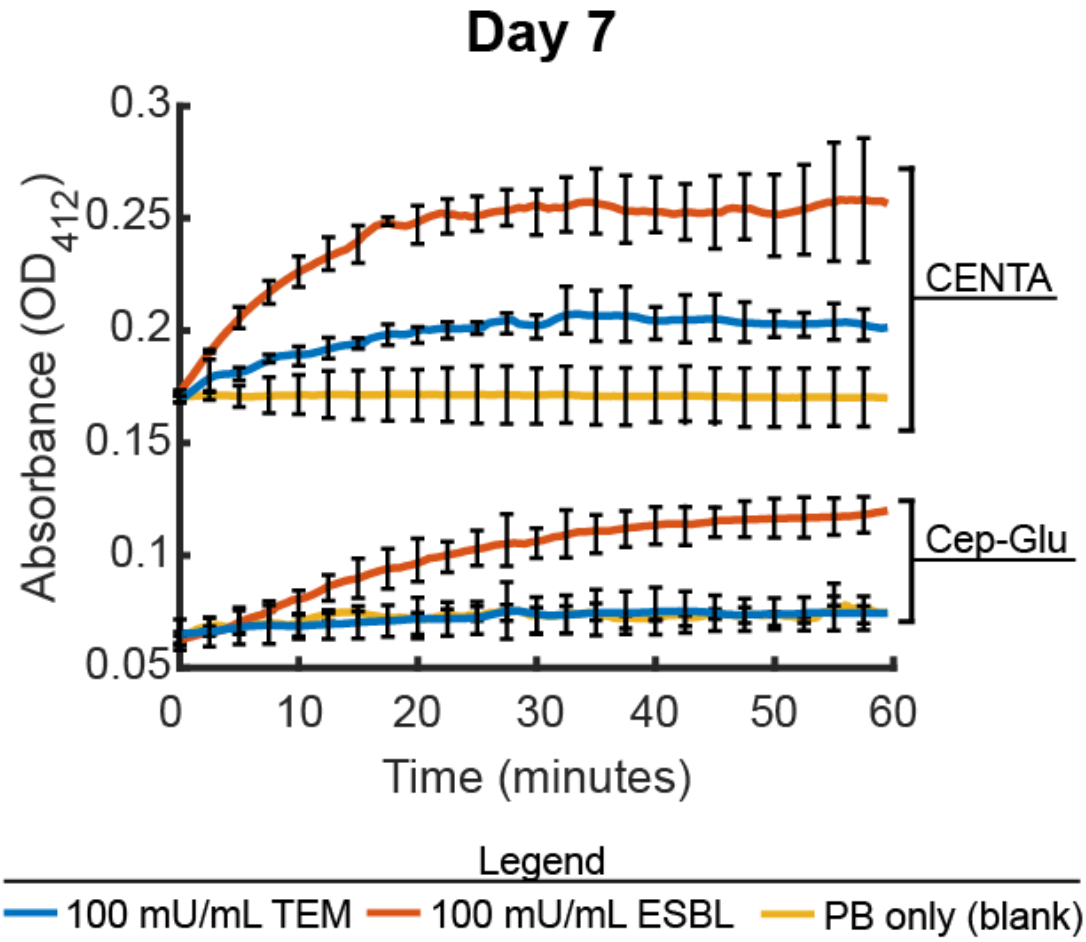
Day 7
Absorbance (OD412)
0.3
0.25
0.2
0.15
0.1
0.05
0
10
20
30
40
50
60
Time (minutes)
CENTA
Cep-Glu
Legend
100 mU/mL TEM
100 mU/mL ESBL
PB only (blank)

Fig. A.4.2

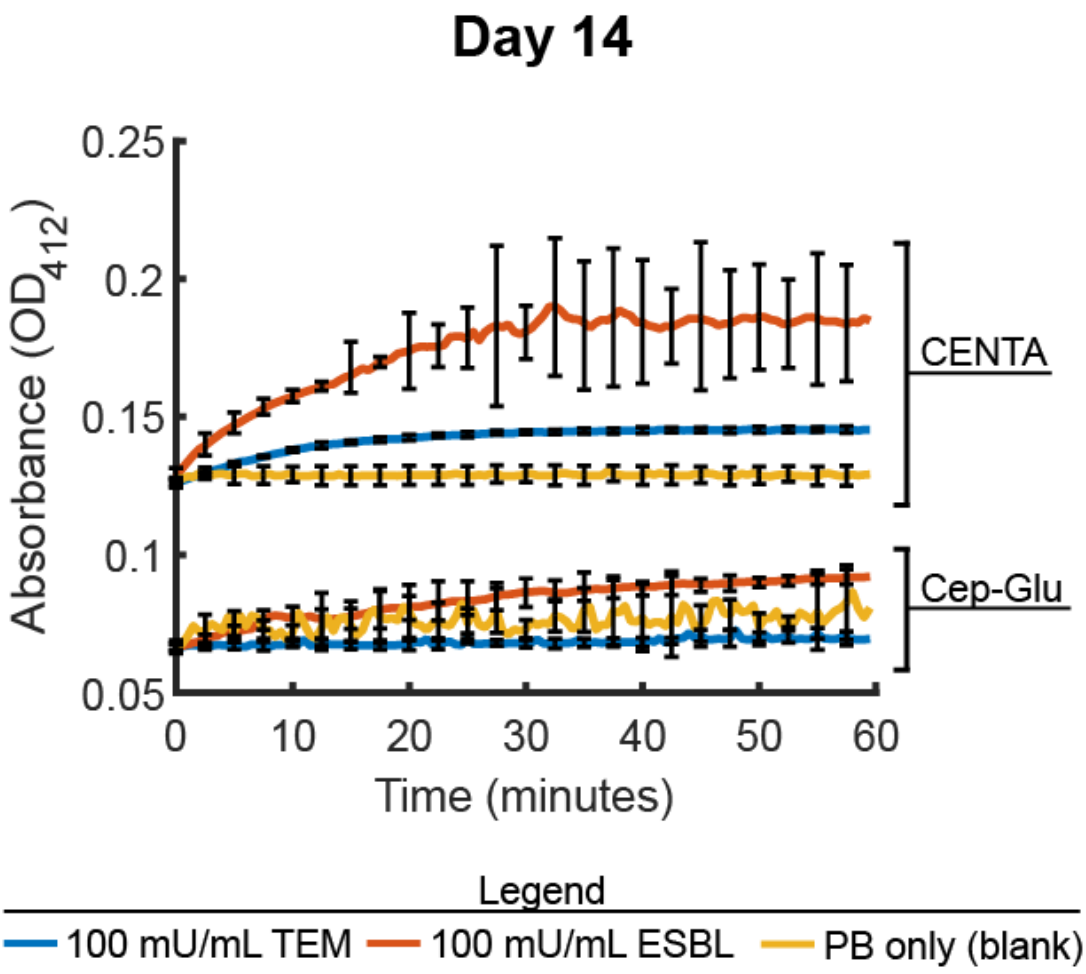
Day 14
0.25
0.2
0.15
0.1
0.05
Absorbance (OD412)
0
10
20
30
40
50
60
Time (minutes)
CENTA
Cep-Glu
Legend
100 mU/mL TEM
100 mU/mL ESBL
PB only (blank)

Fig. A.4.3

Appendix V. Thio-glucose calibration curve in the HRP-inhibition based electrochemical detection of Cep-glucose cleavage by ESBL (Fig. A.5.1).

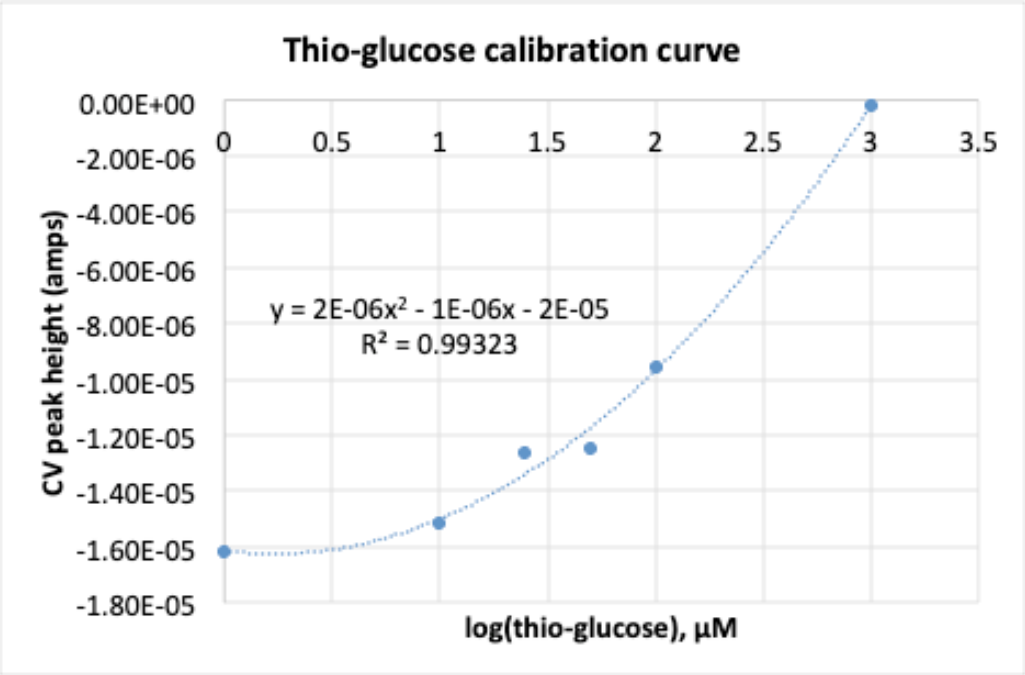

Figure A.5.1. Calibration curve to estimate amount of product generated with chronoamperometric readout.

Bibliography

1. Antibiotic Resistance Threats in the United States, 2013 | Antibiotic/Antimicrobial Resistance | CDC. Available at: https://www.cdc.gov/drugresistance/threat-report-2013/. (Accessed: 13th March 2017)

2. CDC. The biggest antibiotic-resistant threats in the U.S. *Centers for Disease Control and Prevention* (2018). Available at: https://www.cdc.gov/drugresistance/biggest_threats.html. (Accessed: 3rd December 2018)

3. Jorgensen, J. H., Hindler, J. F., Reller, L. B. & Weinstein, M. P. New Consensus Guidelines from the Clinical and Laboratory Standards Institute for Antimicrobial Susceptibility Testing of Infrequently Isolated or Fastidious Bacteria. *Clin. Infect. Dis.* **44**, 280–286 (2007).

4. Dellit, T. H. *et al.* Infectious Diseases Society of America and the Society for Healthcare Epidemiology of America Guidelines for Developing an Institutional Program to Enhance Antimicrobial Stewardship. *Clin. Infect. Dis.* **44**, 159–177 (2007).

5. Reller, L. B., Weinstein, M., Jorgensen, J. H. & Ferraro, M. J. Antimicrobial Susceptibility Testing: A Review of General Principles and Contemporary Practices. *Clin. Infect. Dis.* **49**, 1749–1755 (2009).

6. Wintermans, B. B., Reuland, E. A., Wintermans, R. G. F., Bergmans, A. M. C. & Kluytmans, J. A. J. W. The cost-effectiveness of ESBL detection: towards molecular detection methods? *Clin. Microbiol. Infect.* **19**, 662–665 (2013).

7. LaPlante, K., Cunha, C., Morrill, H., Rice, L. & Mylonakis, E. *Antimicrobial Stewardship: Principles and Practice*. (CABI, 2016).

8. Jorgensen, J. H., Lee, J. C. & Alexander, G. A. Rapid Penicillinase Paper Strip Test for Detection of Beta-Lactamase-Producing Haemophilus influenzae and Neisseria gonorrhoeae. *Antimicrob. Agents Chemother.* **11**, 1087–1088 (1977).

9. Catlin, B. W. Iodometric Detection of Haemophilus influenzae Beta-Lactamase: Rapid Presumptive Test for Ampicillin Resistance. *Antimicrob. Agents Chemother.* **7**, 265–270 (1975).

10. Livermore, D. M. & Brown, D. F. J. Detection of β-lactamase-mediated resistance. *J. Antimicrob. Chemother.* **48**, 59–64 (2001).

11. Bebrone, C. *et al.* CENTA as a Chromogenic Substrate for Studying β-Lactamases. *Antimicrob. Agents Chemother.* **45**, 1868–1871 (2001).

12. Orenga, S., James, A. L., Manafi, M., Perry, J. D. & Pincus, D. H. Enzymatic substrates in microbiology. *J. Microbiol. Methods* **79**, 139–155 (2009).

13. HardyDisks - disk diffusion susceptibility test procedure - Kirby Bauer - HardyDiskASTProceduresandChart.pdf. Available at: https://catalog.hardydiagnostics.com/cp_prod/Content/hugo/HardyDiskASTProceduresandChart.pdf. (Accessed: 13th March 2017)

14. Réglier-Poupet, H. *et al.* Performance of chromID ESBL, a chromogenic medium for detection of Enterobacteriaceae producing extended-spectrum β-lactamases. *J. Med. Microbiol.* **57**, 310–315 (2008).

15. Gao, W., Xing, B., Tsien, R. Y. & Rao, J. Novel Fluorogenic Substrates for Imaging β-Lactamase Gene Expression. *J. Am. Chem. Soc.* **125**, 11146–11147 (2003).

16. Zlokarnik, G. *et al.* Quantitation of Transcription and Clonal Selection of Single Living Cells with β-Lactamase as Reporter. *Science* **279**, 84–88 (1998).

17. Xing, B., Khanamiryan, A. & Rao, J. Cell-Permeable Near-Infrared Fluorogenic Substrates for Imaging β-Lactamase Activity. *J. Am. Chem. Soc.* **127**, 4158–4159 (2005).

18. Watanabe, S., Mizukami, S., Hori, Y. & Kikuchi, K. Multicolor Protein Labeling in Living Cells Using Mutant β-Lactamase-Tag Technology. *Bioconjug. Chem.* **21**, 2320–2326 (2010).

19. Kong, Y. *et al.* Imaging tuberculosis with endogenous β-lactamase reporter enzyme fluorescence in live mice. *Proc. Natl. Acad. Sci.* **107**, 12239–12244 (2010).

20. Jiang, J., Zhang, J. & Li, S. Detecting protein interactions in live cellsvia complementation of a hydrolysis-deficient β-lactamase. *Chem. Commun.* **47**, 182–184 (2010).

21. Zhang, J., Shen, Y., May, S. L., Nelson, D. C. & Li, S. Ratiometric Fluorescence Detection of Pathogenic Bacteria Resistant to Broad-Spectrum β-Lactam Antibiotics. *Angew. Chem.* **124**, 1901–1904 (2012).

22. da Silva, E. T. S. G. *et al.* Electrochemical Biosensors in Point-of-Care Devices: Recent Advances and Future Trends. *ChemElectroChem* **4**, 778–794 (2017).

23. Lan, T., Zhang, J. & Lu, Y. Transforming the blood glucose meter into a general healthcare meter for in vitro diagnostics in mobile health. *Biotechnol. Adv.* **34**, 331–341 (2016).

24. Xu, J. *et al.* Sensitive point-of-care monitoring of HIV related DNA sequences with a personal glucometer. *Chem. Commun.* **48**, 10733–10735 (2012).

25. Gu, C., Lan, T., Shi, H. & Lu, Y. Portable Detection of Melamine in Milk Using a Personal Glucose Meter Based on an in Vitro Selected Structure-Switching Aptamer. *Anal. Chem.* **87**, 7676–7682 (2015).

26. Rochelet, M. *et al.* Amperometric detection of extended-spectrum β-lactamase activity: application to the characterization of resistant E. coli strains. *Analyst* **140**, 3551–3556 (2015).

27. ND4BB | IMI - Innovative Medicines Initiative. Available at: http://www.imi.europa.eu/content/nd4bb. (Accessed: 13th March 2017)

28. IDSA : Antibiotic Development: The 10 x ’20 Initiative. Available at: http://www.idsociety.org/10x20/. (Accessed: 13th March 2017)

29. Joshi, S. Hospital antibiogram: a necessity. *Indian J. Med. Microbiol.* **28**, 277–280 (2010).

30. CDC. Antibiotic Prescribing Putting Patients at Risk. *Centers for Disease Control and Prevention* (2014). Available at: http://www.cdc.gov/media/dpk/antibiotic-resistance/safer-healthcare/dpk-vs-safer-health-care.html. (Accessed: 13th March 2017)

31. Dancer, S. J. The problem with cephalosporins. *J. Antimicrob. Chemother.* **48**, 463–478 (2001).

32. Nordmann, P. & Guibert, M. Extended-spectrum beta-lactamases in Pseudomonas aeruginosa. *J. Antimicrob. Chemother.* **42**, 128–131 (1998).

33. McNulty, C. *et al.* Successful control of Clostridium difficile infection in an elderly care unit through use of a restrictive antibiotic policy. *J. Antimicrob. Chemother.* **40**, 707–711 (1997).

34. Slimings, C. & Riley, T. V. Antibiotics and hospital-acquired Clostridium difficile infection: update of systematic review and meta-analysis. *J. Antimicrob. Chemother.* **69**, 881–891 (2014).

35. Chen, H. Y., Yuan, M. & Livermore, D. M. Mechanisms of resistance to beta-lactam antibiotics amongst Pseudomonas aeruginosa isolates collected in the UK in 1993. *J. Med. Microbiol.* **43**, 300–309 (1995).

36. Zeng, X. & Lin, J. Beta-lactamase induction and cell wall metabolism in Gram-negative bacteria. *Front. Microbiol.* **4**, 128 (2013).

37. Fountain, R. H. & Russell, A. D. Studies on the Mode of Action of Some Cephalosporin Derivatives. *J. Appl. Bacteriol.* **32**, 312–321 (1969).

38. Jacoby, G. A. AmpC β-Lactamases. *Clin. Microbiol. Rev.* **22**, 161–182 (2009).

39. Knox, J. R., Moews, P. C. & Frere, J.-M. Molecular evolution of bacterial β-lactam resistance. *Chem. Biol.* **3**, 937–947 (1996).

40. Oates, J. A., Wood, A. J., Donowitz, G. R. & Mandell, G. L. Drug Therapy: Beta-Lactam Antibiotics. *N. Engl. J. Med. Boston* **318**, 419–426 (1988).

41. Neu, H. C. Factors that affect the in-vitro activity of cephalosporin antibiotics. *J. Antimicrob. Chemother.* **10**, 11–23 (1982).

42. Curtis, N. A., Orr, D., Ross, G. W. & Boulton, M. G. Affinities of penicillins and cephalosporins for the penicillin-binding proteins of Escherichia coli K-12 and their antibacterial activity. *Antimicrob. Agents Chemother.* **16**, 533–539 (1979).

43. Fu, K. P. & Neu, H. C. Beta-Lactamase Stability of HR 756, a Novel Cephalosporin, Compared to That of Cefuroxime and Cefoxitin. *Antimicrob. Agents Chemother.* **14**, 322–326 (1978).

44. Stapley, E. O. *et al.* Cefoxitin and Cephamycins: Microbiological Studies. *Rev. Infect. Dis.* **1**, 73–87 (1979).

45. O'Callaghan, C. H. Description and classification of the newer cephalosporins and their relationships with the established compounds. *J. Antimicrob. Chemother.* **5**, 635–671 (1979).

46. Bush, K. Alarming β-lactamase-mediated resistance in multidrug-resistant Enterobacteriaceae. *Curr. Opin. Microbiol.* **13**, 558–564 (2010).

47. Papp-Wallace, K. M., Endimiani, A., Taracila, M. A. & Bonomo, R. A. Carbapenems: Past, Present, and Future. *Antimicrob. Agents Chemother.* **55**, 4943–4960 (2011).

48. Sykes, R. B. & Bonner, D. P. Aztreonam: The first monobactam. *Am. J. Med.* **78**, 2–10 (1985).

49. English, A. R., Retsema, J. A., Girard, A. E., Lynch, J. E. & Barth, W. E. CP-45,899, a Beta-Lactamase Inhibitor That Extends the Antibacterial Spectrum of Beta-Lactams: Initial Bacteriological Characterization. *Antimicrob. Agents Chemother.* **14**, 414–419 (1978).

50. Reading, C. & Cole, M. Clavulanic Acid: a Beta-Lactamase-Inhibiting Beta-Lactam from Streptomyces clavuligerus. *Antimicrob. Agents Chemother.* **11**, 852–857 (1977).

51. Reading, C. & Farmer, T. The inhibition of β-lactamases from Gram-negative bacteria by clavulanic acid. *Biochem. J.* **199**, 779–787 (1981).

52. Labia, R., Lelievre, V. & Peduzzi, J. Inhibition kinetics of three R-factor-mediated β-lactamases by a new β-lactam sulfone (CP 45899). *Biochim. Biophys. Acta BBA - Enzymol.* **611**, 351–357 (1980).

53. Sawai, T. & Tsukamoto, K. CEFOXITIN, N-FORMIMIDOYL THIENAMYCIN, CLAVULANIC ACID, AND PENICILLANIC ACID SULFONE AS SUICIDE INHIBITORS FOR DIFFERENT TYPES OF β-LACTAMASES PRODUCED BY GRAM-NEGATIVE BACTERIA. *J. Antibiot. (Tokyo)* **35**, 1594–1602 (1982).

54. Labia, R., Morand, A., Lelievre, V., Mattioni, D. & Kazmierczak, A. Sulbactam: Biochemical Factors Involved in Its Synergy with Ampicillin. *Rev. Infect. Dis.* **8**, S496–S502 (1986).

55. Drusano, G. L., Schimpff, S. C. & Hewitt, W. L. The Acylampicillins: Mezlocillin, Piperacillin, and Azlocillin. *Rev. Infect. Dis.* **6**, 13–32 (1984).

56. Parry, M. F. & Neu, H. C. Ticarcillin for Treatment of Serious Infections with Gram-Negative Bacteria. *J. Infect. Dis.* **134**, 476–485 (1976).

57. Winston, D. J., Murphy, W., Young, L. S. & Hewitt, W. L. Piperacillin therapy for serious bacterial infections. *Am. J. Med.* **69**, 255–261 (1980).

58. Brown, C. H., Natelson, E. A., Bradshaw, M. W., Alfrey, C. P. & Williams, T. W. Study of the Effects of Ticarcillin on Blood Coagulation and Platelet Function. *Antimicrob. Agents Chemother.* **7**, 652–657 (1975).

59. Holt, H. A., Broughall, J. M., McCarthy, M. & Reeves, D. S. Interactions between aminoglycoside antibiotics and carbenicillin or ticarcillin. *Infection* **4**, 107–109 (1976).

60. Pickering, L. K. & Rutherford, I. Effect of concentration and time upon inactivation of tobramycin, gentamicin, netilmicin and amikacin by azlocillin, carbenicillin, mecillinam, mezlocillin and piperacillin. *J. Pharmacol. Exp. Ther.* **217**, 345–349 (1981).

61. Brogden, R. N., Heel, R. C., Speight, T. M. & Avery, G. S. Ticarcillin: A Review of its Pharmacological Properties and Therapeutic Efficacy. *Drugs* **20**, 325–352 (1980).

62. Ervin, F. R. & Bullock, W. E. Clinical and Pharmacological Studies of Ticarcillin in Gram-Negative Infections. *Antimicrob. Agents Chemother.* **9**, 94–101 (1976).

63. Pancoast, S. J., Jahre, J. A. & Neu, H. C. Mezlocillin in the therapy of serious infections. *Am. J. Med.* **67**, 747–752 (1979).

64. LeFrock, J. L. *et al.* In-vitro and in-vivo comparison of mezlocillin and cefoxitin. *J. Antimicrob. Chemother.* **11**, 83–90 (1983).

65. Ramirez-Ronda, C. H., Gutiérrez, J. & Bermúdez, R. H. Comparative effectiveness, safety and tolerance of mezlocillin and ticarcillin: A prospective randomized trial. *J. Antimicrob. Chemother.* **9**, 125–129 (1982).

66. Madsen, P. O. & Nielsen, O. S. Treatment of complicated urinary tract infections with mezlocillin and ticarcillin, a comparative study. *J. Antimicrob. Chemother.* **9**, 179–181 (1982).

67. Rolandi, E. *et al.* Comparison of mezlocillin and carbenicillin as therapy for various infectious diseases. *Clin. Ther.* **4**, 321–325 (1981).

68. Lewandowski, A., Orlowski, T. & Weuta, H. Mezlocillin and carbenicillin: A clinical comparison of serious systemic infections in surgical patients. *Infection* **10**, S121–S124 (1982).

69. Pancoast, S., Prince, A. S., Francke, E. L. & Neu, H. C. Clinical Evaluation of Piperacillin Therapy for Infection. *Arch. Intern. Med.* **141**, 1447–1450 (1981).

70. Lutz, B., Mogabgab, W., Holmes, B., Pollock, B. & Beville, R. Clinical evaluation of the therapeutic efficacy and tolerability of piperacillin. *Antimicrob. Agents Chemother.* **22**, 10–14 (1982).

71. Eron, L. J., Goldenberg, R. I., Poretz, D. M. & Park, C. H. Piperacillin therapy for Pseudomonas infections. *South. Med. J.* **76**, 859–862 (1983).

72. Lavery, J. P. *et al.* Mezlocillin prophylaxis against infection after cesarean section: a comparison of techniques. *South. Med. J.* **79**, 1248–1251 (1986).

73. Cartwright, P. S., Pittaway, D. E., Jones, H. W. I. & Entman, S. S. The Use of Prophylactic Antibiotics in Obstetrics and Gynecology. A Review. *Obstet. Gynecol. Surv.* **39**, 537 (1984).

74. Gruber, U. F., Elke, R. & Widmer, M. Mezlocillin prophylaxis in biliary tract surgery. Results of a retrospective and a prospective trial. *Infection* **10**, S144–S147 (1982).

75. Baker, R. J. *et al.* A prospective double-blind comparison of piperacillin, cephalothin and cefoxitin in the prevention of postoperative infections in patients undergoing intra-abdominal operations. *Surg. Gynecol. Obstet.* **161**, 409–415 (1985).

76. Benigno, B. B. *et al.* A comparison of piperacillin, cephalothin and cefoxitin in the prevention of postoperative infections in patients undergoing vaginal hysterectomy. *Surg. Gynecol. Obstet.* **163**, 421–427 (1986).

77. Wallace, R. L. & Yonekura, M. L. The use of prophylactic antibiotics in patients undergoing emergency primary cesarean section. *Am. J. Obstet. Gynecol.* **147**, 533–536 (1983).

78. Lewis, R. T. *et al.* A single preoperative dose of cefazolin prevents postoperative sepsis in high-risk biliary surgery. *Can. J. Surg. J. Can. Chir.* **27**, 44–47 (1984).

79. Woodford, N. & Ellington, M. J. The emergence of antibiotic resistance by mutation. *Clin. Microbiol. Infect.* **13**, 5–18 (2007).

80. Lewis, D. A. The Gonococcus fights back: is this time a knock out? *Sex. Transm. Infect.* **86**, 415–421 (2010).

81. Rossolini, G. M., Arena, F., Pecile, P. & Pollini, S. Update on the antibiotic resistance crisis. *Curr. Opin. Pharmacol.* **18**, 56–60 (2014).

82. Babic, M., Hujer, A. M. & Bonomo, R. A. What's new in antibiotic resistance? Focus on beta-lactamases. *Drug Resist. Updat.* **9**, 142–156 (2006).

83. Jacoby, G. A., Chow, N. & Waites, K. B. Prevalence of Plasmid-Mediated Quinolone Resistance. *Antimicrob. Agents Chemother.* **47**, 559–562 (2003).

84. Mammeri, H., Loo, M. V. D., Poirel, L., Martinez-Martinez, L. & Nordmann, P. Emergence of Plasmid-Mediated Quinolone Resistance in Escherichia coli in Europe. *Antimicrob. Agents Chemother.* **49**, 71–76 (2005).

85. Martinez-Martinez, L., Pascual, A. & Jacoby, G. A. Quinolone resistance from a transferable plasmid. *Lancet* **351**, 797–799 (1998).

86. Wang, M., Sahm, D. F., Jacoby, G. A. & Hooper, D. C. Emerging Plasmid-Mediated Quinolone Resistance Associated with the qnr Gene in Klebsiella pneumoniae Clinical Isolates in the United States. *Antimicrob. Agents Chemother.* **48**, 1295–1299 (2004).

87. Martínez-Martínez, L. *et al.* Energy-Dependent Accumulation of Norfloxacin and Porin Expression in Clinical Isolates of Klebsiella pneumoniae and Relationship to Extended-Spectrum β-Lactamase Production. *Antimicrob. Agents Chemother.* **46**, 3926–3932 (2002).

88. Shen, D., Winokur, P. & Jones, R. N. Characterization of extended spectrum β-lactamase-producing Klebsiella pneumoniae from Beijing, China. *Int. J. Antimicrob. Agents* **18**, 185–188 (2001).

89. Baraniak, A., Sadowy, E., Hryniewicz, W. & Gniadkowski, M. Two Different Extended-Spectrum β-Lactamases (ESBLs) in One of the First ESBL-Producing Salmonella Isolates in Poland. *J. Clin. Microbiol.* **40**, 1095–1097 (2002).

90. Bradford, P. A., Cherubin, C. E., Idemyor, V., Rasmussen, B. A. & Bush, K. Multiply resistant Klebsiella pneumoniae strains from two Chicago hospitals: identification of the extended-spectrum TEM-12 and TEM-10 ceftazidime-hydrolyzing beta-lactamases in a single isolate. *Antimicrob. Agents Chemother.* **38**, 761–766 (1994).

91. Babini, G. S. & Livermore, D. M. Antimicrobial resistance amongst Klebsiella spp. collected from intensive care units in Southern and Western Europe in 1997–1998. *J. Antimicrob. Chemother.* **45**, 183–189 (2000).

92. Crowley, B. D. Extended-spectrum beta-lactamases in blood culture isolates of Klebsiella pneumoniae: seek and you may find! *J. Antimicrob. Chemother.* **47**, 728–729 (2001).

93. Kim, Y.-K. *et al.* Bloodstream Infections by Extended-Spectrum β-Lactamase-Producing Escherichia coli and Klebsiella pneumoniae in Children: Epidemiology and Clinical Outcome. *Antimicrob. Agents Chemother.* **46**, 1481–1491 (2002).

94. Paterson, D. L. *et al.* Outcome of Cephalosporin Treatment for Serious Infections Due to Apparently Susceptible Organisms Producing Extended-Spectrum β-Lactamases: Implications for the Clinical Microbiology Laboratory. *J. Clin. Microbiol.* **39**, 2206–2212 (2001).

95. Ambrose, P. G., Bhavnani, S. M. & Jones, R. N. Pharmacokinetics-Pharmacodynamics of Cefepime and Piperacillin- Tazobactam against Escherichia coli and Klebsiella pneumoniae Strains Producing Extended-Spectrum β-Lactamases: Report from the ARREST Program. *Antimicrob. Agents Chemother.* **47**, 1643–1646 (2003).

96. Paterson, D. L. *et al.* Antibiotic Therapy for Klebsiella pneumoniae Bacteremia: Implications of Production of Extended-Spectrum β-Lactamases. *Clin. Infect. Dis.* **39**, 31–37 (2004).

97. Zanetti, G. *et al.* Cefepime versus Imipenem-Cilastatin for Treatment of Nosocomial Pneumonia in Intensive Care Unit Patients: a Multicenter, Evaluator-Blind, Prospective, Randomized Study. *Antimicrob. Agents Chemother.* **47**, 3442–3447 (2003).

98. Bedenić, B., Beader, N. & Žagar, Ž. Effect of inoculum size on the antibacterial activity of cefpirome and cefepime against Klebsiella pneumoniae strains producing SHV extended-spectrum β-lactamases. *Clin. Microbiol. Infect.* **7**, 626–635 (2001).

99. Jett, B. D., Ritchie, D. J., Reichley, R., Bailey, T. C. & Sahm, D. F. In vitro activities of various beta-lactam antimicrobial agents against clinical isolates of

Escherichia coli and Klebsiella spp. resistant to oxyimino cephalosporins. *Antimicrob. Agents Chemother.* **39**, 1187–1190 (1995).

100. Thomson, K. S. & Moland, E. S. Cefepime, Piperacillin-Tazobactam, and the Inoculum Effect in Tests with Extended-Spectrum β-Lactamase-Producing Enterobacteriaceae. *Antimicrob. Agents Chemother.* **45**, 3548–3554 (2001).

101. Bonnet, R. *et al.* A Novel CTX-M β-Lactamase (CTX-M-8) in Cefotaxime-ResistantEnterobacteriaceae Isolated in Brazil. *Antimicrob. Agents Chemother.* **44**, 1936–1942 (2000).

102. Elkhaïli, H. *et al.* In vitro time-kill curves of cefepime and cefpirome combined with amikacin, gentamicin or ciprofloxacin against Klebsiella pneumoniae producing extended-spectrum beta-lactamase. *Chemotherapy* **43**, 245–253 (1997).

103. Paterson, D. L. Recommendation for treatment of severe infections caused by Enterobacteriaceae producing extended-spectrum β-lactamases (ESBLs). *Clin. Microbiol. Infect.* **6**, 460–463 (2000).

104. Pangon, B. *et al.* In Vivo Selection of a Cephamycin-Resistant, Porin-Deficient Mutant of Klebsiello pneumoniae Producing a TEM-3 β-Lactamase. *J. Infect. Dis.* **159**, 1005–1006 (1989).

105. Bradford, P. A. *et al.* Imipenem resistance in Klebsiella pneumoniae is associated with the combination of ACT-1, a plasmid-mediated AmpC beta-lactamase, and the foss of an outer membrane protein. *Antimicrob. Agents Chemother.* **41**, 563–569 (1997).

106. Siu, L. K. *et al.* Bacteremia Due to Extended-Spectrum β-Lactamase-Producing Escherichia coli andKlebsiella pneumoniae in a Pediatric Oncology Ward: Clinical Features and Identification of Different Plasmids Carrying both SHV-5 and TEM-1 Genes. *J. Clin. Microbiol.* **37**, 4020–4027 (1999).

107. Karadenizli, A., Mutlu, B., Okay, E., Kolayli, F. & Vahaboglu, H. Piperacillin with and without Tazobactam against Extended-Spectrum Beta-Lactamase-Producing Pseudomonas aeruginosa in a Rat Thigh Abscess Model. *Chemotherapy* **47**, 292–296 (2001).

108. Burgess, D. S., Hall, R. G., Lewis, J. S., Jorgensen, J. H. & Patterson, J. E. Clinical and Microbiologic Analysis of a Hospital's Extended-Spectrum β-Lactamase-Producing Isolates Over a 2-Year Period. *Pharmacother. J. Hum. Pharmacol. Drug Ther.* **23**, 1232–1237 (2003).

109. Du, B. *et al.* Extended-spectrum beta-lactamase-producing Escherichia coli and Klebsiella pneumoniae bloodstream infection: risk factors and clinical outcome. *Intensive Care Med.* **28**, 1718–1723 (2002).

110. Endimiani, A. *et al.* Bacteremia Due to Klebsiella pneumoniae Isolates Producing the TEM-52 Extended-Spectrum β-Lactamase: Treatment Outcome of Patients Receiving Imipenem or Ciprofloxacin. *Clin. Infect. Dis.* **38**, 243–251 (2004).

111. Kang, C.-I. *et al.* Bloodstream Infections Due to Extended-Spectrum β-Lactamase-Producing Escherichia coli and Klebsiella pneumoniae: Risk Factors for Mortality and Treatment Outcome, with Special Emphasis on Antimicrobial Therapy. *Antimicrob. Agents Chemother.* **48**, 4574–4581 (2004).

112. Massova, I. & Mobashery, S. Kinship and Diversification of Bacterial Penicillin-Binding Proteins and β-Lactamases. *Antimicrob. Agents Chemother.* **42**, 1–17 (1998).

113. Livermore, D. M. beta-Lactamases in laboratory and clinical resistance. *Clin. Microbiol. Rev.* **8**, 557–584 (1995).

114. Jacoby, G. A. & Medeiros, A. A. More extended-spectrum beta-lactamases. *Antimicrob. Agents Chemother.* **35**, 1697–1704 (1991).

115. Martínez-Martínez, L. *et al.* In vivo selection of porin-deficient mutants of Klebsiella pneumoniae with increased resistance to cefoxitin and expanded-spectrum-cephalosporins. *Antimicrob. Agents Chemother.* **40**, 342–348 (1996).

116. Vatopoulos, A. C., Philippon, A., Tzouvelekis, L. S., Komninou, Z. & Legakis, N. J. Prevalence of a transferable SHV-5 type β-lactamase in clinical isolates of Klebsiella pneumoniae and Escherichia coli in Greece. *J. Antimicrob. Chemother.* **26**, 635–648 (1990).

117. Chambers, H. F. Methicillin resistance in staphylococci: molecular and biochemical basis and clinical implications. *Clin. Microbiol. Rev.* **10**, 781–791 (1997).

118. Jacoby, G. A., Mills, D. M. & Chow, N. Role of β-Lactamases and Porins in Resistance to Ertapenem and Other β-Lactams in Klebsiella pneumoniae. *Antimicrob. Agents Chemother.* **48**, 3203–3206 (2004).

119. Otero, F. *et al.* Rapid Detection of Antibiotic Resistance in Gram-Negative Bacteria Through Assessment of Changes in Cellular Morphology. *Microb. Drug Resist.* **23**, 157–162 (2016).

120. Unemo, M. & Nicholas, R. A. Emergence of multidrug-resistant, extensively drug-resistant and untreatable gonorrhea. *Future Microbiol.* **7**, 1401–1422 (2012).

121. Lee, N.-Y. *et al.* Cefepime Therapy for Monomicrobial Bacteremia Caused by Cefepime-Susceptible Extended-Spectrum Beta-Lactamase–Producing Enterobacteriaceae: MIC Matters. *Clin. Infect. Dis.* **56**, 488–495 (2013).

122. Nordmann, P., Poirel, L., Walsh, T. R. & Livermore, D. M. The emerging NDM carbapenemases. *Trends Microbiol.* **19**, 588–595 (2011).

123. Gould, I. M. & Bal, A. M. New antibiotic agents in the pipeline and how they can help overcome microbial resistance. *Virulence* **4**, 185–191 (2013).

124. Ambler R. P., Baddiley James & Abraham Edward Penley. The structure of β-lactamases. *Philos. Trans. R. Soc. Lond. B Biol. Sci.* **289**, 321–331 (1980).

125. Medeiros, A., Mayer, K. H. & Opal, S. M. Plasmid-mediated beta-lactamases. *Antimicrob. Newsl.* **5**, 61–65 (1988).

126. Bush, K., Jacoby, G. A. & Medeiros, A. A. A functional classification scheme for beta-lactamases and its correlation with molecular structure. *Antimicrob. Agents Chemother.* **39**, 1211–1233 (1995).

127. Sougakoff, W., Goussard, S. & Courvalin, P. The TEM-3 β-lactamase, which hydrolyzes broad-spectrum cephalosporins, is derived from the TEM-2 penicillinase by two amino acid substitutions. *FEMS Microbiol. Lett.* **56**, 343–348 (1988).

128. Tzouvelekis, L. S. & Bonomo, R. A. SHV-type beta-lactamases. *Curr. Pharm. Des.* **5**, 847–864 (1999).

129. Ishii, Y. *et al.* Cloning and sequence of the gene encoding a cefotaxime-hydrolyzing class A beta-lactamase isolated from Escherichia coli. *Antimicrob. Agents Chemother.* **39**, 2269–2275 (1995).

130. Ma, L., Ishii, Y., Ishiguro, M., Matsuzawa, H. & Yamaguchi, K. Cloning and Sequencing of the Gene Encoding Toho-2, a Class A β-Lactamase Preferentially Inhibited by Tazobactam. *Antimicrob. Agents Chemother.* **42**, 1181–1186 (1998).

131. Tzouvelekis, L. S., Tzelepi, E., Tassios, P. T. & Legakis, N. J. CTX-M-type β-lactamases: an emerging group of extended-spectrum enzymes. *Int. J. Antimicrob. Agents* **14**, 137–142 (2000).

132. Humeniuk, C. *et al.* β-Lactamases of Kluyvera ascorbata, Probable Progenitors of Some Plasmid-Encoded CTX-M Types. *Antimicrob. Agents Chemother.* **46**, 3045–3049 (2002).

133. Lobkovsky, E. *et al.* Evolution of an enzyme activity: crystallographic structure at 2-A resolution of cephalosporinase from the ampC gene of Enterobacter

cloacae P99 and comparison with a class A penicillinase. *Proc. Natl. Acad. Sci.* **90**, 11257–11261 (1993).

134. Bradford, P. A. Extended-spectrum beta-lactamases in the 21st century: characterization, epidemiology, and detection of this important resistance threat. *Clin. Microbiol. Rev.* **14**, 933–951, table of contents (2001).

135. Canton, R., Gonzalez-Alba, J. M. & Galán, J. C. CTX-M Enzymes: Origin and Diffusion. *Front. Microbiol.* **3**, (2012).

136. Bradford, P. A. *et al.* CTX-M-5, a Novel Cefotaxime-Hydrolyzing β-Lactamase from an Outbreak of Salmonella typhimuriumin Latvia. *Antimicrob. Agents Chemother.* **42**, 1980–1984 (1998).

137. Sabaté, M. *et al.* Cloning and Sequence of the Gene Encoding a Novel Cefotaxime-Hydrolyzing β-Lactamase (CTX-M-9) fromEscherichia coli in Spain. *Antimicrob. Agents Chemother.* **44**, 1970–1973 (2000).

138. Hall, L. M., Livermore, D. M., Gur, D., Akova, M. & Akalin, H. E. OXA-11, an extended-spectrum variant of OXA-10 (PSE-2) beta-lactamase from Pseudomonas aeruginosa. *Antimicrob. Agents Chemother.* **37**, 1637–1644 (1993).

139. Danel, F., Hall, L. M. C., Duke, B., Gur, D. & Livermore, D. M. OXA-17, a Further Extended-Spectrum Variant of OXA-10 β-Lactamase, Isolated from Pseudomonas aeruginosa. *Antimicrob. Agents Chemother.* **43**, 1362–1366 (1999).

140. Palzkill, T. Metallo-β-lactamase structure and function. *Ann. N. Y. Acad. Sci.* **1277**, 91–104 (2013).

141. Drawz, S. M. & Bonomo, R. A. Three Decades of β-Lactamase Inhibitors. *Clin. Microbiol. Rev.* **23**, 160–201 (2010).

142. Bou, F. J. P.-L. and G. β-Lactamase Inhibitors: The Story so Far. *Current Medicinal Chemistry* (2009). Available at: http://www.eurekaselect.com/70025/article. (Accessed: 11th July 2019)

143. Stachyra, T. *et al.* Mechanistic Studies of the Inactivation of TEM-1 and P99 by NXL104, a Novel Non-β-Lactam β-Lactamase Inhibitor. *Antimicrob. Agents Chemother.* **54**, 5132–5138 (2010).

144. Lim, H. M., Pène, J. J. & Shaw, R. W. Cloning, nucleotide sequence, and expression of the Bacillus cereus 5/B/6 beta-lactamase II structural gene. *J. Bacteriol.* **170**, 2873–2878 (1988).

145. Walsh, T. R. *et al.* Sequence analysis of the L1 metallo-β-lactamase from Xanthomonas maltophilia. *Biochim. Biophys. Acta BBA - Gene Struct. Expr.* **1218**, 199–201 (1994).

146. Lauretti, L. *et al.* Cloning and Characterization of bla VIM, a New Integron-Borne Metallo-β-Lactamase Gene from a Pseudomonas aeruginosa Clinical Isolate. *Antimicrob. Agents Chemother.* **43**, 1584–1590 (1999).

147. Laraki, N. *et al.* Structure of In31, abla IMP-Containing Pseudomonas aeruginosa Integron Phyletically Related to In5, Which Carries an Unusual Array of Gene Cassettes. *Antimicrob. Agents Chemother.* **43**, 890–901 (1999).

148. Cornaglia, G., Giamarellou, H. & Rossolini, G. M. Metallo-β-lactamases: a last frontier for β-lactams? *Lancet Infect. Dis.* **11**, 381–393 (2011).

149. Bennett, P. M. Plasmid encoded antibiotic resistance: acquisition and transfer of antibiotic resistance genes in bacteria. *Br. J. Pharmacol.* **153**, S347–S357 (2008).

150. Yong, D. *et al.* Characterization of a New Metallo-β-Lactamase Gene, blaNDM-1, and a Novel Erythromycin Esterase Gene Carried on a Unique Genetic Structure in Klebsiella pneumoniae Sequence Type 14 from India. *Antimicrob. Agents Chemother.* **53**, 5046–5054 (2009).

151. Blazquez, J., Morosini, M.-I., Negri, M.-C. & Baquero, F. Selection of Naturally Occurring Extended-Spectrum TEM β-Lactamase Variants by Fluctuating β-Lactam Pressure. *Antimicrob. Agents Chemother.* **44**, 2182–2184 (2000).

152. Jacoby, G. A. Genetics of extended-spectrum beta-lactamases. *Eur. J. Clin. Microbiol. Infect. Dis.* **13**, S2–S11 (1994).

153. Christensen, H., Martin, M. T. & Waley, S. G. Beta-lactamases as fully efficient enzymes. Determination of all the rate constants in the acyl-enzyme mechanism. *Biochem. J.* **266**, 853–861 (1990).

154. Bush, K. & Singer, S. B. Biochemical characteristics of extended broad spectrum β-lactamases. *Infection* **17**, 429–433 (1989).

155. Jacoby, G. A. & Carreras, I. Activities of beta-lactam antibiotics against Escherichia coli strains producing extended-spectrum beta-lactamases. *Antimicrob. Agents Chemother.* **34**, 858–862 (1990).

156. Petit, A., Ben Yaghlane-Bouslama, H., Sofer, L. & Labia, R. Does high level production of SHV-type penicillinase confer resistance to ceftazidime in enterobacteriaceae? *FEMS Microbiol. Lett.* **92**, 89–94 (1992).

157. Darfeuille-Michaud, A. *et al.* R-plasmid-encoded adhesive factor in Klebsiella pneumoniae strains responsible for human nosocomial infections. *Infect. Immun.* **60**, 44–55 (1992).

158. Mabilat, C. & Courvalin, P. Development of 'oligotyping' for characterization and molecular epidemiology of TEM beta-lactamases in members of the family Enterobacteriaceae. *Antimicrob. Agents Chemother.* **34**, 2210–2216 (1990).

159. Prinarakis, E. E., Miriagou, V., Tzelepi, E., Gazouli, M. & Tzouvelekis, L. S. Emergence of an inhibitor-resistant beta-lactamase (SHV-10) derived from an SHV-5 variant. *Antimicrob. Agents Chemother.* **41**, 838–840 (1997).

160. Bradford, P. A. *et al.* SHV-7, a novel cefotaxime-hydrolyzing beta-lactamase, identified in Escherichia coli isolates from hospitalized nursing home patients. *Antimicrob. Agents Chemother.* **39**, 899–905 (1995).

161. Harrif-Heraud, Z. E., Arpin, C., Benliman, S. & Quentin, C. Molecular epidemiology of a nosocomial outbreak due to SHV-4-producing strains of Citrobacter diversus. *J. Clin. Microbiol.* **35**, 2561–2567 (1997).

162. Naas, T., Philippon, L., Poirel, L., Ronco, E. & Nordmann, P. An SHV-Derived Extended-Spectrum β-Lactamase in Pseudomonas aeruginosa. *Antimicrob. Agents Chemother.* **43**, 1281–1284 (1999).

163. Rasheed, J. K. *et al.* Evolution of extended-spectrum beta-lactam resistance (SHV-8) in a strain of Escherichia coli during multiple episodes of bacteremia. *Antimicrob. Agents Chemother.* **41**, 647–653 (1997).

164. Marchandin, H., Carriere, C., Sirot, D., Pierre, H. J.- & Darbas, H. TEM-24 Produced by Four Different Species ofEnterobacteriaceae, Including Providencia rettgeri, in a Single Patient. *Antimicrob. Agents Chemother.* **43**, 2069–2073 (1999).

165. Morosini, M. I. *et al.* New extended-spectrum TEM-type beta-lactamase from Salmonella enterica subsp. enterica isolated in a nosocomial outbreak. *Antimicrob. Agents Chemother.* **39**, 458–461 (1995).

166. Palzkill, T. *et al.* New variant of TEM-10 beta-lactamase gene produced by a clinical isolate of proteus mirabilis. *Antimicrob. Agents Chemother.* **39**, 1199–1200 (1995).

167. Perilli, M. *et al.* TEM-72, a New Extended-Spectrum β-Lactamase Detected in Proteus mirabilis and Morganella morganii in Italy. *Antimicrob. Agents Chemother.* **44**, 2537–2539 (2000).

168. Tessier, F., Arpin, C., Allery, A. & Quentin, C. Molecular Characterization of a TEM-21 β-Lactamase in a Clinical Isolate of Morganella morganii. *Antimicrob. Agents Chemother.* **42**, 2125–2127 (1998).

169. Milatovic, D. & Braveny, I. Development of resistance during antibiotic therapy. *Eur. J. Clin. Microbiol.* **6**, 234–244 (1987).

170. Hancock, R. E. W. & Speert, D. P. Antibiotic resistance in Pseudomonas aeruginosa: mechanisms and impact on treatment. *Drug Resist. Updat.* **3**, 247–255 (2000).

171. Vu, H. & Nikaido, H. Role of beta-lactam hydrolysis in the mechanism of resistance of a beta-lactamase-constitutive Enterobacter cloacae strain to expanded-spectrum beta-lactams. *Antimicrob. Agents Chemother.* **27**, 393–398 (1985).

172. Mah, T.-F. *et al.* A genetic basis for Pseudomonas aeruginosa biofilm antibiotic resistance. *Nature* **426**, 306 (2003).

173. Nüesch-Inderbinen, M. T., Hächler, H. & Kayser, F. H. Detection of genes coding for extended-spectrum SHV beta-lactamases in clinical isolates by a molecular genetic method, and comparison with the E test. *Eur. J. Clin. Microbiol. Infect. Dis.* **15**, 398–402 (1996).

174. M'Zali, F.-H., Gascoyne-Binzi, D. M., Heritage, J. & Hawkey, P. M. Detection of mutations conferring extended-spectrum activity on SHV β-lactamases using polymerase chain reaction single strand conformational polymorphism (PCR-SSCP). *J. Antimicrob. Chemother.* **37**, 797–802 (1996).

175. M'Zali, F. H., Heritage, J., Gascoyne-Binzi, D. M., Snelling, A. M. & Hawkey, P. M. PCR single strand conformational polymorphism can be used to detect the gene encoding SHV-7 extended-spectrum beta-lactamase and to identify different SHV genes within the same strain. *J. Antimicrob. Chemother.* **41**, 123–125 (1998).

176. Chanawong, A., M'Zali, F. H., Heritage, J., Lulitanond, A. & Hawkey, P. M. Characterisation of extended-spectrum β-lactamases of the SHV family using a combination of PCR-single strand conformational polymorphism (PCR-SSCP) and PCR-restriction fragment length polymorphism (PCR-RFLP). *FEMS Microbiol. Lett.* **184**, 85–89 (2000).

177. Bradford, P. A. Automated Thermal Cycling Is Superior to Traditional Methods for Nucleotide Sequencing ofbla SHV Genes. *Antimicrob. Agents Chemother.* **43**, 2960–2963 (1999).

178. Veenemans, J. *et al.* Next-Generation Sequencing for Typing and Detection of Resistance Genes: Performance of a New Commercial Method during an

Outbreak of Extended-Spectrum-Beta-Lactamase-Producing Escherichia coli. *J. Clin. Microbiol.* **52**, 2454–2460 (2014).

179. Sundsfjord, A. *et al.* Genetic methods for detection of antimicrobial resistance. *APMIS* **112**, 815–837 (2004).

180. Arlet, G. *et al.* Molecular characterisation by PCR-restriction fragment length polymorphism of TEM β-lactamases. *FEMS Microbiol. Lett.* **134**, 203–208 (1995).

181. Edelstein, M., Pimkin, M., Palagin, I., Edelstein, I. & Stratchounski, L. Prevalence and Molecular Epidemiology of CTX-M Extended-Spectrum β-Lactamase-Producing Escherichia coli and Klebsiella pneumoniae in Russian Hospitals. *Antimicrob. Agents Chemother.* **47**, 3724–3732 (2003).

182. Kirkland, K. B. & Weinstein, J. M. Adverse effects of contact isolation. *The Lancet* **354**, 1177–1178 (1999).

183. Shibata, N. *et al.* PCR Typing of Genetic Determinants for Metallo-β-Lactamases and Integrases Carried by Gram-Negative Bacteria Isolated in Japan, with Focus on the Class 3 Integron. *J. Clin. Microbiol.* **41**, 5407–5413 (2003).

184. Cockerill, F. R. Genetic Methods for Assessing Antimicrobial Resistance. *Antimicrob. Agents Chemother.* **43**, 199–212 (1999).

185. Clinical and Laboratory Standards Institute. (2006). Methods for dilution antimicrobial susceptibility tests for bacteria that grow aerobically. Approved standard, 26, 14-16.

186. Clinical and Laboratory Standards Institute. Performance standards for antimicrobial susceptibility testing. Supplement M100-S16. Clinical and Laboratory Standards Institute: Wayne, PA: Clinical and Laboratory Standards Institute, 2006.

187. NCCLS. Methods for antimicrobial susceptibility testing of anaerobic bacteria. Approved standard M11-A6. Wayne, PA: NCCLS, 2004.

188. Jarlier, V., Nicolas, M.-H., Fournier, G. & Philippon, A. Extended Broad-Spectrum β-Lactamases Conferring Transferable Resistance to Newer β-Lactam Agents in Enterobacteriaceae: Hospital Prevalence and Susceptibility Patterns. *Rev. Infect. Dis.* **10**, 867–878 (1988).

189. Drieux, L., Brossier, F., Sougakoff, W. & Jarlier, V. Phenotypic detection of extended-spectrum β-lactamase production in Enterobacteriaceae: review and bench guide. *Clin. Microbiol. Infect.* **14**, 90–103 (2008).

190. Hall, M. A. L. *et al.* Evaluation of the Etest ESBL and the BD Phoenix, VITEK 1, and VITEK 2 Automated Instruments for Detection of Extended-Spectrum Beta-Lactamases in Multiresistant Escherichia coli and Klebsiella spp. *J. Clin. Microbiol.* **40**, 3703–3711 (2002).

191. Brun-Buisson, C. *et al.* TRANSFERABLE ENZYMATIC RESISTANCE TO THIRD-GENERATION CEPHALOSPORINS DURING NOSOCOMIAL OUTBREAK OF MULTIRESISTANT KLEBSIELLA PNEUMONIAE. *The Lancet* **330**, 302–306 (1987).

192. Rice, L. B., Yao, J. D. C., Klimm, K., Eliopoulos, G. M. & Moellering, R. C. Efficacy of Different β-Lactams against an Extended-Spectrum β-Lactamase-Producing Klebsiella pneumoniae Strain in the Rat Intra-Abdominal Abscess Model. *Antimicrob. Agents Chemother.* **35**, 1243–1244 (1991).

193. Fast, W. & Sutton, L. D. Metallo-β-lactamase: Inhibitors and reporter substrates. *Biochim. Biophys. Acta BBA - Proteins Proteomics* **1834**, 1648–1659 (2013).

194. Jones, R. N., Wilson, H. W., Novick, W. J., Barry, A. L. & Thornsberry, C. In vitro evaluation of CENTA, a new beta-lactamase-susceptible chromogenic cephalosporin reagent. *J. Clin. Microbiol.* **15**, 954–958 (1982).

195. Schindler, P. & Huber, G. Chromophoric cephalosporins. (1982).

196. Bieniarz, C., Young, D. F. & Cornwell, M. J. Chromogenic redox assay for β-lactamases yielding water-insoluble products: I. Kinetic behavior and redox chemistry. *Anal. Biochem.* **207**, 321–328 (1992).

197. Bieniarz, C., Cornwell, M. J. & Young, D. F. Beta-lactamase assay employing chromogenic precipitating substrates. (1990).

198. Boyd, D. B. & Lunn, W. H. W. Electronic structures of cephalosporins and penicillins. 9. Departure of a leaving group in cephalosporins. *J. Med. Chem.* **22**, 778–784 (1979).

199. Faraci, W. S. & Pratt, R. F. Elimination of a good leaving group from the 3'-position of a cephalosporin need not be concerted with .beta.-lactam ring opening: TEM-2 .beta.-lactamase-catalyzed hydrolysis of pyridine-2-azo-4'-(N',N'-dimethylaniline) cephalosporin (PADAC) and of cephaloridine. *J. Am. Chem. Soc.* **106**, 1489–1490 (1984).

200. Toney, J. H. *et al.* Succinic Acids as Potent Inhibitors of Plasmid-borne IMP-1 Metallo-β-lactamase. *J. Biol. Chem.* **276**, 31913–31918 (2001).

201. Toney, J. H. *et al.* Antibiotic sensitization using biphenyl tetrazoles as potent inhibitors of Bacteroides fragilis metallo-β-lactamase. *Chem. Biol.* **5**, 185–196 (1998).

202. Minond, D. *et al.* Inhibitors of VIM-2 by screening pharmacologically active and click-chemistry compound libraries. *Bioorg. Med. Chem.* **17**, 5027–5037 (2009).

203. Thomas, P. W. *et al.* An altered zinc-binding site confers resistance to a covalent inactivator of New Delhi metallo-beta-lactamase-1 (NDM-1) discovered by high-throughput screening. *Bioorg. Med. Chem.* **21**, 3138–3146 (2013).

204. Minond, D. *et al.* HTS Assay for Discovery of Novel Metallo-Beta-lactamase (MBL) Inhibitors. in *Probe Reports from the NIH Molecular Libraries Program* (National Center for Biotechnology Information (US), 2010).

205. Gazin, M., Paasch, F., Goossens, H. & Malhotra-Kumar, S. Current Trends in Culture-Based and Molecular Detection of Extended-Spectrum-β-Lactamase-Harboring and Carbapenem-Resistant Enterobacteriaceae. *J. Clin. Microbiol.* **50**, 1140–1146 (2012).

206. Overdevest, I. T. M. A., Willemsen, I., Elberts, S., Verhulst, C. & Kluytmans, J. A. J. W. Laboratory Detection of Extended-Spectrum-Beta-Lactamase-Producing Enterobacteriaceae: Evaluation of Two Screening Agar Plates and Two Confirmation Techniques. *J. Clin. Microbiol.* **49**, 519–522 (2011).

207. Färber, J. *et al.* Extended-Spectrum Beta-Lactamase Detection with Different Panels for Automated Susceptibility Testing and with a Chromogenic Medium. *J. Clin. Microbiol.* **46**, 3721–3727 (2008).

208. Huang, T.-D., Bogaerts, P., Berhin, C., Guisset, A. & Glupczynski, Y. Evaluation of Brilliance ESBL Agar, a Novel Chromogenic Medium for Detection of Extended-Spectrum-Beta- Lactamase-Producing Enterobacteriaceae. *J. Clin. Microbiol.* **48**, 2091–2096 (2010).

209. Randall, L. P. *et al.* Evaluation of CHROMagar CTX, a novel medium for isolating CTX-M-ESBL-positive Enterobacteriaceae while inhibiting AmpC-producing strains. *J. Antimicrob. Chemother.* **63**, 302–308 (2009).

210. Oliver, A. *et al.* Mechanisms of Decreased Susceptibility to Cefpodoxime in Escherichia coli. *Antimicrob. Agents Chemother.* **46**, 3829–3836 (2002).

211. Hancock, R. E. W. The bacterial outer membrane as a drug barrier. *Trends Microbiol.* **5**, 37–42 (1997).

212. Bellido, F., Pechère, J. C. & Hancock, R. E. Novel method for measurement of outer membrane permeability to new beta-lactams in intact Enterobacter cloacae cells. *Antimicrob. Agents Chemother.* **35**, 68–72 (1991).

213. Sabath, L. D., Jago, M. & Abraham, E. P. Cephalosporinase and penicillinase activities of a β-lactamase from Pseudomonas pyocyanea. *Biochem. J.* **96**, 739–752 (1965).

214. Hamilton-Miller, J. M. T., Newton, G. G. F. & Abraham, E. P. Products of aminolysis and enzymic hydrolysis of the cephalosporins. *Biochem. J.* **116**, 371–384 (1970).

215. Lowe, J. P. Is this a concerted reaction? *J. Chem. Educ.* **51**, 785 (1974).

216. P. Laws, A. & I. Page, M. The effect of the carboxy group on the chemical and β-lactamase reactivity of β-lactam antibiotics. *J. Chem. Soc. Perkin Trans. 2* **0**, 1577–1581 (1989).

217. Ivama, V. M., Rodrigues, L. N. C., Guaratini, C. C. I. & Zanoni, M. V. B. Spectrophotometric determination of cefaclor in pharmaceutical preparations. *Quím. Nova* **22**, 201–204 (1999).

218. Quotadamo, A. *et al.* An Improved Synthesis of CENTA, a Chromogenic Substrate for β-Lactamases. *Synlett* **27**, 2447–2450 (2016).

219. van Berkel, S. S. *et al.* Assay Platform for Clinically Relevant Metallo-β-lactamases. *J. Med. Chem.* **56**, 6945–6953 (2013).

220. Hrbac, J., Halouzka, V., Trnkova, L. & Vacek, J. eL-Chem Viewer: a freeware package for the analysis of electroanalytical data and their post-acquisition processing. *Sensors* **14**, 13943–13954 (2014).

221. Ellman's reagent: 5,5′-dithiobis(2-nitrobenzoic acid)—a reexamination - ScienceDirect. Available at: https://www.sciencedirect.com/science/article/pii/0003269779907929. (Accessed: 11th December 2018)

222. Saa, L. & Pavlov, V. Enzymatic Growth of Quantum Dots: Applications to Probe Glucose Oxidase and Horseradish Peroxidase and Sense Glucose. *Small* **8**, 3449–3455 (2012).

223. Zhou, M., Diwu, Z., Panchuk-Voloshina, N. & Haugland, R. P. A Stable Nonfluorescent Derivative of Resorufin for the Fluorometric Determination of Trace Hydrogen Peroxide: Applications in Detecting the Activity of Phagocyte NADPH Oxidase and Other Oxidases. *Anal. Biochem.* **253**, 162–168 (1997).

224. Savizi, I. S. P., Kariminia, H.-R., Ghadiri, M. & Roosta-Azad, R. Amperometric sulfide detection using Coprinus cinereus peroxidase immobilized on screen printed electrode in an enzyme inhibition based biosensor. *Biosens. Bioelectron.* **35**, 297–301 (2012).

225. Fleischmann, M., Hendra, P. J. & McQuillan, A. J. Raman spectra of pyridine adsorbed at a silver electrode. *Chem. Phys. Lett.* **26**, 163–166 (1974).

226. Albrecht, M. G. & Creighton, J. A. Anomalously intense Raman spectra of pyridine at a silver electrode. *J. Am. Chem. Soc.* **99**, 5215–5217 (1977).

227. Jeanmaire, D. L. & Van Duyne, R. P. Surface raman spectroelectrochemistry: Part I. Heterocyclic, aromatic, and aliphatic amines adsorbed on the anodized silver electrode. *J. Electroanal. Chem. Interfacial Electrochem.* **84**, 1–20 (1977).

228. Moskovits, M. Surface roughness and the enhanced intensity of Raman scattering by molecules adsorbed on metals. *J. Chem. Phys.* **69**, 4159–4161 (1978).

229. Moskovits, M. Surface-enhanced spectroscopy. *Rev. Mod. Phys.* **57**, 783–826 (1985).

230. Kneipp, K., Kneipp, H., Itzkan, I., Dasari, R. R. & Feld, M. S. Ultrasensitive Chemical Analysis by Raman Spectroscopy. *Chem. Rev.* **99**, 2957–2976 (1999).

231. Michaels, A. M., Nirmal, M. & Brus, L. E. Surface Enhanced Raman Spectroscopy of Individual Rhodamine 6G Molecules on Large Ag Nanocrystals. *J. Am. Chem. Soc.* **121**, 9932–9939 (1999).

232. Nie, S. & Emory, S. R. Probing Single Molecules and Single Nanoparticles by Surface-Enhanced Raman Scattering. *Science* **275**, 1102–1106 (1997).

233. Mosier-Boss, P. A. Review of SERS Substrates for Chemical Sensing. *Nanomaterials* **7**, 142 (2017).

234. Tian, Z.-Q., Ren, B. & Wu, D.-Y. Surface-Enhanced Raman Scattering: From Noble to Transition Metals and from Rough Surfaces to Ordered Nanostructures. *J. Phys. Chem. B* **106**, 9463–9483 (2002).

235. Weaver, M. J., Zou, S. & Chan, H. Y. H. Peer Reviewed: The New Interfacial Ubiquity of Surface-Enhanced Raman Spectroscopy. *Anal. Chem.* **72**, 38 A-47 A (2000).

236. Campion, A. & Kambhampati, P. Surface-enhanced Raman scattering. *Chem. Soc. Rev.* **27**, 241–250 (1998).

237. Kennedy, B. J., Spaeth, S., Dickey, M. & Carron, K. T. Determination of the Distance Dependence and Experimental Effects for Modified SERS Substrates Based on Self-Assembled Monolayers Formed Using Alkanethiols. *J. Phys. Chem. B* **103**, 3640–3646 (1999).

238. Yan, X., Li, J. & Möhwald, H. Templating Assembly of Multifunctional Hybrid Colloidal Spheres. *Adv. Mater.* **24**, 2663–2667 (2012).

239. Su, Y. *et al.* Peptide Mesocrystals as Templates to Create an Au Surface with Stronger Surface-Enhanced Raman Spectroscopic Properties. *Chem. – Eur. J.* **17**, 3370–3375 (2011).

240. Cao, Y. C., Jin, R. & Mirkin, C. A. Nanoparticles with Raman Spectroscopic Fingerprints for DNA and RNA Detection. *Science* **297**, 1536–1540 (2002).

241. Faulds, K., Smith, W. E. & Graham, D. Evaluation of Surface-Enhanced Resonance Raman Scattering for Quantitative DNA Analysis. *Anal. Chem.* **76**, 412–417 (2004).

242. McCall, S. L. & Platzman, P. M. Raman scattering from chemisorbed molecules at surfaces. *Phys. Rev. B* **22**, 1660–1662 (1980).

243. Gersten, J. & Nitzan, A. Electromagnetic theory of enhanced Raman scattering by molecules adsorbed on rough surfaces. *J. Chem. Phys.* **73**, 3023–3037 (1980).

244. Skadtchenko, B. O. & Aroca, R. Surface-enhanced Raman scattering of p-nitrothiophenol: Molecular vibrations of its silver salt and the surface complex formed on silver islands and colloids. *Spectrochim. Acta. A. Mol. Biomol. Spectrosc.* **57**, 1009–1016 (2001).

245. Sharma, B., Frontiera, R. R., Henry, A.-I., Ringe, E. & Van Duyne, R. P. SERS: Materials, applications, and the future. *Mater. Today* **15**, 16–25 (2012).

246. Sylvia, J. M., Janni, J. A., Klein, J. D. & Spencer, K. M. Surface-Enhanced Raman Detection of 2,4-Dinitrotoluene Impurity Vapor as a Marker To Locate Landmines. *Anal. Chem.* **72**, 5834–5840 (2000).

247. Mazet, V., Carteret, C., Brie, D., Idier, J. & Humbert, B. Background removal from spectra by designing and minimising a non-quadratic cost function. *Chemom. Intell. Lab. Syst.* **76**, 121–133 (2005).